GLUTAMATE IN CANCER-INDUCED BONE PAIN

SYSTEM XC- MEDIATED GLUTAMATE TRANSPORT INHIBITION IN CANCER-INDUCED BONE PAIN

By

ROBERT G. UNGARD, B.A.S. (HONOURS)

A Thesis

Submitted to the School of Graduate Studies

In Partial Fulfilment of the Requirements

for the Degree

Master of Science

McMaster University

MASTER OF SCIENCE (2012) McMaster University

(Medical Sciences) Hamilton, Ontario, Canada

TITLE: System x_C^- Mediated Glutamate Transport Inhibition in Cancer-Induced Bone Pain

AUTHOR: Robert Gavin Ungard, B.A.S. (Honours) (University of Guelph)

SUPERVISOR: Professor Gurmit Singh

NUMBER OF PAGES: xii, 137

Abstract

Breast cancers are the most common source of metastases to bone of which cancer-induced bone pain is a frequent pathological feature. Cancer-induced bone pain is a unique pain state with a multiplicity of determinants that remains to be well understood and managed. Current standard treatments are limited by dose-dependent side effects that can depress the quality of life of patients. Glutamate is a neurotransmitter and bone cell-signalling molecule that has been found to be released *via* the system x_C^- cystine/glutamate antiporter on cancer cells of types that frequently metastasize to bone, including breast cancers. This project examines the hypothesis that limiting glutamate release from cancer cells metastasized to bone will reduce bone tissue disruption and cancer-induced bone pain. A mouse model of cancer-induced bone pain was established with intrafemoral human breast cancer cells (MDA-MB-231), and behavioural measurements were taken for weight bearing and induced paw withdrawal thresholds. The system x_C^- inhibitors sulfasalazine and (S)-4-carboxyphenylglycine both attenuated glutamate release from cancer cells in a dose-dependent manner *in vitro*. Treatment with sulfasalazine induced a moderate delay in the onset of behavioural indicators of pain in mouse models, and treatment with (S)-4-carboxyphenylglycine had no apparent results. This data suggests that the limitation of extracellular glutamate released from cancers in bone with sulfasalazine may provide some alleviation of the often severe and intractable pain associated with bone metastases.

Acknowledgements

My most heartfelt appreciation and thanks go to my supervisor Dr. Gurmit Singh for accepting me into your lab, entrusting me with this project, and mentoring me throughout it. I appreciate this opportunity more than I can convey in this paragraph. To Dr. Eric Seidlitz, thank you for holding my hand for the past two years and for making sure I didn't ruin everything for everyone else. I depended on you daily for help and advice and I hope that this thesis may finally find me teaching you something you don't already know, although I doubt it. To my supervisory committee Dr. James L. Henry and Dr. Margaret Fahnestock, thank you both very much for accepting me under your supervision. Your critical analysis has greatly improved this project and has led me to learn a great deal of which I would have otherwise been ignorant. Thanks to Dr. Jim Julian and Dr. Chu-Shu Gu for your guidance into the realm of practical statistics. Thanks to Natalie Zacal for arriving on a Monday and outpacing me at IHC by Friday. Your help with the final stages of this project was great. Thanks to Vikas Sridhar for taking the blame for most of my mistakes and for befriending all my mice. And, thank you to all my lab-mates at the JCC. The opportunity to have worked with each of you has been a privilege and a window into the world of some of the most clever and dedicated students and researchers there are.

Most importantly, thank you to my family and friends for your love and support. To Sashaina, thank you for sharing your amazing love of life and for always brightening the darkest of days. To my parents, thank you for having every confidence in me to

accomplish my goals. Your approach to life has shaped mine immensely and I am so proud of that.

Table of Contents

List of Figures and Tables

List of Abbreviations

(S)-4-CPG	(S)-4-Carboxyphenylglycine
AMPA	α-amino-3-hydroxyl-5-methyl-4-isoxazolepropionic acid
AMPAR	α-amino-3-hydroxyl-5-methyl-4-isoxazolepropionic acid receptor
ASIC	Acid-sensing ion channel
ATP	Adenosine triphosphate
BBB	Blood-brain barrier
BDNF	Brain-derived neurotrophic factor
cAMP	Cyclic adenosine monophosphate
CGRP	Calcitonin gene-related peptide
CNS	Central nervous system
CSF	Cerebrospinal fluid
DAG	Diacylglycerol
DMEM	Dulbecco's Modified Eagle Medium
DNA	Deoxyribonucleic acid
DPA	Dynamic Plantar Aesthesiometer
DRG	Dorsal root ganglion
DWB	Dynamic Weight Bearing
EAAC	Excitatory amino acid carrier
EAAT	Excitatory amino acid transporter
ECF	Extracellular fluid
EPSP	Excitatory postsynaptic potential
FBS	Fetal bovine serum
GC	Mitochondrial glutamate carrier
GFAP	Glial fibrillary acidic protein
GLAST	Glutamate aspartate transporter
GLT-1	Glutamate transporter-1
GSH	Glutathione
Hsp90	Heat shock protein 90
IASP	International Association for the Study of Pain
iGluR	Ionotropic glutamate receptor
IP_3	Inositol 1,4,5-trisphosphate
KA	Kainate
KAR	Kainate receptor
M-CSF	Macrophage colony-stimulating factor
mGluR	Metabotropic glutamate receptor
MS	Multiple sclerosis
MMP	Matrix metalloproteinase
NGF	Nerve growth factor
NK_1	Neurokinin receptor 1

NMDA	N-methyl-D-aspartate
NMDAR	NMDA receptor
NSAID	Non-steroidal anti-inflammatory drug
OPG	Osteoprotegerin
PBS	Phosphate-buffered saline
PTH	Parathyroid hormone
PTH1R	Parathyroid hormone type 1 receptor
PTHrP	Parathyroid hormone related peptide
RANK	Receptor activator of nuclear factor-κB
RANKL	Receptor activator of nuclear factor-κB ligand
ROS	Reactive oxygen species
SEM	Standard error of the mean
SSZ	Sulfasalazine
TBS	Tris-buffered saline
TGF-β	Transforming growth factor-β
TRAP	Tartrate-resistant acid phosphatase
Trk	Tropomyosin receptor kinase
TRPV1	Transient receptor potential channel-vanilloid subfamily member 1
V-ATPase	Vacuolar-ATPase
VGLUT	Vesicular glutamate transporter
WHO	World Health Organization

Chapter 1: Introduction

Cancer in bone occurs most frequently as a result of metastases from distant sites rather than as the growth of a primary cancer in bone. Bone metastases are extremely disruptive to normal bone cell metabolism, often resulting in the development of lesions featuring the dysregulated destruction and formation of mineralized bone tissue and the release of pro-inflammatory and algogenic substances into the bone microenvironment. This disruption is responsible for a host of pathologic consequences including multiple fractures, spinal cord compression, hypercalcaemia, and severe and often intractable pain (Coleman, 2006). As a result, patients with bone metastases experience reductions in functional status, quality of life and survival (Mercadante, 1997).

The primary site of origin of bone metastases is not evenly distributed, rather some cancers display a propensity to metastasize to bone that far outstrips that of other cancers. In particular, cancers of the lung, prostate, kidney, thyroid and breast are the most likely to produce a bone metastasis, with lung, prostate and breast cancer accounting for the vast majority of these cases, and breast cancer as the most common source (Coleman, 2006). The exact incidence of bone metastases from breast cancer is unknown; however, one study radiographically confirmed bone metastases in approximately 70% of patients with advanced breast cancer, making bone the most common site of breast cancer metastasis, and also the most common site of distant breast cancer relapse (Coleman & Rubens, 1987). If it is the case that even a conservative 50%

of terminal breast, prostate, and lung cancers have produced a bone metastasis, then it is possible that approximately one million people die each year while burdened with a tumour in bone (IARC, 2010). With treatment, breast cancer patients now frequently survive for several years following the diagnosis of a bone metastasis, increasing the prevalence of the condition and allowing the many associated morbidities of bone metastases to develop into chronic conditions (Coleman & Rubens, 1987; Solomayer et al., 2000; Yavas et al., 2007). As the number of patients living with bone metastases is so great, there is more than ever a vital need for interventions that focus on the preservation of a patient's quality of life to become commonplace and accessible.

Cancer-induced pain can be debilitating and intractable and is a major impediment to the maintenance of quality of life and functional status in cancer patients. Cancer pain is reported to be experienced by 30–50% of all cancer patients, and by 75–90% of late stage metastatic cancer patients (Sabino & Mantyh, 2005). Metastatic cancer-induced bone pain is the most common source of cancer pain reported by patients (Mercadante, 1997). The effective management of cancer pain is largely performed in accordance with the principles of the World Health Organization (WHO) guidelines for cancer pain relief. The guidelines are based upon adherence to the WHO Analgesic Ladder (Figure 1.1) which stipulates a treatment progression from non-opioid analgesics through weak opioids to strong opioids as is necessary to treat progressively worsening pain. Adjuvant drug supplementation and other supplementary interventions including radiotherapy and alternative treatments are applicable throughout as necessary (WHO, 1996). Adherence to this treatment paradigm has been validated as effective for good or satisfactory pain

relief in the majority of cancer patients; however, 24% of treated patients do not experience complete pain control, with 12% reporting inadequate pain control (Mercadante, 1999; Zech et al., 1995). It has also been reported that approximately two-thirds of patients undergoing treatment with opioids experience episodes of breakthrough pain which is a transitory exacerbation of pain that exceeds the control of a patient's regular analgesic regimen (Caraceni & Portenoy, 1999). Episodes of breakthrough pain are treated usually with a "rescue dose" of the patient's current analgesic, or more recently with a different fast-acting transmucosal μ-opioid agonist (Casuccio et al., 2009).

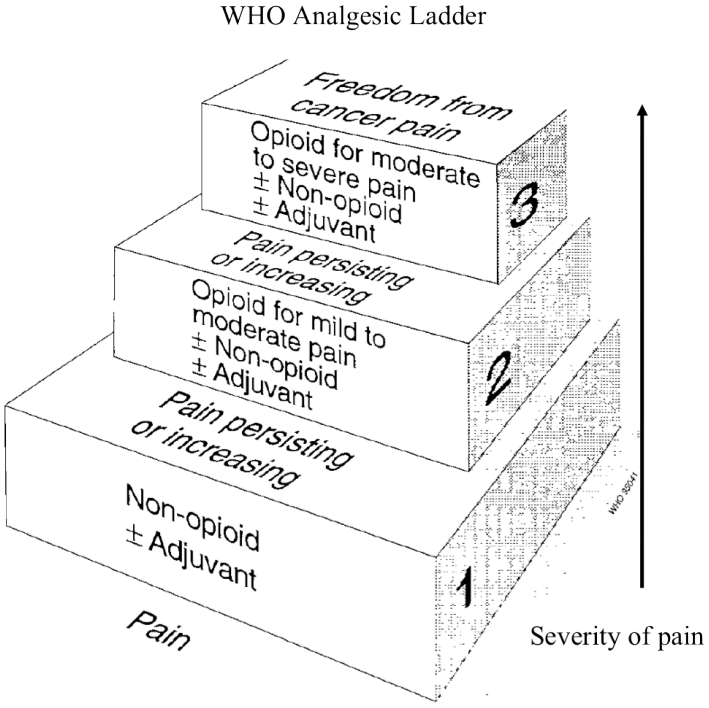

Figure 1.1 World Health Organization Analgesic Ladder. Stipulates a treatment progression from non-opioid analgesics through weak opioids to strong opioids as is necessary to treat progressively worsening pain (adapted from WHO, 1996).

Current analgesic treatment practices are often effective at their priority of reducing the experience of pain for the cancer patient, but that pain relief often comes at the cost of otherwise impairing the patient's quality of life through treatment side effects. Opioids in particular induce a number of serious dose-limiting side effects including but not limited to nausea, constipation, vomiting, respiratory depression, sedation, somnolence, and cognitive impairment, and prolonged use can induce the development of physical dependence, tolerance and addiction (Benyamin et al., 2008; Meuser et al., 2001). Non-steroidal anti-inflammatory drugs (NSAIDs) are most often the first analgesic treatment for cancer pain, and they too are associated with several dose-dependent adverse effects, most predominantly, gastrointestinal and renal side-effects (Brater, 1999; Wolfe et al., 1999). Patient or caregiver concern about treatment-associated side effects or of the consequences of dependence on pain treatment with analgesics can often result in the insufficient control of otherwise manageable pain, as can layers of regulation governing access to controlled pain medications (Cleeland et al., 1997; Pargeon & Hailey, 1999). For these patients who cannot or do not access adequate pain relief, in addition to those patients whose pain cannot be fully controlled with available analgesics, inadequate cancer pain management yet remains a global public health concern.

It is for these reasons that there is a need to investigate new targets for pain management. Approaches that limit side-effects while allowing good background and breakthrough pain management would serve to maintain a patient's quality of life and

independence longer than current therapies do. At a time when there is a palpable shift in the paradigm of cancer research towards the control and management of the disease in addition to its eradication, therapies for pain that do not incapacitate the patient are more necessary than ever. It is in this interest that we have embarked upon this course of research. My project as follows is to investigate the mechanistic potential for a novel method of pain control in cancer patients with bone metastases that acts through the removal of a stimulus of pain by inhibiting the release of the signalling molecule glutamate from the cancer cell into the host bone tissue environment. As the most common source of metastases to bone is breast cancer, I have chosen to focus this project on models of that type.

Glutamate

Glutamate is the anionic form of the nonessential amino acid glutamic acid. L-glutamic acid is ubiquitous in nature, abundant as a free amino acid and comprising 11-22% by weight of all animal protein and as much as 40% of plant protein (Giacometti, 1979). L-glutamate is utilized across several kingdoms in animals, plants, and bacteria in a multiplicity of roles, including as a nutrient, a catalytic intermediate, and most importantly for the purposes of this project, as a cell-signalling molecule in many human tissues. In mammalian cells, glutamate is primarily synthesized from glutamine through glutaminase, and from the transamination of the citric-acid cycle intermediate α-ketoglutarate through glutamate dehydrogenase (Figure 1.2).

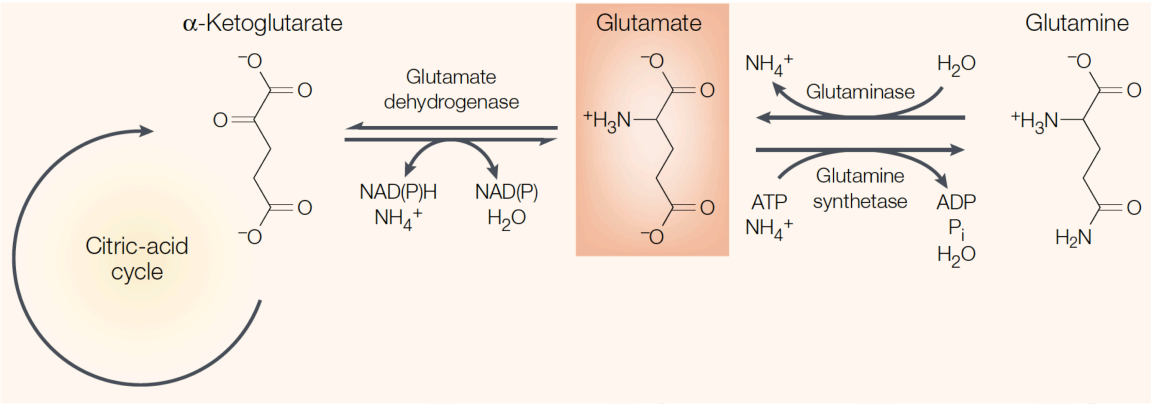

Figure 1.2 Glutamate synthesis in mammals from α-ketoglutarate and glutamine (adapted from Nedergaard et al., 2002).

The most famously studied role of glutamate is that of the predominant excitatory neurotransmitter in the central nervous system (CNS) of vertebrates, where glutamatergic signalling is a mediator of normal brain function including roles in brain development, synaptic plasticity, learning, memory, anxiety, and pain perception (Dingledine et al., 1999). In humans, plasma glutamate levels are reported between 20-130 μM and vary within that range depending on a subject's exercise and diet (Bergstrom et al., 1974; Forslund et al., 2000). Despite being the most abundant free amino acid in the CNS (Perry, 1982), glutamate concentrations in the brain fall far below those of plasma. Glutamate in brain extracellular fluid (ECF) is between 0.5 – 2 μM (Meldrum, 2000), and is even less prevalent in the cerebrospinal fluid (CSF) (Perry, 1982), measured in a variety of conditions at < 0.4 μM (Ferrarese et al., 1993). This discrepancy is maintained by the blood-brain barrier (BBB) which is largely impermeable to the influx of glutamate,

and serves to isolate the delicately balanced glutamatergic signalling of the CNS from the relatively high concentration of circulating plasma glutamate. In high concentrations, glutamate in the ECF of the CNS becomes neurotoxic, inciting the death of neurons and glial cells through excessive glutamate receptor activation, a process termed excitotoxicity (Choi, 1988). The BBB is not entirely impermeable to glutamate, slow influx occurs along protected areas, and the circumventricular organs do not bar the passage of glutamate; however, there is a very limited effect on the CSF through those passages (Hawkins et al., 1995). Glutamate transporters are also present on the BBB; however, they function to remove glutamate to the endothelial cells of the vasculature rather than the reverse (O'Kane et al., 1999), and so the glutamate in the CNS is almost entirely synthesized in the CNS (Gruetter et al., 1998). Unlike glutamate, glutamine can be imported to the CNS via the sodium-dependent amino acid transporter System N, which allows glutamate synthesis to continue in the face of a defunct citric-acid cycle (W. J. Lee et al., 1998).

As the predominant excitatory neurotransmitter, glutamate is stored in membrane-bound vesicles in the presynaptic nerve terminal at ~100 mM (Meldrum, 2000). The exocytosis of these vesicles is induced at the synaptic cleft upon stimulation by a Ca^{2+} influx through voltage-gated channels induced to open by a preceding depolarizing action potential (Llinas et al., 1981). Glutamate released to the synaptic cleft then rapidly binds to one of several glutamate receptors on the postsynaptic neuron prior to its reuptake to the presynaptic neuron or to nearby glial cells. As glutamate is an excitatory neurotransmitter, one of the consequences of its postsynaptic neuronal binding is to

depolarize and induce an excitatory postsynaptic potential (EPSP) in the dendrite which may, in sufficient numbers, induce the propagation of a postsynaptic action potential. The molecular machinery involved in this process and again in non-excitable peripheral and pathological glutamatergic signalling pathways including normal bone cell signalling and nociception involves several classes of glutamate receptors and transporters which will be described independently in the following section.

Glutamate Receptors

There are two major families of glutamate receptors: ionotropic (iGluR) and metabotropic (mGluR). The iGluRs are ligand-gated cation channels and include the NMDA Receptor (NMDAR), AMPA receptor (AMPAR), and Kainate receptor (KAR). The mGluRs induce an intracellular second messenger system through membrane-bound G-proteins, and include eight receptors, mGluR1 through mGluR8 classified into three groups.

Ionotropic Glutamate Receptors

The iGluRs are named for their respective selective synthetic agonists. All iGluR subunits consist of an extracellular N-terminus, intracellular C-terminus, three transmembrane domains and a re-entrant loop that forms the pore of the ion channel (Armstrong & Gouaux, 2000). AMPA Receptors (AMPAR) are named for α-amino-3-hydroxyl-5-methyl-4-isoxazolepropionic acid (AMPA) and consist of four distinct subunits (GluR1-4), each with an agonist binding site (Mayer, 2005). When more than one of these subunits is bound to glutamate, AMPARs undergo a conformational change

opening their ion channel that is permeable to Na^+ influx and K^+ efflux, which rapidly depolarizes the cell. If the AMPAR lacks a GluR2 subunit, the ion channel is also permeable to Ca^{2+} influx (Fundytus, 2001). AMPARs have a lower affinity for glutamate than the NMDA receptors (NMDARs), (200–500 μM and 2.5–3 μM, respectively); however, during a synaptic transmission AMPARs are quick to react and quick to desensitize, making them the first receptors to propagate a signal (Meldrum, 2000).

Kainate receptors (KAR) are named for kainaic acid (KA) and are structurally and functionally similar to the AMPAR. They consist of five subunits (GluR5–7, and KA1–2), and require the binding of two receptor sites to open the ion channel (Mayer, 2005). Like AMPARs, KARs respond quickly to glutamate and are permeable to Na^+ influx, and K^+ efflux (Fundytus, 2001).

NMDARs are named for their selective agonist N-methyl-D-aspartate (NMDA). NMDARs consists of seven subunits (NR1, NR2A–D, NR3A and NR3B), four of which contain a glutamate binding site and one which contains a site for the NMDAR co-agonists glycine or D-serine (Wolosker, 2006). The NMDAR ion channel is permeable to the influx of Ca^{2+} and Na^+ and the efflux of K^+; however, a resting NMDAR also contains a voltage-dependent extracellular Mg^{2+} block of the ion channel which must be removed through membrane depolarization to allow the ion channel to open (Bleakman et al., 2006). During a synaptic transmission the necessity for removal of the NMDAR Mg^{2+} block through membrane depolarization allows the KARs and AMPARs to be the first to open in response to a glutamate signal. It is the largely AMPAR-induced membrane-depolarization that allows the removal of the NMDAR Mg^{2+} block as the final step in the

opening of the NMDAR ion channel, which, relative to the AMPAR is also slower to inactivate (Bleakman et al., 2006).

There is a fourth member of the iGluR family, the delta receptors, δ1 and δ2, which have modulatory effects on the expression of other iGluRs at synapses (Yamasaki et al., 2011). Their inclusion in the iGluR family; however, is an inference based on sequence homology, and there is not yet evidence that the delta receptors can bind glutamate (MacLean, 2009).

Metabotropic Glutamate Receptors

The mGluRs are classified as part of class C of the G-protein-coupled receptor superfamily that act through the GTP activation of a receptor coupled G-protein and second-messenger system. They contain seven transmembrane domains, an extracellular N-terminal domain and an intracellular C-terminal domain. There are eight mGluRs subdivided into three groups based on sequence homology; group I (mGluR1 and 5), group II (mGluR2 and 3), and group III (mGluR4, 6, 7, and 8) (Niswender & Conn, 2010). In neurotransmission, mGluRs play differing roles from each other. In general, group I mGluRs activate phospholipase C, which generates inositol 1,4,5-trisphosphate (IP_3) and diacylglycerol (DAG) to activate protein kinase C and induce the release of vesicular Ca^{2+} to the cytosol (Niswender & Conn, 2010). When located postsynaptically this action serves alongside the iGluRs to increase depolarization and further propagate an EPSP, when located presynaptically, group I mGluRs have been associated with an increase in glutamate release. Group II and III mGluRs are generally associated with the inhibition of adenylyl cyclase and the downregulation of cyclic adenosine monophosphate

(cAMP), which, when located presynaptically, reduces neurotransmitter release in opposition to the function of the Group I mGluRs (Niswender & Conn, 2010).

Glutamate Transporters

There are two major classes of glutamate transporters; the excitatory amino acid transporters (EAATs), and the vesicular glutamate transporters (VGLUTs), as well as a family of mitochondrial glutamate carriers. There is also a lone glutamate transporter in the family of heteromeric amino acid transporters, system x_C^-, which features heavily in the project of this thesis.

EAATs and VGLUTs

The EAATs include five transporters; the glutamate aspartate transporter (GLAST or EAAT1), glutamate transporter-1 (GLT-1 or EAAT2), the excitatory amino acid carrier (EAAC or EAAT3 or system X_{AG}^-), EAAT4, and EAAT5. They all consist of six to eight transmembrane domains, one to two re-entrant loops, and cytoplasmic N- and C-termini, although this structure has been disputed (Shigeri et al., 2004). These transporters have a relatively high affinity for glutamate (~4–40 mM), and all transport both glutamate and aspartate (Shigeri et al., 2004). In addition the EAATs are all Na^+ and K^+ gradient dependent, specifically, every glutamate molecule is accompanied by the transport of two or three molecules of Na^+ and the antiport of one K^+ (Danbolt, 2001). At a synapse, EAATs on glial cells and neurons function to rapidly remove glutamate from the synaptic cleft and the surrounding area which serves to terminate the neurotransmitter signal and to avoid excitotoxicity (Shigeri et al., 2004).

The VGLUTs include four transporters; VGLUT1, 2 and 3, and the glutamate/aspartate transporter sialin. VGLUTs 1, 2, and 3 consist of 8–10 transmembrane domains and have a much lower affinity for glutamate (~1mM), than do the EAATs (Shigeri et al., 2004). At synapses VGLUTs serve to package intracellular glutamate into vesicles for release by exocytosis. All the VGLUTs are dependent on an H^+ gradient which is maintained by vesicular ATPase proton pumps (Shigeri et al., 2004). While VGLUTs 1, 2, and 3 only transport glutamate; sialin, a recent addition to the VGLUT family, transports both glutamate and aspartate (Miyaji et al., 2008).

The mitochondrial glutamate carriers (GC1 and 2) are two isoforms of the H^+ dependent glutamate/aspartate transporter located on the inner mitochondrial membrane. These transporters remove glutamate from the cytosol to the mitochondrial matrix where glutamate dehydrogenase is available for the transamination of glutamate to the citric-acid cycle intermediate α-ketoglutarate (Fiermonte et al., 2002).

System x_C^-

System x_C^- is the pharmacological target of the project of this thesis. It is a Na^+ independent electroneutral exchanger of L-cystine and L-glutamate that was first described in human fibroblasts in 1980 (Figure 1.3) (Bannai & Kitamura, 1980). The name system x_C^- is in accordance with the 1984 abbreviation code for amino acid transporters in which the lowercase of the x denotes a sodium-independent transport system, the x itself denotes a dicarboxylic amino acid transporter, the superscript – indicates that the substrates are anionic, and the subscript C indicates the preferred substrate cystine (the same transporter is less often referred to as system x_{CG}^- to include

glutamate) (Christensen, 1984). System x_C^- is a member of the family of heteromeric amino acid transporters, all of which consist of a single heavy polypeptide subunit (SLC3 family) and a single light subunit (SLC7 family) coupled via a disulfide bridge (Chillarón et al., 2001). The heavy subunit of system x_C^- is 4F2hc (SLC3A2), a type II membrane glycoprotein common to many amino acid transporters (Verrey et al., 2004). It includes one transmembrane domain and has a molecular weight of ~85 kDa (Lim & Donaldson, 2011). 4F2hc is not essential to the transporter action of system x_C^-, it plays a role in the traffic and adherence of the complete transporter complex to the cell membrane, and can be supplanted entirely with another heavy chain polypeptide with similar capabilities, such as rBAT, without losing antiporter function (H. Wang et al., 2003). The light subunit of system x_C^- is xCT, officially named: solute carrier family 7 (anionic amino acid transporter light chain, x_C^- system) member 11, (SLC7A11), which is entirely responsible for the amino acid exchange function of the transporter and unique to system x_C^- (Giacometti, 1979). Human xCT consists of 501 amino acids, has a molecular weight of ~40 kDa and features 12 transmembrane domains, intracellular N- and C-termini, and a re-entrant loop involved in substrate binding or transportation (Gasol et al., 2004). Extracellular cystine is exchanged for intracellular glutamate with a 1:1 stoichiometry in a Na^+ independent manner. System x_C^- is often described as Cl^- dependent, and indeed cystine/glutamate exchange has been found to take place in some instances only in the presence of Cl^- (Gochenauer & Robinson, 2001; Koyama et al., 1995). However, this dependence has also been reported to occur only when cystine is in relatively low extracellular concentrations (~10 μM) and the uptake of cystine when extracellular

concentrations are higher is unaffected by the presence of Cl^-, suggesting a role for Cl^- in the affinity of system x_C^- for cystine rather than as an ionic gradient (Murphy et al., 1989; Warr et al., 1999). Both cystine and glutamate are moved along their respective gradients in transport, the driving force for this exchange provided by the outwardly driven concentration gradient of intracellularly synthesized glutamate (Bannai & Ishii, 1988). If the concentration gradient of glutamate is reversed, this can induce the transporter to similarly reverse direction, a process that may occur during synaptic transmission (Cho & Bannai, 1990).

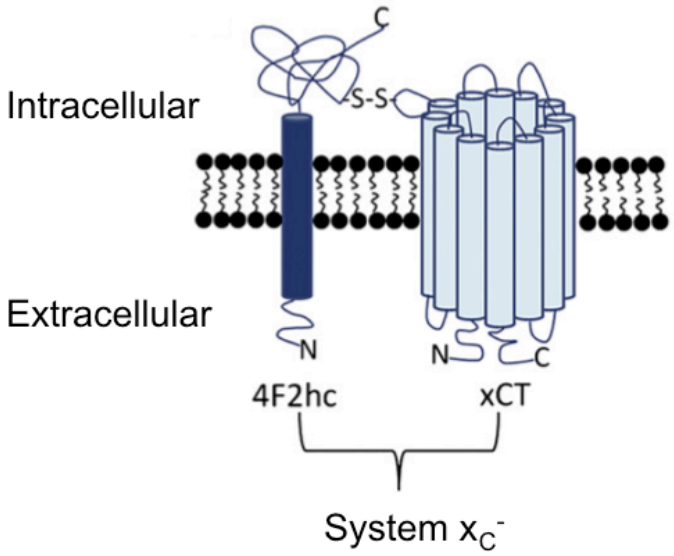

Figure 1.3 Structure of system x_C^- (adapted from Lo, Wang, et al., 2008).

System x_C^- has been localized in a great number of mammalian tissues both in the CNS and peripherally. In human tissues, xCT has been detected peripherally in the

pancreas (Bassi et al., 2001; J. Y. Kim et al., 2001), fibroblasts (Bannai, 1986), monocytes (Eck & Droge, 1989), macrophages (Rimaniol et al., 2001), antigen-presenting dendritic cells (Angelini et al., 2002), the brush border membranes of the kidney and duodenum (Burdo et al., 2006), chondrocytes (L. Wang et al., 2006), osteoclasts (Takarada & Yoneda, 2008), and osteoblasts (Uno et al., 2007). In the CNS, xCT has been detected in the spinal cord (J. Y. Kim et al., 2001), astrocytes (Cho & Bannai, 1990; Gochenauer & Robinson, 2001), microglia (Piani & Fontana, 1994), retinal Müller glia (Kato et al., 1993), and immature cortical neurons (Murphy et al., 1990). It must be acknowledged; however, that xCT expression in a tissue does not necessarily translate into functional system x_C^- transport action.

Functional system x_C^- is retained in several human cancer cell lines including glioma (Cho & Bannai, 1990; J. Y. Kim et al., 2001), lymphoma (Gout et al., 2001), pancreatic cancer (Lo, Ling, et al., 2008), colon cancer (Y. Huang et al., 2005), ovarian cancer (Y. Huang et al., 2005), lung cancer (Guan et al., 2009; Y. Huang et al., 2005), prostate cancer (Doxsee et al., 2007), and breast cancer (Narang et al., 2003; Sharma et al., 2010). It has been noted; however, that system x_C^- in cell culture may not reflect expression patterns *in vivo*, as system x_C^- activity can be rapidly induced upon the establishment of a culture environment (Takada & Bannai, 1984; Watanabe & Bannai, 1987). Functional expression of system x_C^- has been confirmed both in cultured cell lines and in patient-derived tumour samples in glioma (Lyons et al., 2007), and pancreatic cancer (Bassi et al., 2001).

Cystine uptake

The role of system x_C^- in normal conditions is to exchange intracellular glutamate for extracellular cystine. Cystine is a dimer of two oxidized cysteine amino acids, and is the major form of the amino acid in the oxidizing environment of the extracellular space (Ottaviano et al., 2008). The cytosol is considered to be a reducing environment, and so imported cystine is rapidly reduced to its two constituent cysteines, which are therefore predominant intracellularly (Hwang et al., 1992). Cysteine is a nonessential amino acid as it is synthesized intracellularly from methionine through the transsulfuration pathway; however, this synthesis is predominantly active in the liver, and other tissues including the CNS must rely on cysteine or cystine import (I. Ishii et al., 2004). It is thought that the major physiological role of system x_C^- is as a component in two pathways for which intracellular cysteine is the rate-limiting factor: the synthesis of the antioxidant molecule glutathione (GSH), and the cystine/cysteine redox cycle. Both pathways are involved in mediating the protection of the cell from damage by reactive oxygen species (ROS).

Many mammalian cells have the machinery to directly import cysteine; however, the cystine transporters system x_C^-, system X_{AG}^-, and system $b^{o,+}$, allow cells the ability to import the much more prevalent extracellular cystine. Cancer cells have been demonstrated to rely almost entirely on system x_C^- for cystine uptake and cysteine synthesis (Narang et al., 2003; Okuno et al., 2003). In the case of system x_C^-, this cystine import has been demonstrated to increase oxidative stress protection for the cell and the surrounding environment through increasing the availability of rate-limiting intracellular cysteine available for the synthesis of GSH and for the cycling of the cystine/cysteine

cycle (Figure 1.4). GSH is a tripeptide thiol synthesized intracellularly from the amino acids glutamate, cysteine and glycine. GSH is synthesized in the cytosol through the enzymes γ-glutamylcysteine synthetase and GSH synthetase, the rate-limiting factor in this synthesis is the availability of intracellular cysteine (T. Ishii et al., 1987). In the cell, GSH performs a number of functions, one of which is as the predominant cellular antioxidant in the body (Wu et al., 2004). The uptake of extracellular cystine also completes one half of the extracellular/intracellular cystine/cysteine redox cycle. Extracellular cysteine is less prevalent than cystine due to the oxidizing extracellular environment; however, the uptake of cystine to the cell allows the intracellular reduction of cystine dimers to cysteine and is followed by the export of some of that cysteine to the extracellular environment *via* the amino acid transporters system L or system ASC (Verrey et al., 2004). Extracellularly, cysteine acts as an antioxidant, able to effectively protect cells from lipid peroxidation. In the induced absence of GSH, the cystine/cysteine cycle has been found to provide sufficient antioxidation to sustain cell growth (Banjac et al., 2008).

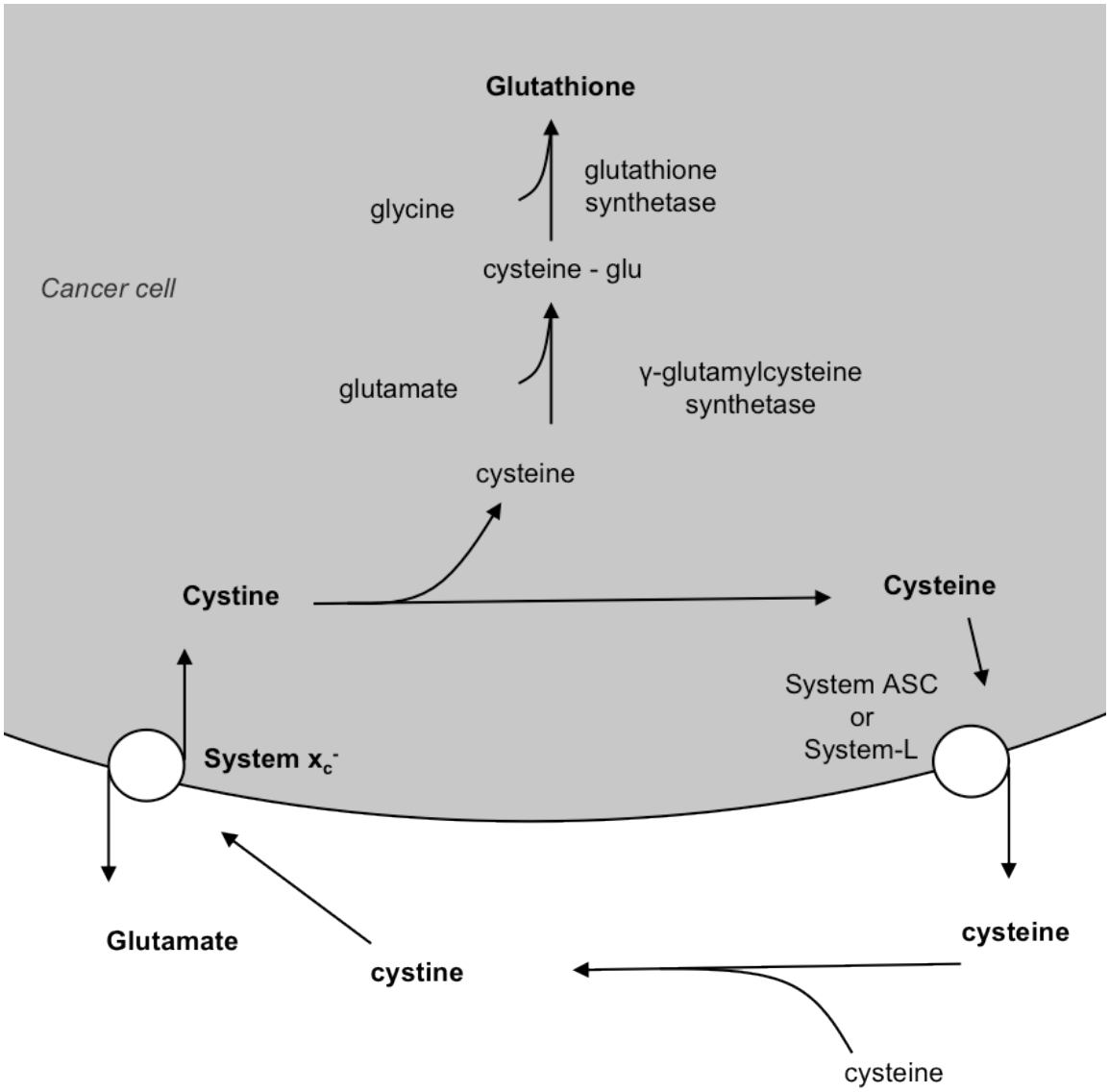

Figure 1.4 System x_C^- in the cycling of the cystine/cysteine cycle and GSH synthesis in cancer cells.

This role as a mediator of cellular protection from oxidative damage is critical to cancer cells, which are consistently under elevated oxidative stress. The rapid and

dysregulated tumour growth and angiogenesis response to the hypoxic and low-glucose tumour environment, and the characteristic of cancer cells to rely heavily on glycolysis for energy supply rather than on the citric acid cycle even in the presence of oxygen, is well-established (Kroemer & Pouyssegur, 2008). In most well oxygenated non-cancer cells, glucose metabolism is relied upon to generate energy for the cell by way of glycolysis in the cytoplasm followed by pyruvate transport to the mitochondria and the circulation of the citric acid cycle. This linked system can only function if oxygen is present to act as the final electron acceptor of the citric acid cycle. In hypoxic environments, glucose metabolism is limited to the process of anaerobic glycolysis in which the citric acid cycle cannot accept pyruvate which is alternatively converted to lactate in the cytosol (J. W. Kim & Dang, 2006). In temporary hypoxic conditions, anaerobic glycolysis is a rapid alternative for ATP production; however, it is too inefficient to be relied upon as a long-term energy source.

In cancer cells, a characteristic shift away from the citric acid cycle towards a reliance upon glycolysis for energy production occurs even in the presence of oxygen. This process is described as aerobic glycolysis, or the Warburg effect, a process that has been established in cancer cells since the early 20th century (Warburg et al., 1927). The result of this metabolic abnormality is that cancer cells become chronic inefficient utilizers of glucose, and rely upon an increased rate of glucose uptake for glycolytic ATP production. This allows the cell a number of advantages including the use of glycolytic intermediates for anabolic reactions, without which, rapidly proliferating cells in conditions of fluctuating oxygen availability could not survive (Kroemer & Pouyssegur,

2008). For the cancer cell in an aerobic environment, glycolysis takes its toll through the generation of reactive oxygen species (ROS) as the normal by-products of respiration (Balendiran et al., 2004). In the cancer cell this ROS production is raised to a level that demands the upregulation of antioxidant systems in order to survive (Halliwell, 2007). Aerobic glycolysis has been identified as a key factor in the increased oxidative stress that cancer cells face, and has also been directly implicated in the activation of oncogenes and the loss of tumour suppressor genes (Le et al., 2010).

One cellular adaptation to increased oxidative stress in cancer cells is the upregulation of the expression of xCT and the activity of system x_C^-, which has been found to confer a survival advantage on the cell. Inhibition of system x_C^- transport activity in normal cell lines (Murphy et al., 1989) and in cancer cell lines (Chung et al., 2005; Kato et al., 1992) has been found to induce GSH depletion, increase oxidative stress, and initiate cell death. System x_C^- mediated resistance to oxidative stress has also been implicated in resistance to chemotherapy and radiation therapy in cancer treatment; therapies that rely to some extent on cell death through ROS. A coordination of transporter gene expression in 60 cancer cell lines with the action of 1400 anticancer drugs revealed 39 drugs that positively correlate with the expression of xCT and 296 that negatively correlate (Y. Huang & Sadée, 2006). The activity of L-alanosine, an amino acid analogue whose uptake is mediated by system x_C^-, was found to positively correlate with xCT. Inhibition of system x_C^- reduced the efficacy of L-alanosine treatment by impeding its uptake to the cell. The activity of geldanamycin, an antibiotic that targets heat shock protein 90 (Hsp90), was found to negatively correlate with xCT expression.

System x_C^- inhibition increased the efficacy of geldanamycin through a reduction of intracellular GSH which reduced cellular resistance to the drug's cytotoxicity (Y. Huang et al., 2005). Celastrol is another antitumoral Hsp90 targeting drug that very negatively correlated with xCT expression (Y. Huang et al., 2008). Inhibition of system x_C^- in celastrol-resistant glioma cells reduced chemoresistance to celastrol treatment, as did other negative modulators of GSH synthesis, indicating that celastrol resistance in glioma is at least in part mediated through the availability of GSH (Pham et al., 2010). The activity of system x_C^- can therefore allow a survival advantage to cancer cells in highly oxidizing conditions.

Glutamate Release

The corollary effect of cystine uptake *via* system x_C^- is the obligatory secretion of glutamate into the extracellular space. This function is largely understood to be a side-effect of cystine uptake, and not a purposeful function in itself. The consequences of this glutamate release depend on the surrounding host tissue, but given the ubiquity of glutamate as a signalling molecule, excess extracellular glutamate has the potential to be devastating in multiple tissues. Similarly to its principal role in cell cystine uptake, system x_C^- has been identified as the mediator of the majority of glutamate secretion from cancer cell lines (Sharma et al., 2010; Ye et al., 1999). The amount of glutamate released in these cultures was dependent on the availability of cystine in the media. In the CNS, glutamate released by system x_C^- from glioma cells is sufficient to exceed the glutamate reuptake capabilities of the EAATs and to incite brain edema and excitotoxic cell death through chronic glutamate receptor activation in neurons (Takano et al., 2001; Ye &

Sontheimer, 1999). This action has been found to impart a functional advantage on the tumour, allowing increased growth and migration relative to glioma that secrete less glutamate (Takano et al., 2001).

Autocrine and paracrine signalling by glutamate on cancer cells also promote growth and migration. AMPA, NMDA, Kainate, and the metabotropic glutamate receptors mGluR3 and mGluR5 have all been identified in cancer cells, and growth-effects have been demonstrated through the manipulation of several of these receptor types. Exogenous glutamate has been found to have a stimulatory effect on growth when applied to glioma and lung cancer cells in culture, and in the same study, antiproliferative effects were observed following treatment with AMPAR and NMDAR antagonists in several cancer cell lines including glioma, lung, thyroid, colon, and breast cancers (Rzeski et al., 2001). To some extent this growth stimulation has been linked to the availability of intracellular Ca^{2+} which can also stimulate tumour growth (Meloni et al., 1998). In addition to regularly Ca^{2+} permeable NMDARs, glioma cell lines have been shown to predominantly feature AMPARs that are also permeable to Ca^{2+} through low or no expression of the GluR2 subunit. Induced expression of GluR2 increased glioma cell apoptosis and reduced tumour growth *in vivo*, suggesting a role of Ca^{2+} influx in proliferative glutamate signalling (Ishiuchi et al., 2002). Inhibition of mGluR2 and 3 on glioma cells also reduced cell proliferation both *in vitro* and *in vivo* (Arcella et al., 2005).

In addition to tumour progression, glutamate released by system x_C^- has been associated with the recurring epileptic seizures that are a prominent feature of glioma. In mouse models of glioma, the inhibition of system x_C^- reduced extracellular peritumoural

glutamate, and was found to reduce epileptic activity following treatment (Buckingham et al., 2011).

The action of system x_C^- has also been implicated in the excitotoxic cell death of oligodendrocytes that is a characteristic feature of multiple sclerosis (MS). Immune cells in both the blood and CNS of animal models of MS and MS patients are induced through high oxidative stress to increase xCT expression and glutamate release (Pampliega et al., 2011). Similarly, xCT has been found to be upregulated in the brain following induction of a rat model of Parkinson's disease which is also characterized by oxidative stress and excitotoxic cell death (Massie et al., 2008). System x_C^- has also been identified as the fusion-entry receptor of human herpesvirus 8, the causative virus of Kaposi's sarcoma. It is thought that the presence of system x_C^- transporters further contribute to the proliferation of Kaposi's sarcoma through upregulation of xCT in response to oxidative stress which aids cell survival and provides more ports of entry for the virus (Kaleeba & Berger, 2006). Reduced and impaired system x_C^- transport activity has also been implicated in the physiology of cocaine addiction (Kau et al., 2008).

In this thesis I will propose that as a host tissue of cancer metastases, the sensitivity to glutamate of bone is a similarly destructive quality as it is in glioma. As will be discussed later, bone is a heavily innervated tissue whose cell regulation depends on glutamatergic signalling pathways. The excessive release of glutamate into this environment from a tumour metastasis has the potential to disrupt local cell signalling which may impact the pathologies of cancer in bone.

Regulation and Inhibition

The regulation of system x_C^- activity is a process mediated through oxidative stress and amino acid deprivation. Only changes in the expression of the xCT subunit affect system x_C^- activity, whereas changes in the 4F2hc subunit do not coordinate with transporter function, possibly an indication of 4F2hc expression in excess of its use (Shih & Murphy, 2001). xCT is readily upregulated by an increase in cellular oxidative stress (J. Y. Kim et al., 2001), and by the deficit of several amino acids including cystine (Sato et al., 2004). In addition, xCT has been found to be chronically over-expressed in normal cell lines identified as particularly resistant to oxidative stress (Lewerenz et al., 2011), and in cancer cells (Chung et al., 2005; Sharma et al., 2010). The 5' flanking regions of both mouse (Sato et al., 2001), and human xCT (Sato et al., 2000) have been sequenced. Binding sites for the transcription factors AP-1, NFκB, Nrf2, and ATF4 have been identified in both species' xCT, and Nrf2 and ATF4 are both thought to be principal regulators of xCT expression (Sasaki et al., 2002; Sato et al., 2001; Sato et al., 2004). This exemplifies the possibility of a diverse array of regulatory pathways for xCT expression. The administration of oxidizing agents to cell culture induces Nrf2 to translocate to the nucleus and bind to one of four antioxidant response elements on the xCT gene, promoting transcription and increasing system x_C^- activity (Sasaki et al., 2002). ATF4 has been shown to bind to two amino acid response elements on the xCT gene, and have been shown to upregulate xCT in response to cystine starvation (Sato et al., 2004).

The significance of the transport activity of system x_C^- to so many pathologies has made the inhibition of system x_C^- a keenly investigated topic. A number of effective

inhibitors have been identified in several structural classes. The first inhibitors to be identified were its substrates, L-glutamate and L-cystine, which in high concentrations each inhibit the transport of the other (Bannai & Kitamura, 1980). Since then several studies have set out to examine the potential for different classes of chemicals to inhibit system x_C^-, including amino acid analogues (Patel et al., 2004), AMPA analogues (Patel et al., 2010), and anti-inflammatory drug analogues (Shukla et al., 2011). The search for effective nontoxic inhibitors has yielded several viable classes of compounds including those mentioned above and, interestingly, UV-B irradiation which has been reported to inhibit system x_C^- mediated cystine uptake (M. Zhu & Bowden, 2004). Of these previously investigated inhibitors, the cyclic glutamate analogue (S)-4-carboxyphenylglycine ((S)-4-CPG), and the anti-inflammatory drug sulfasalazine (SSZ) were chosen as most promising for the purposes of this project (Figure 1.5).

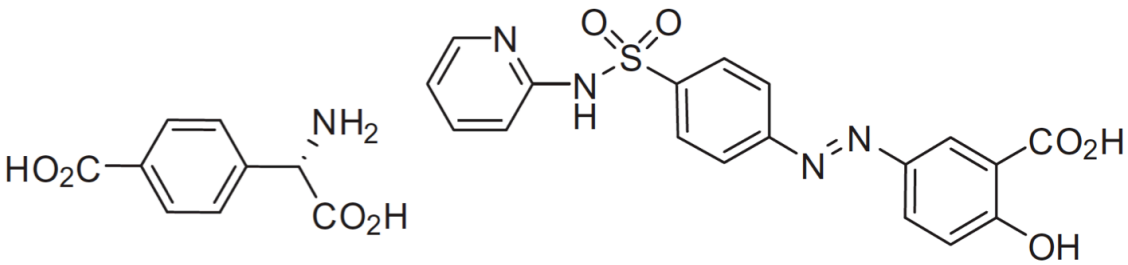

(s)-4-carboxyphenylglycine Sulfasalazine

Figure 1.5 Chemical structure of both inhibitors of the system x_C^- transporter: the cyclic glutamate analogue (S)-4-carboxyphenylglycine and the anti-inflammatory drug sulfasalazine (adapted from Shukla et al., 2011).

(S)-4-CPG is a cyclic glutamate analogue that inhibits system x_C^- in a non-substrate manner. (S)-4-CPG was chosen for its relative lack of action on other glutamatergic targets excluding group I mGluRs, and as it was found to be among the most potent inhibitors of system x_C^- of all amino acid analogues and the least likely to act as a substrate (Patel et al., 2004). It was found to have an IC_{50} of 15 μM in the inhibition of cystine uptake in human glioma cells (Shukla et al., 2011). Advantageously, (S)-4-CPG does not readily cross the BBB, which limits disruption of its group I mGluR antagonism on our pain model (Reichel et al., 2000). (S)-4-CPG has been successfully used as an inhibitor of system x_C^- *in vitro* in many cell cultures including cancer cells (Chung et al., 2005).

SSZ is a FDA and Health Canada approved drug for the treatment of ulcerative colitis that is also frequently used in the treatment of rheumatoid arthritis. It is a combination of sulfapyridine, an antibiotic, and 5-aminosalicylic acid, an anti-inflammatory, bound with an azo bridge. When taken orally, ~30% of sulfasalazine is absorbed intact, where the rest is separated by colonic bacteria at the azo bond to its constituent drugs (Wahl et al., 1998). It is intact SSZ only that inhibits system x_C^-, and it was found to have an IC_{50} of 30 μM in the inhibition of cystine uptake in human glioma cells (Shukla et al., 2011). The route of drug delivery in this project is intraperitoneal which avoids drug digestion in the GI tract allowing SSZ to remain intact in circulation. Unlike (S)-4-CPG, intact SSZ does permeate the BBB, which is an advantageous feature for the treatment of cancers in the CNS (Robe et al., 2004). Several physiological functions in addition to system x_C^- inhibition have been attributed to intact SSZ, one of

which is to inhibit the activation of the immunomodulatory NFκB (Wahl et al., 1998). In addition to its lengthy history in human treatments SSZ has been successfully used as an inhibitor of system x_C^- *in vitro* in many cell cultures including cancer cells in our lab (Sharma et al., 2010), and *in vivo* in murine cancer models (Chung et al., 2005). Recently a small (n = 10) Phase I clinical trial to evaluate the safety of SSZ in the treatment of advanced recurrent glioma was terminated early due to concerns for patient safety (Robe et al., 2009). This trial, however, included only very late stage patients (median Karnofsky score = 50) who had previously undergone other treatments. Its interests were in investigating SSZ safety in the interests of use as a NFκB inhibitor (Robe et al., 2006). Another phase I trial to evaluate SSZ safety in low-grade newly diagnosed glioma patients is currently in its infancy. This trial is utilizing SSZ in the interests of its system x_C^- inhibition, and has the objective to measure glutamate release in the brain before and after treatment inhibition (de Groot & Sontheimer, 2011).

Bone Physiology

Bones consist of dynamic tissues that undergo regular turnover and remodelling. The skeletal system has three major functions, the first is as a structural frame for the shape, locomotion and protection of the body, the second is as a reserve of minerals and growth factors, and the third is for the production of blood cells in the marrow of the bone matrix. The outer surface of bone is sheathed by the periosteum, a densely innervated and vascularized fibrous membrane. There are two types of mineralized bone structure, both with the same molecular composition: cortical bone and trabecular bone. Cortical bone comprises the outer surface of a bone, it is more dense and rigid and undergoes much

lower rates of turnover than does the trabecular bone which has much more surface area, and is located on the interior surfaces of the cortical bone and at the epiphyses of the long bones (Hadjidakis & Androulakis, 2006). Both cortical and trabecular bone are composed of the same tissues and cells. Those include bone matrix, and the osteoclasts, osteoblasts, and osteocytes found within it.

Bone matrix is the osseous tissue that forms the majority of a bone structure, and mostly consists of mineralized type I collagen fibres and several non-collagenous proteins. The collagen is initially deposited by osteoblasts and then mineralized by crystals of hydroxyapatite ($[Ca_3(PO_4)_2]_3Ca(OH)_2$). In normal bone these two processes generally occur at a similar rate (Hadjidakis & Androulakis, 2006). In cortical bone, matrix is arranged to form repeated parallel cylindrical osteons that are the fundamental unit of cortical bone. Matrix is deposited in concentric circles around a central Haversian canal through which blood vessels and nerves can pass. Volkman's canals run perpendicular through the matrix allowing the connection of Haversian canals (Hadjidakis & Androulakis, 2006). In response to injury or loading, matrix is rapidly produced by osteoblasts in a disorganized pattern to form woven bone that in normal bones is gradually replaced by ordered osteons (McKenzie et al., 2011). Osteocytes are the most common cells of bone. They are formed from osteoblasts that incorporate themselves into the bone matrix, become quiescent, and live for many years. They connect to each other through a network of long cytoplasmic channels that allow signal transmission (Noble, 2008). The precise role of osteocytes is not entirely clear; however, it has been shown that they produce factors involved in the regulation of bone turnover in response to

mechanical stimuli. In particular, this involves the influence of mineralization and matrix metalloproteinase (MMP) production, and through the production of a Wnt pathway inhibitor in response to mechanical loading and parathyroid hormone (PTH) signalling (as reviewed by Noble, 2008).

Bone Remodelling

Bone turnover and remodelling is accomplished through the balanced antithetical roles of osteoblasts and osteoclasts. Osteoblasts mediate bone apposition while osteoclasts mediate bone degradation. These processes are closely coordinated both systemically and locally, and dysregulation of this communication is a feature of several diseases including osteoporosis, osteopetrosis, Paget's disease, and cancers in the bone. Glutamate signalling is a feature of both cell types, and has recently become understood to play a role in the maturation and regulation of osteoblasts and osteoclasts, and their functional outcomes.

Osteoblasts are the cells responsible for the synthesis and mineralization of the bone matrix. They are cuboidal with a single nucleus, and originate through the process of osteoblastogenesis from multipotent mesenchymal stem cells through osteoprogenitor cells and pre-osteoblasts (Marie, 2008). Several transcription factors have been identified in this process, with Runx2 distinguished as the critical and principal positive regulator. It acts through binding to the osteoblast specific element regulatory sequence featured on all genes responsible for components of the bone matrix (Marie, 2008). Osteoblasts are found at the bone matrix surface in clusters, joined to each other through tight junctions.

They are polarized and secrete matrix proteins exclusively at the bone surface (Mackie, 2003). Mostly osteoblasts primarily secrete type I collagen, but also several proteoglycans, glycoproteins and γ-carboxylated proteins (Mackie, 2003). Following protein secretion, osteoblasts initiate mineralization of the newly formed collagen matrix by the release of preformed hydroxyapatite crystals to the bone surface in membrane bound vesicles (Anderson, 2003). The fate of an osteoblast is to either become encased in matrix thus becoming an osteocyte, to undergo apoptosis, or once its matrix secretion properties are finished, to become a bone lining cell which covers the exposed surfaces of bone tissue (Mackie, 2003).

Osteoclasts are the cells largely responsible for bone lysis and resorption. They are large, multinucleated cells that form through the fusion of multiple monocytes originated from hematopoietic stem cells (Hadjidakis & Androulakis, 2006). Osteoclastogenesis is determined primarily through exposure to two cytokines: macrophage colony-stimulating factor (M-CSF) and receptor activator of NFκB ligand (RANKL) (Väänänen & Laitala-Leinonen, 2008). Osteoclasts, like osteoblasts, are found at the bone matrix surface. They are polarized cells with the bone surface side featuring a ruffled membrane responsible for the bone resorption action of the cell, surrounded by a sealing zone which binds tightly to the bone surface, isolating the environment of the resorptive pit at the ruffled border from the ECF (Väänänen & Laitala-Leinonen, 2008). Osteoclasts resorb both the crystallized hydroxyapatite and the underlying collagen matrix through direct secretion and the exocytosis of vesicles containing hydrochloric acid, cathepsin K, tartrate-resistant acid phosphatase (TRAP), and several MMPs at the

ruffled border. Acid is secreted both by membrane bound vesicles and through direct secretion by the active transporter proton pumps, vacuolar-ATPase (V-ATPase), that function first to load the intracellular vesicles and then for cross-membrane proton transport (Väänänen et al., 1990). This secreted acid enables dissolution of hydroxyapatite, the rate-limiting step in bone resorption. The dissolved mineral contents, largely calcium and phosphate, must then be transported away to prevent neutralizing the low pH of the resorption pit. This transport occurs by transcytosis by VGLUT1 through the osteoclast where it is secreted from the apical end of the cell, or through the sealing zone periphery (Morimoto et al., 2006). This mechanism of bone matrix dissolution and mineral transport through the cell is a feature exploited by drugs that target osteoclasts. Following the de-mineralization of the bone matrix, the other secreted factors from osteoclasts bind and resorb the protein component. Cathepsin K binds and degrades type I collagen, and activates TRAP which acts as a phosphatase and a generator of ROS, both shown to be essential in matrix resorption (Ljusberg et al., 2005). Osteoclasts also secrete several MMPs, most regularly MMP-9 and 14; however, the effect on bone resorption of inhibiting these enzymes in osteoclasts is small (Fuller et al., 2007).

The maturation and activity of osteoblasts and osteoclasts is tightly coupled. Osteoblastogenesis as previously mentioned is determined by several transcription factors including Runx2. The systemic hormone PTH, secreted from the chief cells of the parathyroid gland, acts to maintain circulating calcium and phosphate homeostasis through action on several organs including through both anabolic and catabolic effects on bone, as determined by the pattern of its release. PTH itself is negatively regulated by

serum Ca^{2+}, and positively regulated by serum phosphate and vitamin D (Naveh-Many, 2010). A drop in essential serum Ca^{2+}, then, results in the steady upregulation of PTH production, and indirectly acts to mobilize the hydroxyapatite reserves of bone through osteoblast induced osteoclast proliferation (Naveh-Many, 2010). Through its effects on osteoblasts, PTH increases both bone formation and resorption at once; however, it has been demonstrated that constant high expression of PTH as in the case of hyperparathyroidism has overall catabolic effects on bone (el-Hajj Fuleihan et al., 1989), whereas intermittent expression is more anabolic (W. Zhu et al., 2011). In either case, these results are realized through PTH binding of the PTH type 1 receptor (PTH1R), which is expressed on pre-osteoblasts and mature osteoblasts but not on osteoclasts (Aslan et al., 2012). PTH acts on several transcription factors in osteoblasts including through the phosphorylation and activation of Runx2, and also activates anti-apoptotic pathways in the cell, increasing the proliferation of osteoblasts (Bellido et al., 2003). Mature osteoblasts produce and secrete osteoclast stimulating RANKL, and M-CSF, and the decoy receptor for RANKL, osteoprotegerin (OPG), which sequesters RANKL and limits its signalling. Stimulation with steady PTH has been shown to differentially suppress osteoblast expression of OPG while increasing that of RANKL, resulting in increased osteoclastogenesis in co-cultures (J. C. Huang et al., 2004). Osteoblast proliferation then has a corresponding stimulatory effect on the proliferation of osteoclasts (Aslan et al., 2012). A mathematical model has been developed that suggests the differential role of constant and intermittent PTH stimulation on bone resorption is due to the longer survival and action of osteoblasts after PTH stimulus is removed,

relative to osteoclasts. Intermittent PTH would then allow more periods of osteoblast matrix synthesis without corresponding osteoclast resorption (Komarova, 2005).

Systemically, other hormones are also involved in bone homeostasis. Estrogens have been shown to induce bone anabolism through osteoblastogenesis and osteoblast survival by activating Runx2 and other transcription factors (Kousteni et al., 2007). The thyroid hormone calcitonin has also been shown to increase bone formation by inhibiting osteoclast activity in response to high serum Ca^{2+} (de Paula & Rosen, 2010).

Glutamate in Bone

In addition to the RANKL and M-CSF systems of local regulation, glutamate has been implicated in intercellular signalling pathways involved in bone turnover. Cells of bone have repeatedly been found to express the requisite machinery for glutamatergic signalling, and more recently, the effects of glutamate signalling on bone cell homeostasis have begun to be elucidated. There is evidence that cells of bone express the following glutamatergic complexes: osteocytes express the glutamate transporter EAAT1 (Mason et al., 1997). Osteoblasts express the ionotropic receptors AMPAR (Hinoi, Fujimori, Takemori, et al., 2002), NMDAR (Chenu et al., 1998), KAR (Hinoi, Fujimori, Takemori, et al., 2002), the group III mGluRs mGluR 4 and 8 (Hinoi et al., 2001), and the glutamate transporters EAAT 1, 2, and 3 (Takarada et al., 2004), VGLUT1 (Hinoi, Fujimori, Takarada, et al., 2002), and system x_C^- (Uno et al., 2007). Osteoclasts express NMDARs (Chenu et al., 1998), EAAT 2 and 4 (Takarada & Yoneda, 2008), VGLUT1 (Morimoto et al., 2006)and system x_C^- (Figure 1.6) (Takarada & Yoneda, 2008).

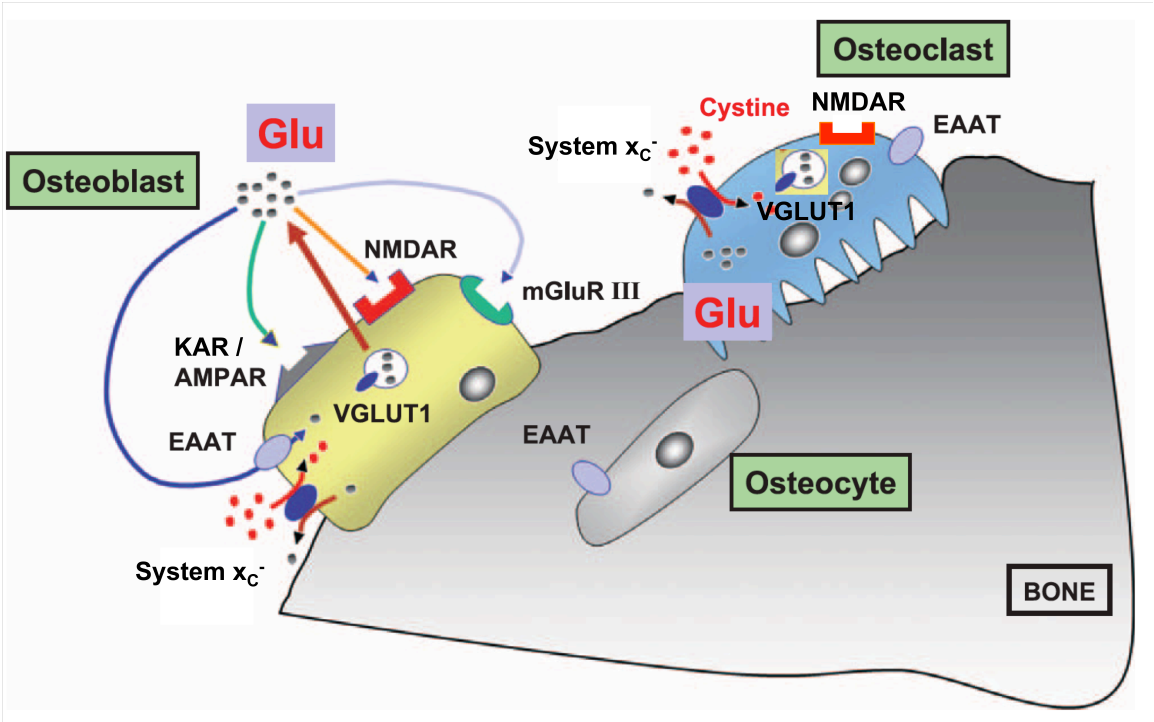

Figure 1.6 Glutamate receptors and transporters in bone. Osteocytes express the EAAT1. Osteoblasts express AMPAR, NMDAR, KAR, mGluR 4 and 8, EAAT 1, 2, and 3, VGLUT1, and system x_C^-. Osteoclasts express NMDAR, EAAT 2 and 4, VGLUT1, and system x_C^- (adapted from Hinoi et al., 2004).

A comprehensive picture of glutamate signalling in bone has yet to emerge, but individual snapshots of signalling interactions are steadily being compiled into a more cohesive whole. Early in their differentiation, NMDAR antagonism inhibits the development of both osteoblasts (Hinoi et al., 2003), and osteoclasts (Peet et al., 1999), and AMPAR inhibition has been shown to inhibit the early differentiation of osteoblasts only (Skerry, 2008). System x_C^- inhibition with SSZ was able to inhibit the early

differentiation of osteoclasts (Suematsu et al., 2007). As they differentiate, both osteoblasts (Genever & Skerry, 2001), and osteoclasts (Morimoto et al., 2006), have been demonstrated to release glutamate. In fully differentiated osteoclasts, bone resorption was reduced by NMDAR inhibition in one instance (Chenu et al., 1998), but not in another (Peet et al., 1999). NMDAR and AMPAR inhibition has also been reported to reduce the activity of mature osteoblasts (Ho et al., 2005; Lin et al., 2008). *In vivo,* infusion of AMPAR, and NMDAR inhibitors have been demonstrated to have differential growth effects on bone; however, as the inhibitors used are BBB permeable, indirect effects through CNS glutamate receptor inhibition cannot be discounted in this instance (Skerry, 2008).

Most recently, our laboratory has investigated the impact of modulating glutamatergic signalling in fully differentiated osteoclasts, and in osteoblast differentiation and activity through treatment with several glutamate transporter and NMDAR inhibitors and with the direct application of high concentrations of glutamate itself. Osteoclasts reacted only to SSZ treatment with a decrease in cell number, and to SSZ and an NMDAR inhibitor treatment with an increase in the number and size of resorption pits. Osteoblast proliferation was not impacted by any treatments, but markers of mature osteoblast activity were increased following glutamate treatment at concentrations far beyond what would cause excitotoxicity in neurons of the CNS (Seidlitz et al., 2010b). Electrophysiological investigation of the response of bone cells to glutamate has indicated that the ionotropic receptors depolarize the cell in the same rapid manner as in the CNS (Gu et al., 2002). The need for a rapid glutamatergic signalling

system in the bone is not as immediately apparent as the need for rapid signalling in the CNS. However, Skerry (2008) has pointed out the ability of bone to adjust its growth to very brief periods of stimuli including moments of high rate-of-change strain such as jumping, that would necessitate a rapid signalling mechanism. The utilization of glutamatergic signalling for the maturation and activity of bone cells allows the possibility that an unprecedented source of extracellular glutamate, as in the case of a glutamate-secreting metastasis, could directly disrupt intercellular bone cell signalling and in turn, result in the dysregulation of bone remodelling.

Bone is also densely innervated with sympathetic and sensory nerve fibres including glutamatergic neurons that may release glutamate to impact bone remodelling (Chenu, 2002). Sensory fibres in bone include A-β fibres and the recognized nociceptive A-δ and C-fibres, which all have been identified in the periosteum, as well as throughout mineralized bone and the bone marrow (Figure 1.7) (Mach et al., 2002). These fibre types have each been confirmed to express glutamate receptors whose stimulation may be involved in nociceptive signal transmission (Carlton et al., 1995; Coggeshall & Carlton, 1998).

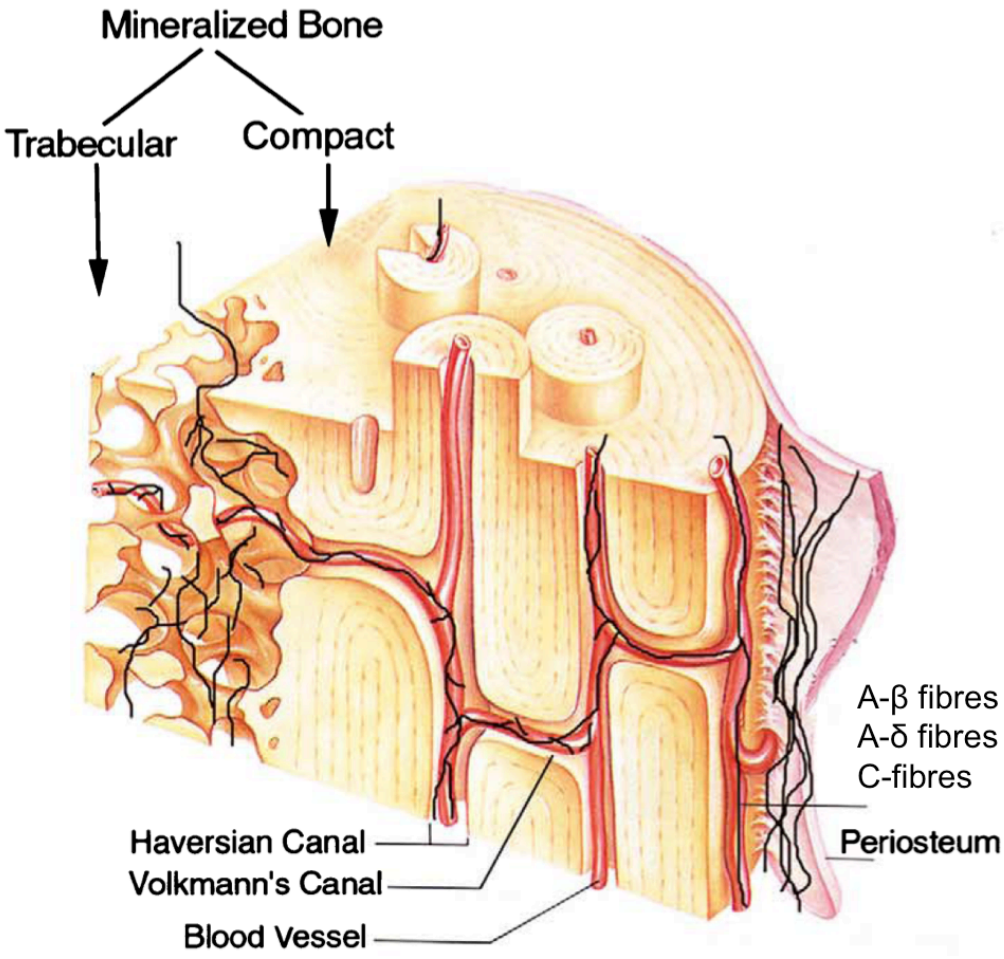

Figure 1.7 Sensory innervation throughout the periosteum, cortical and trabecular bone (adapted from Mach et al., 2002).

Cancer Metastasis to Bone

Prior to the establishment of a metastatic tumour, the primary cancer cell must first develop several qualities that allow its travel and survival in abnormal conditions beyond the original host organ. As summarized by Hanahan and Weinberg (2011), the invasion-

metastasis cascade is a highly inefficient process that consists of local tumour growth and angiogenesis followed by intravasation of cancer cells into circulation, survival until arrest in a distant tissue, extravasation through the vessel wall into the host tissue, and the colonization of that tissue with micrometastatic lesions ultimately developing into a metastatic tumour (Hanahan & Weinberg, 2011). As mentioned earlier, the host site of these metastases is not due solely to chance or proximity. It has been observed that certain cancers will preferentially metastasize to particular tissues and that this relationship is mediated by features of both the cancer cell and the secondary host. A familiar trope among the discussion of site-preferential metastatic cancers is that of the "seed and soil" from Stephen Paget's famous 1889 paper which spoke of the metastatic cell as a seed able only to grow in favourable tissue soils (Paget, 1889). The mechanisms of this soil-specificity have not been entirely elucidated; however, evidence for three methods of site-selection has been presented, each of which is independent of the rate of blood flow or the number of circulating tumour cells that pass by the site. The first is a requirement for specific growth factors exuded from the host tissue, the second is a requirement for cell adhesion molecules compatible with the tumour cell to be expressed on the endothelium of the host tissue vasculature, and the third is chemo-attraction through cytokines secreted from the host tissue into circulation (as reviewed by Liotta, 2001).

Breast cancers have a strong predilection to metastasize to bone. One factor that has been identified in this interaction is the expression on breast cancer cells of the chemokine receptors CXCR4 and CCR7, and the highest expression of their respective

ligands CXCL12 and CCL21, in the most common sites of breast cancer metastasis: the lymph nodes, lung, liver and bone marrow (Müller et al., 2001). CXCL12 is chemotactic to breast cancer cells in culture, and the inhibition of the CXCL12- CXCR4 interaction *in vivo* has reduced metastases in both breast and prostate cancer animal models (Müller et al., 2001; Sun et al., 2005). The cell adhesion molecule αvβ3 integrin is also expressed by breast cancer cells and has been shown to be particularly involved in metastases to bone (Zhao et al., 2007).

Metastatic Lesions

Bone metastases produce lesions that are most often characterized as osteolytic or osteoblastic in their effects on the host bone. Occult metastases in which there are no radiologically detectable symptoms of a lesion in bone are more rare and often difficult to detect (Vukmirovic-Popovic et al., 2002). This title designation is based on the net effect of the lesions which are most often mixed in their local effects on bone, but are predominantly either lytic or blastic (Mundy, 2002). These effects on host bone occur from the influence of tumour cells in the promotion of dysregulated intercellular signalling between bone cells, and also, in the case of lytic lesions, from the direct effects of tumour cells on mineralized bone.

Lesions of a type can often be associated with distinct cancers. Osteoblastic lesions commonly arise from prostate cancers and from ~25% of breast cancers (Mundy, 2002). Their promotion of bone formation has been associated with the production by the tumour of a number of factors secreted into the bone microenvironment. The most well-

characterized of the many associated factors is the ubiquitous growth factor endothelin-1 which has been confirmed to be expressed in osteoblastic prostate and breast cancer cell lines (Yin et al., 2003). Endothelin-1 stimulates osteoblast proliferation and activity through action on the endothelin-A receptor (Yin et al., 2003). A number of other tumour associated factors are involved in the promotion of bone volume including OPG, transforming growth factor-β (TGF-β), the serine protease urokinase, fibroblast growth factors, and possibly also prostate-specific antigen, all of which are associated with osteoblast proliferation (as reviewed by Mundy, 2002). Pathological osteoblast activity from a bone metastasis is not just the overactive production of normal mineralized woven or osteons; autopsy results have demonstrated osteoblastic lesions from prostate cancer metastases to be dysregulated and osteosclerotic (Roudier et al., 2003).

Most breast cancers produce osteolytic lesions which extensively degrade mineralized bone. Other conditions including postmenopausal osteoporosis, hormone-ablative therapies in cancer treatment, and other cancers including 95-100% of multiple myeloma are also associated with osteolysis (Coleman, 1997). The majority of this osteolytic degradation from metastatic cancer is a result of the pathological activation of osteoclasts by the tumour; however, it has also been demonstrated that tumour cells can directly resorb bone in the absence of osteoclasts. Like osteoblastic metastases, osteoclastic bone resorption is stimulated by the tumour through the release of a number of stimulatory factors that upregulate osteoclast proliferation and activity. One released factor, parathyroid hormone related peptide (PTHrP) is not identical to PTH, but they share many structural and functional similarities. At the bone, PTHrP acts similarly to

PTH to stimulate osteoclast proliferation through osteoblastic production of RANKL (Thomas et al., 1999). Treatment of tumour-bearing animals with neutralizing antibodies to PTHrP significantly reduces bone metastasis and resorption, leading the possibility that tumour-generated PTHrP is the major factor through which cancer cells stimulate osteolysis (Guise et al., 1996). However, also like PTH, PTHrP may have a dual role in bone remodelling, as its expression by prostate cancer cells has conversely been associated with the extent of osteoblastic lesions (Liao et al., 2008). Other factors either released directly or induced to be released by tumour cells include M-CSF, TGF-β, tumour necrosis factor α and β, and interleukin-1, 6, and 11 (as reviewed by Orr et al., 2000), and Jagged1 of the Notch signalling pathway (Sethi et al., 2011).

One of the roles of mineralized bone matrix is to act as a reservoir of minerals and growth factors that can be stimulated through osteoclastic bone-resorption to be re-released into circulation. Bone resorption in the event of a lytic metastasis results in the pathologic release of these same substances. Ca^{2+} release in this manner is partially responsible for the hypercalcaemia that is characteristic of bone metastases (Yates et al., 1988), and the release of both mineral and growth factor has been implicated in a positive-feedback cycle of tumour growth and bone destruction commonly referred to as the vicious cycle hypothesis. The vicious cycle consists of the release of the osteoclast stimulating factors including PTHrP from the metastatic tumour which increase bone resorption and the release of tumour stimulating cytokines and growth factors from the bone matrix that further stimulate tumour growth, which perpetuates the cycle. Factors

released from bone that stimulate tumour growth include TGF-β, insulin-like growth factor 1, and Ca^{2+} itself (as reviewed by Mundy, 2002).

Bone resorption can also occur independently of osteoclasts through the direct action of cancer cells. This ability has been demonstrated *in vitro* in several cancer types including breast (Eilon & Mundy, 1978), prostate (Sanchez-Sweatman et al., 1998), murine melanoma (Sanchez-Sweatman et al., 1997), and giant cell tumour of bone (Mak et al., 2010). MMPs secreted from these cancer cells are thought to play a significant role in this process, particularly MMP-2 and 9 (J. Lee et al., 2001), and MMP-13 (Mak et al., 2010). Inhibition of MMPs was able to reduce the ability of *in vivo* human breast cancer cells to degrade bone (J. Lee et al., 2001).

Glutamate Release in Cancer Metastases

As described earlier, the release of glutamate into the extracellular environment is a feature of several cancer cell lines. In glioma, this glutamate release *via* the system x_C^- cystine/glutamate antiporter has been confirmed to induce a disruptive influence on normal host tissue cell signalling resulting in a functional advantage to the tumour and in several pathologies common to this condition including malignancy, the excitotoxic death of neurons, and seizures (Buckingham et al., 2011; Chung et al., 2005). Our lab has discovered that glutamate is released from cancer cell types that commonly metastasize to bone also through the system x_C^- transporter (Seidlitz et al., 2009; Sharma et al., 2010). In particular, prostate and breast cancer cells were found to release glutamate *in vitro*, with the highest levels from MDA-MB-231 human breast adenocarcinoma cell line which

readily metastasizes to bone where it reliably induces osteolytic lesions (Duivenvoorden et al., 2002). It has been postulated that glutamate secreted from tumour cells may play a role in the development of this lesion and associated pathologies including severe and intractable cancer-induced bone pain (Seidlitz et al., 2010a).

Pain

Pain is defined by the International Association for the Study of Pain (IASP) as an unpleasant sensory and emotional experience associated with actual or potential tissue damage, or described in terms of such damage (Loeser & Treede, 2008). Pain is a perceptual phenomenon that is emotional and subjective, and in its entirety is difficult to study. Nociception is defined by the IASP as the neural processes of encoding and processing noxious stimuli. It is the physical process of sensation that is ultimately perceived to be painful and is not subjective. Noxious stimuli include any stimuli (mechanical, chemical or thermal) that have the potential for tissue damage, including inflammation. Nociception is not necessary for the sensation of pain, but pain is the necessary outcome of nociception. Nociceptive pain also differs from neuropathic pain which is pain arising as a direct consequence of a lesion or disease affecting the somatosensory system (Loeser & Treede, 2008). Neuropathic pain can arise as a result of sensitization through chronic nociceptive activation. Sensitization is manifested both peripherally and centrally, resulting in hyperalgesia and allodynia whereby a lower stimulus threshold triggers a nociceptive response, and a normally non-nociceptive stimulus becomes painful, respectively.

Glutamate and Pain

Glutamate plays an essential role in the induction, transmission, and modulation of nociceptive signalling. As an excitatory neurotransmitter, glutamatergic signalling has been implicated in nociceptive transmission and sensitization in the periphery and the CNS. Glutamate receptors are active along nociceptive pathways at synapses in the periphery, spinal cord and brain, and are susceptible to pharmacological intervention for the treatment of pain at each location. Glutamate contributes to the development and maintenance of central sensitization as initiated through chronic depolarization of the postsynaptic neuron through activated glutamate receptors. This in turn induces the phosphorylation of regularly dormant postsynaptic NMDARs, and the trafficking of excess AMDARs to the postsynaptic nerve terminal in a process comparable to long-term potentiation (Drdla & Sandkuhler, 2008). Glutamatergic central sensitization is well established in the spinal cord, and has also been recognized supraspinally in nociceptive regions (J. Huang et al., 2006). Peripherally, glutamate is released from afferent neurons as a component of the "inflammatory soup" of signalling molecules that mediate inflammation and peripheral sensitization (Omote et al., 1998), and as a result of nerve injury induced neuropathic pain (Jang et al., 2004). In addition to inflammatory and neuropathic states, increased extracellular glutamate is a feature of several painful human conditions including chronic myalgia (Rosendal et al., 2004), arthritis (McNearney et al., 2000), and herniated intervertebral discs (Harrington et al., 2000). During inflammation, total numbers of ionotropic glutamate receptors on sensory neurons and the proportion of

neurons bearing glutamate receptors in affected cutaneous tissue were found to increase (Carlton & Coggeshall, 1999).

Primary afferent nociceptors are directly sensitive to glutamate in the periphery. AMPARs, NMDARs, and mGluR1 and 5 have been confirmed to be expressed at the peripheral terminals of afferent neurons, and both AMPARs and NMDARs have been demonstrated to be directly involved in nociceptive signalling from noxious stimuli (Bleakman et al., 2006). The subcutaneous injection of exogenous glutamate into a rat hindpaw was able to elicit extended behavioural responses of pain from as little as 100μM (Carlton et al., 1995). This effect has been replicated in humans with the injection of glutamate into the masseter muscle that produced pain which could be controlled through the co-injection of an NMDAR antagonist (Cairns et al., 2006). The subcutaneous injection of glutamate into the human face also produced "moderate" pain, and an increase in local blood flow in a dose-dependent manner. Furthermore there was an observed sex-dependent difference in the response to glutamate induced pain, with women reporting greater pain intensity and longer pain duration than men (Gazerani et al., 2006).

The modulation of glutamatergic neurotransmission is regularly employed for analgesia in animal studies. Antagonists of NMDARs, AMPARs, and KARs have all demonstrated effectiveness in analgesia at the periphery, spinal cord, and CNS, and group I and II mGluR antagonists have demonstrated effectiveness at the spinal cord; however, this analgesia remains to be consistently seen only experimentally (as reviewed by Bleakman et al., 2006). One reason for this is likely the ubiquity of glutamatergic

signalling. NMDAR antagonists have been the subject of much clinical and preclinical study for the treatment of pain, and although there are many reports of successful patient treatment for conditions including cancer pain (with the anaesthetic NMDAR inhibitor ketamine), there are as many unsuccessful treatments and many treatments limited by severe side effects (Fundytus, 2001).

Cancer-Induced Bone Pain

Pain in metastatic cancer afflicted bone can arise from a number of stimuli and from any location within the bone. As mentioned earlier, bone is innervated with sensory and sympathetic neurons throughout the periosteum, mineralized bone and bone marrow. The common perception of disruption of the densely innervated periosteum as the principal source of cancer-induced bone pain does not account for the many painful lesions that entirely lack periosteal involvement (Sabino & Mantyh, 2005). As tumours grow in bone, the character and severity of the pain will often change over time and can be categorized based on its temporal features (onset, duration, frequency, or pattern). There are two major classes of bone pain reported by patients; ongoing or background pain and breakthrough pain. Ongoing pain is described as a dull aching sensation, constant in presentation, progressive in intensity and tending to gradually worsen as the tumours progresses. Breakthrough pain is characterized by a transient and debilitating exacerbation of sharp pain sensations (Mercadante, 1997). Breakthrough pain is so named to indicate that this type of pain can break through analgesic regimens successfully used to treat ongoing pain. This pain can arise spontaneously or as a result of an action or movement committed by the patient in which case it is labelled as incident pain. The

rapid onset and occasional unpredictability of breakthrough pain makes it difficult to control and therefore highly debilitating to the patient's functional status and quality of life (Mercadante, 1997).

Murine models have revealed that cancer-induced bone pain is a unique pain state exhibiting distinct neurochemical and cellular features in the spinal cord and dorsal root ganglia (DRG) that are not shared with inflammatory or neuropathic pain states. In particular, changes in the expression of both substance P and calcitonin gene-related peptide (CGRP) were observed in the dorsal horn of the spinal cord in both inflammatory and neuropathic models, but neither neuropeptide was altered in a bone cancer pain model. Also bone cancer pain resulted in a much greater increase in glial fibrillary acidic protein (GFAP), a marker of astrocyte proliferation and hypertrophy (Honore, Rogers, et al., 2000).

A number of factors involved in tumour metastasis, growth and lesion formation have the potential to cause pain both directly and indirectly. The confluence of algogenic substances and physical disruption of the tumour site and host tissue indicate that the mechanisms responsible for cancer-induced bone pain are heterogeneous and unlikely to be relieved through a single treatment. Also, although cancer pain tends to increase with disease advancement, pain does not correlate with the extent or type of the lesion (Mercadante, 1997).

The growing tumour itself contributes to pain generation through pressure on the periosteum or sensory nerves in bone, and through the destruction of sensory neurons.

The leading edge of tumours in bone were found to come into contact, injure and then destroy the distal processes of sensory fibres in conjunction with the development of neuropathic pain states in animal models (Peters et al., 2005). Both osteolytic and osteoblastic lesions are characterized by weaker bone that is more prone to fracture, compression, and collapse (Halvorson et al., 2006). Microfractures of the bone trabeculae and fractures of the whole bone which compress sensory neurons and distort the periosteum contribute significantly to pain if they occur (Mercadante, 1997).

The mechanisms of osteolysis itself have also been linked to cancer-induced bone pain. Inhibitors of osteoclast activity have reliably been demonstrated to limit bone pain, and the enhancement of resorption has conversely been demonstrated to increase pain, but this could be due to a number of factors (Nagae et al., 2006). As mentioned earlier, osteoclastic bone resorption is initiated through the acidification of the resorption compartment at the bone surface by V-ATPase H^+ transporters. The extracellular environment of various human tumours including breast and prostate cancers becomes progressively acidic as tumours develop (Gatenby et al., 2006). It has been proposed that this acidic microenvironment in bone following tumour growth and osteoclast upregulation may produce sufficient acid to activate the low pH receptors acid-sensing ion channel (ASIC) and transient receptor potential channel-vanilloid subfamily member 1/capsaicin receptors (TRPV1) that are present on nociceptors in bone (Yoneda et al., 2011).

Many other algogenic factors have been found to be secreted from cancer cells and associated tumour stromal cells. These include prostaglandins, bradykinin,

endothelins, tumour necrosis factor-α, interleukins-1 and 6, epidermal growth factor, TGF-β, platelet-derived growth factor, and nerve growth factor (NGF) (as reviewed by Jimenez-Andrade et al., 2010). Several of these are mediators of inflammation and inflammatory pain secreted from immune cells recruited to the tumour site. Recently, our lab characterized a rat model of cancer-induced inflammatory bone pain through the use of the preferential cyclooxygenase-2 (COX-2) enzyme inhibitor meloxicam which effectively reduced the severity of pain behaviours in tumour-bearing animals (De Ciantis et al., 2010).

NGF has been revealed to be a particularly versatile component of the induction of cancer-induced bone pain. NGF can directly activate nociceptors that bear either the tropomyosin receptor kinase (Trk) A receptor or the low-affinity neurotrophin receptor p75, both of which are found on nociceptors in bone. NGF is known to be upregulated in inflammatory pain states, and NGF-TrkA signalling is a mediator of central sensitization through action at the spinal cord and DRG (P. W. Mantyh et al., 2011). In mouse models of osteosarcoma, NGF is also responsible for the rapid neurogenesis of TrkA positive sensory and sympathetic fibres that reach a pathologic density in the periosteum never observed in animals without tumour (W. G. Mantyh et al., 2010). Antibody sequestration of tumour generated NGF has reduced both pain and evidence of neurogenesis in these models of osteosarcoma, prostate cancer, and breast cancer in bone (Bloom et al., 2011; Jimenez-Andrade et al., 2011; W. G. Mantyh et al., 2010). Apart from directly stimulating nociceptors, NGF is able to provoke pain by the development of central sensitization through transcriptional upregulation of neuropeptides and ion channels at the

DRG in nociceptors, including substance P, CGRP, and brain-derived neurotrophic factor (BDNF) (W. G. Mantyh et al., 2010). Substance P is involved in nociceptive signalling through binding the neurokinin receptor 1 (NK_1) on nociceptors. It has been found to be released in the spinal cord following noxious stimuli, and to provoke pain upon direct application intrathecally, and to play a role in the development and maintenance of central sensitization; however NK_1 antagonists as analgesics have not yet found clinical success (as reviewed by Boyce & Hill, 2004). Interestingly, substance P released from neurons in bone has more recently been found to modulate bone resorption through NK_1 receptors on osteoclasts (Liu et al., 2007). BDNF is a neurotrophin that binds the TrkB receptor, and, like NGF, also to p75. The overexpression of BDNF at the spinal cord is likewise involved in the generation of central sensitization in both inflammatory and neuropathic pain states (as reviewed by Merighi et al., 2008). Microglial production of BDNF has recently been found to be involved in the development of central sensitization in an animal model of metastatic breast cancer-induced bone pain. Treatment of these animals with a tetracycline inhibitor of microglial activation, minocycline, reduced BDNF at the dorsal horn and behavioural evidence of pain (L. N. Wang et al., 2012). Currently, a fully humanized monoclonal antibody to NGF called tanezumab that has had much success in the reduction of pain in animal models and preclinical studies is under clinical evaluation for use in a number of conditions including osteoarthritis pain, and more recently, a phase II trial for safety in treatment of bone metastases (Pfizer, 2009).

The release of glutamate from cancer cells of types that commonly metastasize to bone, and the demonstrated disruptive influence of glutamate to normal bone cell

signalling in addition to the direct sensitivity to glutamate of sensory neurons in bone demonstrates the possibility of extracellular glutamate as an additional algogenic substance in cancer metastases to bone.

Cancer-Induced Bone Pain Treatment

An impediment to the effective treatment of cancer-induced bone pain is that current standard treatments are largely based on principles developed from studies of non-cancer pain (Sabino & Mantyh, 2005). Standard treatment for progressive ongoing pain involves adherence to the WHO analgesic ladder following progression from non-opioid analgesics for mild pain through strong opioids in conjunction with non-opioids and adjuvant treatment for moderate to severe pain. Adjuvant treatments in this case are non-analgesics that modify analgesic outcomes. The use of adjuvant treatments in the management of pain is quite common, and standard treatments can include the use of antidepressants or anticonvulsants. In the treatment of cancer-induced bone pain the use of drugs that prevent osteoclastic bone resorption are widely used as adjuvants. Bisphosphonates are a class of antiresorptive compounds with a high affinity to bind Ca^{2+} and therefore to become sequestered in the Ca^{2+} rich bone matrix. When released and absorbed by osteoclasts, bisphosphonates inhibit the enzyme farnesyl diphosphate synthase which then limits the downstream ability of the cell to produce several essential GTP-binding proteins, inducing apoptosis (Rodan & Martin, 2000). This limits the extent of osteoclastic resorption in the bone and therefore limits pain from mechanical stress and osteoclast-associated algogenic factors. Bisphosphonate treatment has also been tentatively shown to reduce metastasis to bone and increase survival in breast cancer

patients without current bone metastases (Powles et al., 2006). These results have fuelled the search for drugs that, like bisphosphonates, inhibit osteoclastic bone resorption. Treatments with OPG, the decoy receptor for RANKL has successfully limited bone pain and tumour growth in animal models (Honore, Luger, et al., 2000). A fully human monoclonal antibody to RANKL, denosumab, has also been developed as a more specific inhibitor of osteoclast activity than bisphosphonates. In multiple phase III clinical trials denosumab was superior to several bisphosphonates in the prevention of skeletal related events including pain in both prostate and breast cancer patients (as reviewed by Honore, Luger, et al., 2000). The inhibition of osteoclasts appears to have several serious side effects that has limited treatment with these drugs. Bisphosphonates are associated with occasional atrial fibrillation, osteomyelitis, and more commonly, osteonecrosis of the jaw of which bisphosphonate treatment is involved in over 90% of cases (Drake et al., 2008). As expected from a slightly more effective inhibitor of osteoclasts, treatment with denosumab has a similar, but slightly higher incidence of osteonecrosis of the jaw (Brown et al., 2010). Standard treatments for cancer in bone can also have an impact on pain including radiotherapy and surgery. Both are applied palliatively with pain control as the primary intention (Clines & Guise, 2008).

Currently, μ-agonist opioids remain the gold standard for the treatment of moderate to severe cancer pain with adherence to the WHO pain ladder. Their efficacy is limited by the occurrence of severe side-effects at the doses necessary for adequate analgesia and patient quality of life suffers as a result. Adjuvant treatments are successfully utilized in cancer-induced bone pain management, but reliable pain relief in

a manner not independently detrimental to patient quality of life remains elusive. The restriction of the algogenic substance glutamate release from cancer cells in bone presents an attractive possibility for the control of pain in patients with bone metastases.

Rationale

The amino acid glutamate has been identified as an intercellular signalling molecule involved in the homeostasis of bone remodelling. Glutamate is also an algogenic compound that can directly sensitize sensory neurons resident throughout bone. Our lab has previously discovered that glutamate is released in significant quantities from cancer cell lines of types that frequently metastasize to bone. They have also identified the responsible mechanism for this release as the cystine/glutamate antiporter system x_C^-. I have predicated this project upon the rationale that the reduction of glutamate release from cancer cells through the pharmacological inhibition of system x_C^- will reduce the disruptive influence of extracellular glutamate in bone and will limit any direct stimulation of nociceptors by that free glutamate. I propose that these outcomes of limiting free glutamate in bone will reduce cancer-induced bone pain in animals with bone metastases.

Hypothesis

Pharmacological inhibition of system x_C^- will limit the release of glutamate from breast cancer cells in bone resulting in a reduction of cancer-induced bone pain in animal models (See Hypothesis Summary Figure on the following page).

Objectives

My project objectives (as presented at my initial supervisory committee meeting) were as follows:

1. To examine if mice display pain behaviours correlated with increased glutamate release from cancer in bone *in vivo*.

2. To determine if glutamate release can be attenuated with system x_C^- inhibitors *in vivo*.

3. To validate the concept that system x_C^- inhibition results in a reduction of pain behaviours in mice.

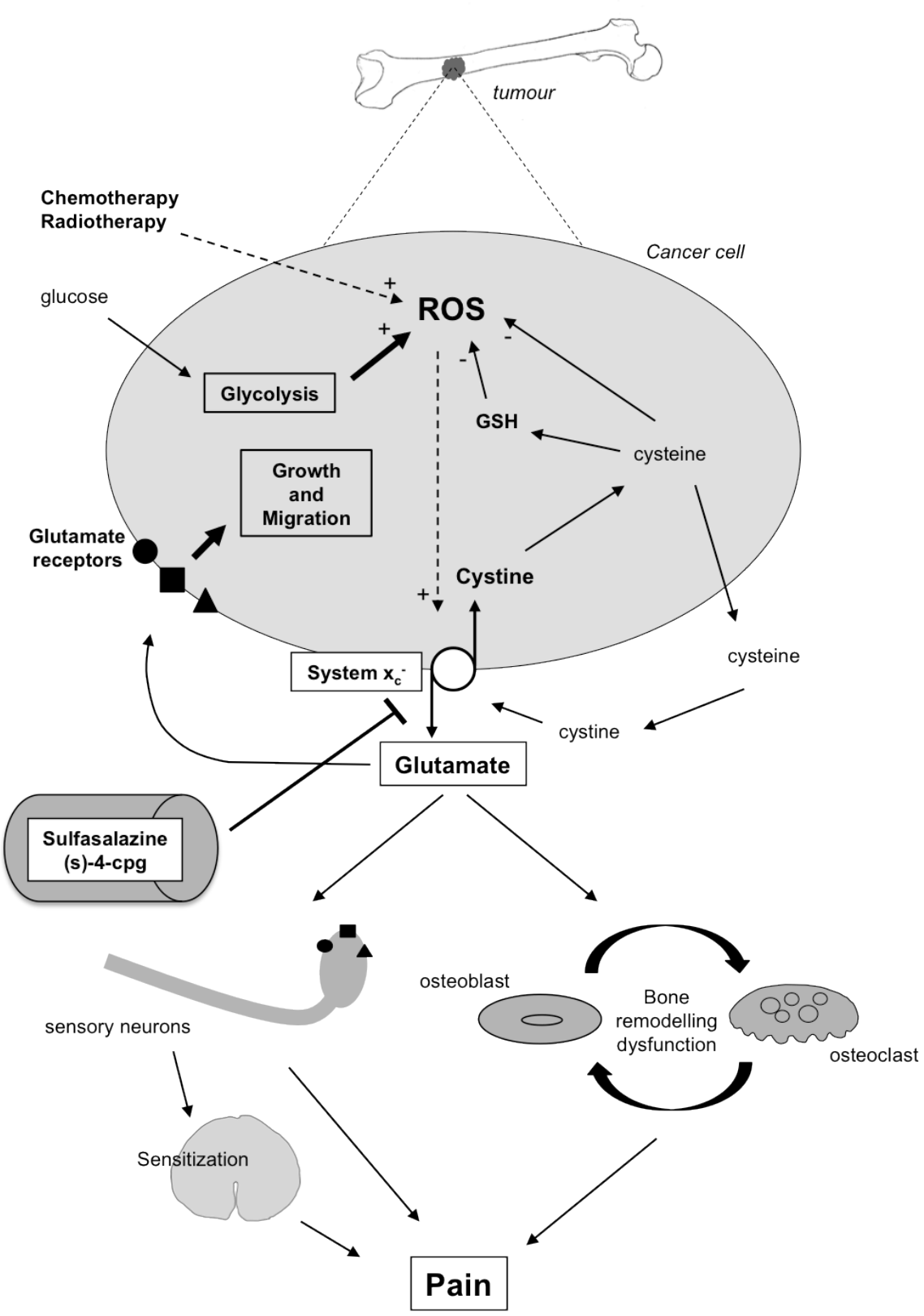
tumour
Chemotherapy
Radiotherapy
Cancer cell
glucose
ROS
Glycolysis
GSH
cysteine
Growth
and
Migration
Glutamate
receptors
Cystine
cysteine
System x_c^-
cystine
Glutamate
Sulfasalazine
(s)-4-cpg
osteoblast
Bone
remodelling
dysfunction
osteoclast
sensory neurons
Sensitization
Pain

Chapter 2: Materials and Methods

Cell Culture

The highly metastatic human breast adenocarcinoma MDA-MB-231 cell line was used in all *in vitro* and *in vivo* work. Mycoplasma free cells were obtained from American Type Culture Collection (Manassas, VA, USA). Testing for mycoplasma contamination was further performed later during the course of this project using the PlasmoTest mycoplasma detection assay kit (Invivogen, San Diego, CA, USA) to ensure cell cultures remained free of contamination.

All cells were maintained at sub-confluent densities in a humidified incubator with 5% CO_2 in room air at 37°C using Dulbecco's Modified Eagle Medium (DMEM) (Invitrogen, Burlington, ON, Canada) supplemented with 10% fetal bovine serum (FBS) and antibiotics (100 U/ml penicillin sodium and 100 μg/ml streptomycin sulfate) (Invitrogen). For the duration of all glutamate release experiments, cells were initially plated with DMEM containing FBS and incubated for 4 hours to allow cell adherence to the plate surface. The media was then aspirated and replaced with DMEM without FBS for the duration of the timed release. DMEM without supplementary FBS contains no glutamate (Invitrogen datasheet), but FBS itself contains a high and variable amount of glutamate depending on the lot. To eliminate this potential source of variance and to ease the ability of the AMPLEX Red glutamic acid kit (Invitrogen/Molecular Probes, Eugene, OR, USA) to detect small changes in secreted glutamate, it was determined that serum-

free media would be most appropriate for cultures undergoing glutamate release experiments. Eliminating exogenous glutamate from the media of cancer cells exporting glutamate by system x_C^- also limits the possibility of substrate transport inhibition through high extracellular glutamate concentrations. Antibiotic was also not used in culture during glutamate release experiments as it has been shown that β-lactam antibiotics can alter the expression of several glutamate transporters other than system x_C^- (Rothstein et al., 2005).

24 hours prior to animal model induction, the growth media of all cells to be injected was replaced with an DMEM + 20% FBS + antibiotic. This was done in order to promote cell growth and division to improve the tumour establishment success of the animal models.

Treatments

All *in vitro* and *in vivo* work was performed with treatment groups of various concentrations of the system x_C^- inhibitors SSZ (Sigma-Aldrich) and (S)-4-CPG (Tocris Bioscience, Minneapolis, MN, USA), both prepared in solution in accordance with their respective manufacturers recommendations. SSZ was prepared by dissolution in 1M NH_4OH, and (S)-4-CPG was prepared by dissolution in 1 mM NaOH.

For all *in vitro* work, the stock solutions of the drug were then added directly to culture media at the desired concentration. For all *in vivo* work, the stock solutions were added to sterile phosphate-buffered saline (PBS) at the desired concentration prior to filling the osmotic pumps used for drug delivery.

Cell Growth

Cell numbers in all experiments were quantified using the crystal violet assay as optimized for use in our lab (Seidlitz et al., 2009). This assay involves the fixation of adhered cells to their 96-well culture plate with 10% neutral buffered formalin (Fisher Scientific), followed by staining with 50 µL of 0.1% (w/v) crystal violet stain (Sigma-Aldrich, St. Louis, MO, USA) in 25% (v/v) methanol, a complete rinse in water to remove excess stain, and a re-solubilization of the crystal violet stain in 100 µL of 0.05 M sodium dihydrogen phosphate (BDH, Toronto, Ontario, Canada) in 50% ethanol. The extent of staining was read with a microplate spectrophotometer (BioTek, Winooski, VT, USA) at λ=570 nm. Crystal violet binds and stains deoxyribonucleic acid (DNA), and so the extent of staining in a culture plate indicates cell number. To establish a custom gradient of cell staining to MDA-MB-231 cell number, cells were seeded in 96-well plates at densities of 0-55,000 cells in increments of 5,000. Following a 4 hour incubation period at 37°C to allow cell adhesion, crystal violet assays were performed to generate a linear relationship of staining at known cell densities. This equation ($y = 4\times10^{-05}x + 0.024$) was used to consistently determine cell number from staining value in all further crystal violet assays. All glutamate release experiment results determined by AMPLEX Red assay were standardized to cell number through the performance of a crystal violet assay following media collection for glutamate quantification.

Glutamate Release

Glutamate release was quantified under normal conditions and in the presence of the system x_C^- inhibitors SSZ and (S)-4-CPG. All cultures were initially seeded in 96-well plates at a density of 10,000 cells/well with DMEM (10% FBS and 1% antibiotic). Following a 4 hour incubation period to allow cell adhesion, the growth media was removed and discarded, and all seeded wells were rinsed once with sterile 37°C PBS and then filled with 200 µL of 37°C DMEM without FBS or antibiotic. SSZ and (S)-4-CPG were added to the DMEM at the relevant concentrations prior to its application to the cells.

To quantify the abilities of both system x_C^- inhibitors to reduce glutamate release from MDA-MB-231 *in vitro*, dose-response curves were generated through serial dilutions of 0-640 µM for both inhibitors applied for 48 hours to 10,000 cells. Negative controls were included for both the vehicle substances and the inhibitors. Vehicle controls were provided where the same serial dilution of the respective vehicles of each inhibitor was applied to 10,000 cells. Drug controls were provided where the same drug concentrations in media were applied to wells free of cells. Following 48 hours of incubation, all media was collected independently and stored at -20°C for later glutamate quantification through the AMPLEX Red assay. All plate wells containing cells were then immediately fixed with 200 µL of 10% neutral buffered formalin and cell numbers in each well were quantified using the crystal violet assay.

Glutamate levels in culture media were quantified using the AMPLEX Red glutamic acid assay kit (Invitrogen) and analyzed on a CytoFluor Series 4000 Fluorescence Multi-Well Plate Reader (PerSeptive Biosystems, Framingham, MA, USA). The AMPLEX Red glutamic acid assay kit quantifies L-glutamate in a sample through the indirect measurement of a fluorescent product, resorufin, linked 1:1 with glutamate in the test sample. Initially, the media sample containing glutamate to be quantified is diluted with proprietary reaction buffer to a concentration that falls within the range of the fluorescence values of a standard curve of 0-25 μM glutamate. This dilution was optimized to be sample 1:2 buffer, for all 48 hour experiments. The diluted sample is then mixed in triplicate with the a reaction mixture containing 0.25 U/mL horseradish peroxidase, 0.08 U/mL L-glutamate oxidase, and 0.026 μg/μL AMPLEX Red reagent in DMSO, all diluted in reaction buffer and incubated at 37°C without added CO_2 for 30 minutes. The reaction steps proceed as follows: L-glutamate is oxidized by L-glutamate oxidase to form α-ketoglutarate, NH_4, and H_2O_2. H_2O_2 goes on to react 1:1 to form resorufin, but if amplification of the H_2O_2 signal is necessary, L-alanine and L-glutamate-pyruvate transaminase are added to the assay to transaminate the α-ketoglutarate product back to glutamate (Figure 2.1). This cycle continues multiple times to amplify the H_2O_2 signal. H_2O_2 then reacts 1:1 with the AMPLEX Red reagent in a reaction catalyzed by horseradish peroxidase to form resorufin which is the fluorescent product measurable in the CytoFluor plate reader.

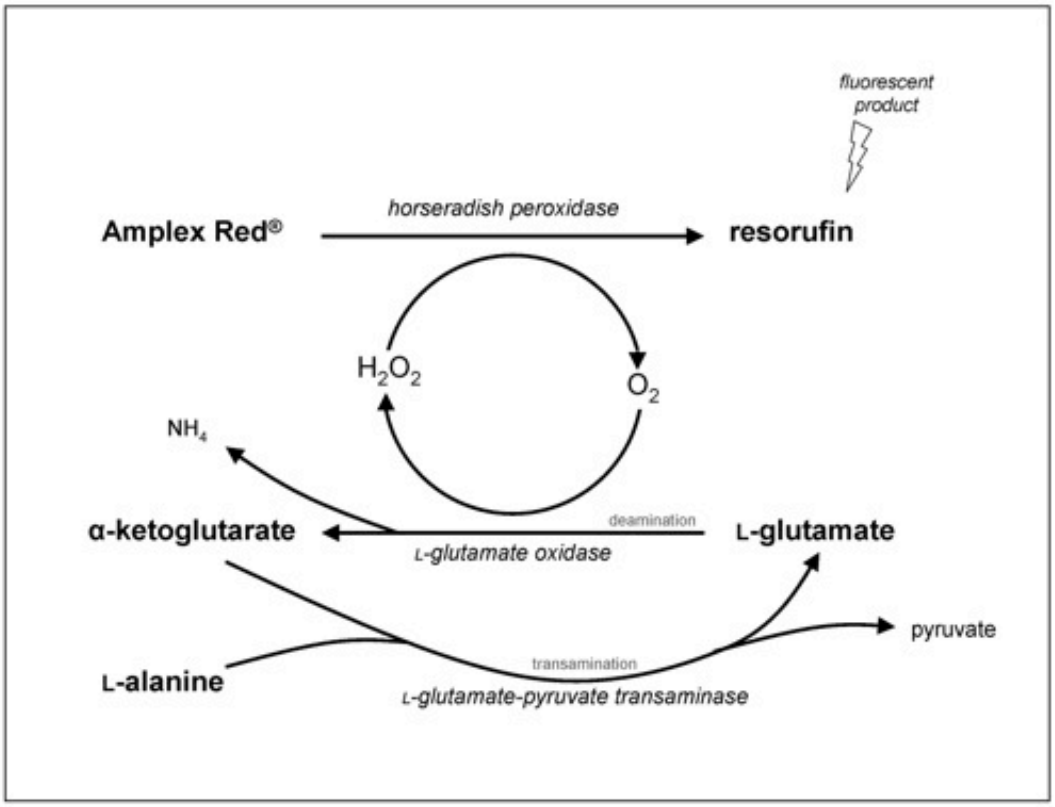

Figure 2.1 Diagrammatical representation of the AMPLEX Red conversion of L-glutamate to fluorescent resorufin measurable by fluorescence plate reader (adapted from Dr. Eric Seidlitz).

For the purposes of these experiments, the AMPLEX Red procedures were completed without the addition of L-alanine and L-glutamate pyruvate transaminase to the reaction, which are included to allow the measurement of very small (nM) amounts of glutamate through signal amplification by recycling glutamate through α-ketoglutarate. This modification was earlier developed by our lab to optimize the assay for the sensitive

measurement of glutamate concentrations above 0.5 μM as is necessary to accommodate the heavy glutamate secretion of cancer cells (Seidlitz et al., 2009). Since the fluorescence value for a set amount of glutamate was found to vary somewhat in preliminary use of the AMPLEX Red assay, a standard curve of three repeats each of L-glutamic acid (Sigma-Aldrich) in ddH_2O at 0, 1, 5, 10, 15, 20, and 25 μM was included with each assay plate to provide a reference to a known quantity of glutamate that would not vary with any inconsistencies between repeats of the assay. The resulting linear equations were used to plot the fluorescence values of the samples to generate a corresponding glutamate amount for each. All absolute glutamate amounts were then standardized to cell number as determined by the crystal violet assay.

Animal Model

All protocols for animal studies were reviewed and approved by the Animal Research Ethics Board of McMaster University, Hamilton, ON, Canada, and adhered to the guidelines of the Canadian Council on Animal Care. Relevant Animal Use Protocols are 08-06-20 and 11-60-29.

A xenograft animal model of cancer-induced bone pain was developed for this project. The MDA-MB-231 cell line was chosen as the most appropriate for the model as it is a highly metastatic human breast adenocarcinoma and thus representative of a large segment of painful human bone metastases. MDA-MB-231 cells also were found to have the highest rate of glutamate secretion of a panel of cell lines and to secrete most of it through the targetable system x_C^- transporter (Sharma et al., 2010). MDA-MB-231 were

also found to retain xCT expression when growing *in vivo* in animal bone (Seidlitz et al., 2009). Immunodeficient mice were needed so as to not reject a xenograft injection. Balb/c nu/nu mice lack a thymus and therefore cannot produce mature T cells or recognize and reject a xenograft. 4-6 week-old female inbred Balb/c nu/nu mice (Charles River, St. Constant, QC, Canada) were chosen as this lab has experience using them in intracardiac injection models of cancer metastasis (Duivenvoorden et al., 2002; Seidlitz et al., 2009). Food and water were provided *ad libitum*.

Model Induction

Mice were obtained at 4-6 weeks old, and following a mandatory week of solitary acclimation to the animal facilities, they were exposed to human handling and the behavioural testing equipment daily for another ~1 week acclimation period, and assigned individual identification. Three days prior to cell implantation, mice were anaesthetized by isoflurane inhalation and 21 day-release pellets containing 0.25 mg of 17β-estradiol (Innovative Research of America, Sarasota, FL, USA), were implanted in each animal subcutaneously. Although MDA-MB-231 are estrogen receptor negative, estrogen receptors are found throughout bone and play a role in the regulation of bone remodelling (Bord et al., 2001). In experiments done previously in this lab, it was found that 17β-estradiol pellets implanted prior to cancer cell inoculation improved the consistency of tumour growth in bone; however, the exact mechanisms for this growth effect have not yet been isolated.

Cell harvesting was performed on sub-confluent cultures and adherent cells were suspended and kept lightly agitated in sterile PBS at a density of 10^6 cells/ 50 μL.

Mice were anaesthetized by isoflurane inhalation and injected subcutaneously with 0.05 mL 1:10 temgesic buprenorphine analgesic (Schering-Plough, Welwyn Garden City, Hertfordshire, UK). 10^6 MDA-MB-231 cells in 50 μL sterile PBS were percutaneously injected intrafemorally into the right distal epiphysis of the femur of all mice. The contralateral hind limb of each animal served as a negative control specific to each animal. One animal was randomly selected using a random number generator (random.org, Dublin, Ireland) for a sham injection of 50 μL sterile PBS only to mimic the disruption of the surgery but not the disruption of the tumour. To minimize necessary tissue damage and resulting pain from surgery, mice were laid supine while the ipsilateral knee is held bent at ~90°, allowing clearance of the patella. A $26^1/_4$ gauge needle is then placed between the medial and lateral condyles of the distal epiphysis parallel to the length of the femur and rotated manually to penetrate the cortical bone and enter the epiphysis. The cell solution is then slowly injected into the bone and the needle is gently removed. No plug is required as is utilized in other intrafemoral osteosarcoma models (Honore, Luger, et al., 2000), as tumour invasion into the periosteum and beyond the confines of the bone more closely mimics a metastasis. This method of intrafemoral injection results in a small hole and little damage to the surrounding tissues, and was used successfully in a rat model in this lab (De Ciantis et al., 2010).

On day 14 following model induction, the animals were randomized into either the treatment or control arm of the study using a random number generator and test substances in osmotic delivery pumps were implanted intraperitoneally. The treatment groups consisted of either SSZ or (S)-4-CPG treatment, and the control groups were the respective vehicle of each treatment, NH_4OH or NaOH, at the same concentration in sterile PBS as the treatment drugs. The drug dosage was rationally selected based on the results of the initial dose-response work with each inhibitor in MDA-MB-231, and the available literature regarding safety and methods of treatment in humans and animals. Both doses were selected to be within the range of clinical possibility. Each dose was selected based on their dose response curves to be at minimum the 50% inhibitory dose of each inhibitor based on glutamate secretion if this could be achieved without more than a 50% decline in cell growth as was achievable for both chosen inhibitors. It was also ensured that a margin for error was included with *in vivo* drug treatment to account for the likelihood that not all the drug would reach its molecular target in the cancer cell. As such, both drugs at the selected doses could withstand more than a 50% failure to attain their target without a large change in efficacy as measured *in vitro*. As SSZ is an approved drug with a known safety profile in humans, the maximum soluble dose was chosen that could be delivered with the osmotic pumps. This dose would circulate at 165.66 μM in the mice which in MDA-MB-231 dose response would allow the release of ~6 μM glutamate/10,000 cells over 48 hours. In a 20g mouse this SSZ dose is 6.6 mg/kg/day. (S)-4-CPG was calculated to circulate at 20 μM in mice which in MDA-MB-231 dose response would allow the release of ~11 μM glutamate/10,000 cells over 48

hours, which was nearly the maximum inhibition/cell achievable with this drug. In a 20g mouse this (S)-4-CPG dose is 0.4 mg/kg/day. (See Results, Figures 3.1, 3.2 for glutamate release data). The restriction of both of these inhibitors to doses that do not significantly affect cell growth allows the isolation of the effect of treatment on glutamate release rather that compounding these effects with a drug-induced reduction in tumour cell number or size.

Drugs were delivered with intraperitoneal Alzet model 1004 mini-osmotic pumps (Durect, Cupertino, CA, USA), which were implanted intraperitoneally on day 14 post-model induction and have the capacity to release 0.11 μL/hour for 28 days. These pumps operate through the expansion of a "salt sleeve" with high osmolality and a semi permeable membrane to the exterior of the pump. As fluid is drawn into the salt sleeve, the resulting expansion compresses an impermeable inner reservoir filled with the test substance which forces the release of that substance through a metal delivery portal (Alzet, 2008). Implantation on day 14 allows sufficient time for the implanted cancer cells to reliably establish a tumour in bone without any drug interference, and more accurately replicates a human cancer treatment model. Filling and implantation of the osmotic pumps was performed in accordance with the manufacturer's specifications and the vehicles used for drug delivery were listed as compatible with the pump delivery mechanism. Prior to surgery, animals were anaesthetized by isoflurane inhalation and were administered 0.5 mL sterile 0.9% saline subcutaneously. Following implantation the peritoneum was sutured with dissolving thread separately from the skin.

All animals were sacrificed between days 36-46 post model induction as necessary by their variable achievement of ethical endpoints. Following sacrifice by CO_2, high resolution radiographic scans of all mice in the prone position were taken with a Faxitron X-ray system MX-20 (Faxitron X-ray Co., Wheeling, IL) on Kodak MIN-R 2000 Mammography Film (Eastman Kodak, Rochester, NY, USA). The ipsilateral and contralateral tibia, fibula, femur, and some surrounding tissue were then dissected and fixed in 2.5% buffered glutaraldehyde solution for 48 hours. The use of glutaraldehyde as a fixative was necessitated to fix glutamate for immunological detection as a glutaraldehyde-glutamate hapten. Following fixation, bone samples were immersed in an agitated 10% EDTA, 4% Formalin buffered solution for decalcification. This process was completed over several weeks with weekly changes of the decalcification solution. All fixed and decalcified tissues were embedded in paraffin blocks to be sectioned for histological staining.

Behavioural Analysis

Behavioural testing was performed for a minimum of five days prior to model induction to obtain baseline data, and three days a week on alternate weekdays beginning on day 1 following model induction and continuing until endpoint. The tests performed include one test for spontaneous pain behaviours, the Dynamic Weight Bearing system (DWB) (BioSeb, Vitrolles, France), and one test for elicited pain behaviours, the Dynamic Plantar Aesthesiometer (DPA) (Ugo Basile, Comerio, Italy).

Dynamic Weight Bearing

The DWB machine allows the recording of weight and time distribution between all points of pressure of freely moving animals. It consists of an enclosed digital recording floor pad in a chamber into which the mouse is placed and a video camera to record the animal's position in the chamber in time with the sensor. The sensory pad in the testing chamber is connected *via* custom interface to a computer for direct capture of the data at a sampling rate of 10 Hz. The advantage of this system over a classical incapacitance device is that it requires no forced restraint of the animal, theoretically limiting stress and allowing a true recording of the animal's posture. The digital recordings from this machine are manually validated with the provided software to allocate the pressure point recordings to their corresponding anatomy on the mouse and to specify the parameters of which moments of capture to include in data analysis. Animals were placed in the testing chamber for seven minutes total over each test. The first two minutes were an acclimation period to eliminate any excited behaviour from the test data, and the final five minutes were recorded and saved.

Weight bearing as measured by the DWB was expressed as a mean weight at a given moment across that five minute capture period for each point of pressure. Postural disequilibrium of the animal could indicate an allodynic response to normal ambulation, and so a reduction in weight bearing by the tumour-afflicted limb of the animal was accepted as evidence of an inability or aversion to utilize that limb and therefore as indirect evidence of pain. To account for the characteristic weight gain of all mice over the testing period and for the accommodation of weight bearing shifted from the tumour-

afflicted limb to all other points of the animal's weight bearing (contralateral hind paw, forepaws, tail, thorax, and abdomen), weight bearing for all points of the animal was expressed as a single measurement of the mean weight borne by the tumour afflicted paw as a percentage of mean total weight bearing of an animal on a given day.

The DWB machine is a relatively new introduction to the arsenal of behavioural research, and as such there is little precedent for the presentation of the resulting data. The expression of ipsilateral limb weight bearing as a percentage of total animal weight; however, has been utilized in two instances of DWB presentation (Dore-Savard et al., 2010; Tetreault et al., 2011), although this data was not standardized to baseline measurements.

To account for any predisposition of the animals to favour particular limbs under normal conditions, as could be expected from evidence of motor laterality in mice (Roubertoux et al., 2003), behavioural results were expressed as a percentage of the animal's baseline scores that were recorded prior to tumour cell injection. Specifically, each day's weight bearing score was expressed as a percentage of the mean of all corresponding baseline scores for that animal. Standardization to baseline values is a common practice in the reporting of behavioural results (Gabriel et al., 2009). This method of standardizing to baseline was also applied to all measurements with the DPA.

Dynamic Plantar Aesthesiometer

The DPA machine measures the threshold force and time to paw withdrawal from a mechanical stimulus to the plantar surface of the animal paw. It consists of an

automated metal filament that is raised by an electrical actuator. The raising action is adjustable to maximum force and ramp speed. The animals are placed in individual chambers with a wire mesh floor elevated above the DPA. When the DPA filament is raised below the plantar surface of an animal's paw the threshold force and time required until paw withdrawal is recorded. The DPA is designed as an automated version of the von Frey hair assessment which measures mechanical allodynia and hyperalgesia. It is intended to reduce subjectivity in testing by way of a constant rate of change of force at the animal paw that cannot be repeated with manual von Frey hairs. DPA testing was performed six times at each of the hind paws of all animals on each testing day. Animals were first given a minimum of five minutes to acclimate in the testing chambers prior to any stimulation.

Threshold force at paw withdrawal as measured by the DPA was expressed as the mean force of six measurements each testing day. A reduction in force withstood by the tumour-afflicted limb of the animal was accepted as evidence of increased sensitivity, both allodynia and hyperalgesia, in that limb manifested as a reflexive or desired withdrawal from stimulus, and therefore as indirect evidence of pain. DPA data is presented for the tumour bearing ipsilateral hindlimb only. Unlike the DWB which measures compensation by other pressure points of the mouse, the isolation of the ipsilateral limb is appropriate in this instance as the measurements of the DPA are not captured simultaneously for both legs, making indications of compensation a less valid measurement than with the DWB. Like the DWB results, all DPA measurements are presented as a percentage of the animal's baseline scores that were recorded prior to

tumour cell injection. This method of data analysis is maintained here again to account for any predisposition of the animals to favour particular limbs under normal conditions.

For all methods of comparison, behavioural results were included only from animals that successfully developed a tumour visible by radiograph. This was done to remove any interference from animals that were not successful tumour models and therefore would not exhibit relevant behaviour. As vehicle groups of the delivery solutions of each drug (1M NH_4OH and 100 μM NaOH diluted in PBS equivalent to drug volumes) did not differ from one another in any measurements of glutamate release, cell survival, or behavioural evidence of pain (See Results, Figure 3.3 for glutamate release data), it was determined that neither substance had an effect on all measured outcomes and it therefore became appropriate to include both vehicle-substances as a single vehicle treatment (drug control) group. The final group numbers of successful tumour models were: (SSZ): n=11; ((S)-4-CPG): n=12; (All Vehicles): n=14; (Sham injection): n=1. All weight bearing and threshold force behavioural data are presented until day 36, past which the n of all groups was decreased due to differential animal achievement of ethical endpoint. All 70% pain threshold data include all data for all tumour-bearing animals until individual endpoint.

Radiograph Lesion Scoring

The extent of osteolytic lesions in the ipsilateral femurs as imaged as a loss of bone density by post-mortem radiograph was scored using a custom four point (0-3) scale of bone destruction similar to other scoring systems of the extent of tumour in bone (Mann

et al., 2008; Schwei et al., 1999). The scale designations are as follows: (0) Normal bone, no visible lesion; (1) minor loss of bone density, minimal lesion; (2) Moderate to substantial loss of bone density, lesion limited to bone trabecula and cortex; (3) substantial loss of bone density, lesion includes clear periosteal involvement or fracture. (Figure 2.2). This scoring was performed for all mice.

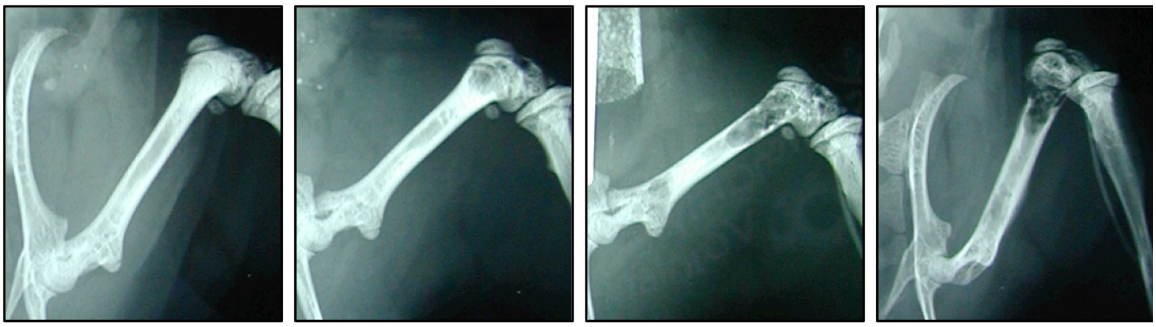

Figure 2.2 Quantification of bone osteolysis in the ipsilateral femurs at endpoint of all cancer cell injected animals on a 0-3 numerical scale. These images are examples of each stage of bone destruction as quantified by this scale. Numbers are to represent: (0) Normal bone, no visible lesion; (1) minor loss of bone density, minimal lesion; (2) Moderate to substantial loss of bone density, lesion limited to bone trabecula and cortex; (3) substantial loss of bone density, lesion includes clear periosteal involvement or fracture.

Histochemistry

Haematoxylin and eosin staining of model animal hindlimbs was undertaken to determine the extent of tumour invasion in injected bone and the surrounding tissues. Paraffin-embedded tissue samples were sliced to a thickness of 4 μm and mounted on glass slides and baked at 70°C for 20–30 minutes prior to haematoxylin and eosin staining. Cool slides were deparaffinized and rehydrated in multiple washes of xylene, ethanol and dH_2O, and then stained in Gill #3 Haematoxylin (Sigma-Aldrich) diluted 1:2 with dH_2O for 3 minutes, followed by two dH_2O rinses and ten seconds in alkaline lithium carbonate to induce the colour change of the haematoxylin stain. Slides were then stained for 45 seconds in 1% eosin diluted 1:3 in 80% ethanol. Following staining, slides were dehydrated in several washes each of ethanol and xylene and coverslipped with xylene miscible permount (Fisher Scientific, Pittsburgh, PA, USA) for visualization with light microscopy.

Glutamate Immunohistochemistry

Immunostaining for glutamate was undertaken to determine sources of glutamate in mouse bone *in vivo* and to determine if SSZ and (S)-4-CPG treatment had any visible effect on glutamate levels in the tumour and in the peritumoural environment in bone. Immunohistochemistry for L-glutamate was performed using a rabbit anti-glutamate polyclonal antibody, AB5018 (Millipore, Billerica, MA, USA). This antibody binds glutamate as a hapten fixed with glutaraldehyde. To produce these haptens, tissue fixation in glutaraldehyde was necessary and applied to all dissected tissues. 4 μm thick

sections on glass slides were baked at 60°C for 2-4 hours, then deparaffinized and rehydrated in multiple washes of xylene, ethanol, and a heated citrate buffer for heat-induced epitope retrieval. Slides were blocked for endogenous peroxidase activity by incubation with 3% hydrogen peroxide for 15 minutes, rinsed with dH_2O and Tris-buffered saline (TBS), and blocked with 3% normal goat serum in TBS for 45 minutes. Primary antibody in 1% normal goat serum and 1% normal goat serum only as a negative control was applied to the slides and left for 12 hours at 4°C. Mouse brain tissue slices were used as positive control. The slides were then rinsed in TBS and secondary biotinylated anti-rabbit immunoglobulin (Sigma-Aldrich) was applied for 30 minutes and then rinsed with TBS. A Vectastain Elite ABC kit (Vector Laboratories; Burlingame, CA, USA) was then applied for 30 minutes to conjugate an avidin-perioxidase to the biotinylated secondary antibody, followed use of a NovaRED substrate kit for peroxidase SK-4800 (Vector Laboratories) for ~5 minutes at room temperature to generate a peroxidase-activated visible colour product. If necessary, slides were counterstained in haematoxylin diluted 1:2 with dH_2O for two minutes followed by a rinse in lukewarm water. Following staining, slides were dehydrated in several washes each of ethanol and xylene and coverslipped with xylene miscible permount for visualization with light microscopy.

Glutamate Stain Scoring

Tissues stained for glutamate in the above manner were photographed and examined for evidence of glutamate in tumour-bearing bone. A qualitative three point (1-3) scale was devised for the comparison of tumours between treatment groups, based on

the extent of the anti-glutamate staining in non-haematoxylin counterstained samples in the tumour near an interface with bone. Since all tumours displayed some staining for glutamate, the scale designations are as follows: (1): mild glutamate staining; (2): moderate glutamate staining; (3): heavy glutamate staining (Figure 2.3). To maintain consistency between samples, all photographs were taken at 100× magnification and included tumour as near to the distal metaphysis of the femur as possible. The scale was also necessarily unique for each batch of immunostaining, as different batches would often exhibit differential background staining that precluded individual stain comparison between batches.

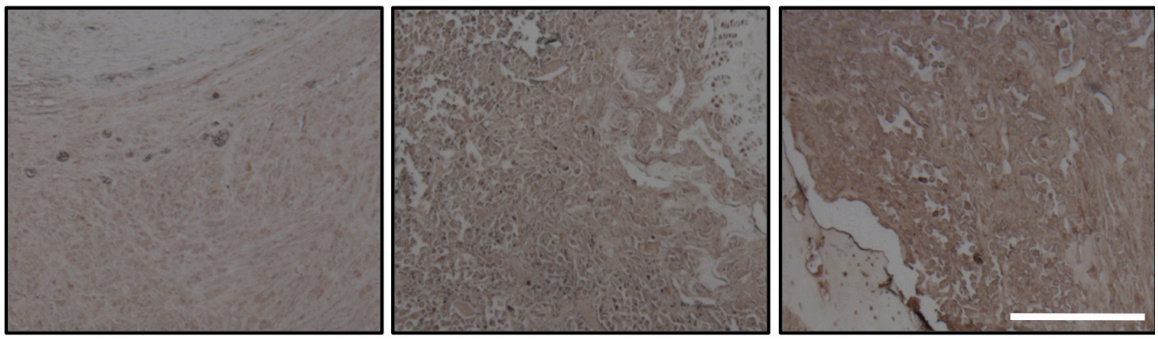

1 2 3

Figure 2.3 Comparison of glutamate staining in tumours in bone on a 1-3 numerical scale. These images are examples of each stage of tumour glutamate staining within a single batch of stained slides. Numbers are to represent: (1): mild glutamate staining; (2): moderate glutamate staining; (3): heavy glutamate staining. Scale bar = 100 μm.

Statistical Analysis

All behavioural data has been confirmed for normal distribution and was analyzed across treatment groups with one-way repeated-measures ANOVA followed by Bonferonni post hoc test. Behavioural treatment effects between groups were calculated from the segment of the curve past day 20 to limit the effect of the long period of minimal tumour growth and surgical interference on the treatment effect. The 70% threshold pain data was plotted as a survival curve, and comparisons between curves were made through logrank tests. All *in vitro* work was analyzed with one-way ANOVA followed by Bonferonni post hoc test where indicated. The significance level was set at $P < 0.05$.

All data are presented as mean ± the standard error of the mean (SEM). GraphPad Prism software version 4.0c for Macintosh (GraphPad Software, Inc., La Jolla, CA, USA) was used for all graphing and statistical analyses.

A retroactive power analysis was performed according to the guidelines for two-group repeated-measures comparisons by Rochon (1991) with a type II error (β=20%), and a type I error (α=5%). This was undertaken to identify the minimum effect size discernible from the sample size of this project (Rochon, 1991).

Chapter 3: Results

Inhibitor Dose Response

Both SSZ and (S)-4-CPG inhibited the release of glutamate from MDA-MB-231 cells in a dose-dependent manner. This was expected as both drugs are potent inhibitors of system x_C^- which was previously found to be expressed on MDA-MB-231 cells; however, the extent and pattern of system x_C^- inhibition with respect to glutamate release was unknown, including the degree of glutamate that may be secreted by other transporters. In serial dose responses of each drug from 0-640 μM on 10,000 cells over 48 hours, (S)-4-CPG was found to be the more effective inhibitor at low doses (0-40 μM), while SSZ effectiveness surpassed the efficacy of (S)-4-CPG at all doses above 40 μM (Figure 3.1). This effect was sustained when absolute glutamate released from all cells was standardized to cell number (Figure 3.2). (S)-4-CPG also demonstrated a lower limit of inhibition at ~11 μM/10,000 cells which was nearly achieved at the lowest dose above control of 10 μM of drug. The glutamate secretion inhibition of SSZ did not level off, both absolute glutamate in the media and glutamate/10,000 cells continued to decline at the highest doses. Negative controls of no cells for all treatments had glutamate levels below the reliable detection level of the assay, but this indicated no fluorescence interference from the test chemicals with the AMPLEX Red assay. Controls for the vehicle substances used to solubilize each drug were also tested for any glutamate secretion inhibition effect on cells to ensure the dose-response results were a result of

drug treatment, rather than an artefact of the vehicle substances. Vehicle substances were tested at the highest dose of the serial dose response (Figure 3.3).

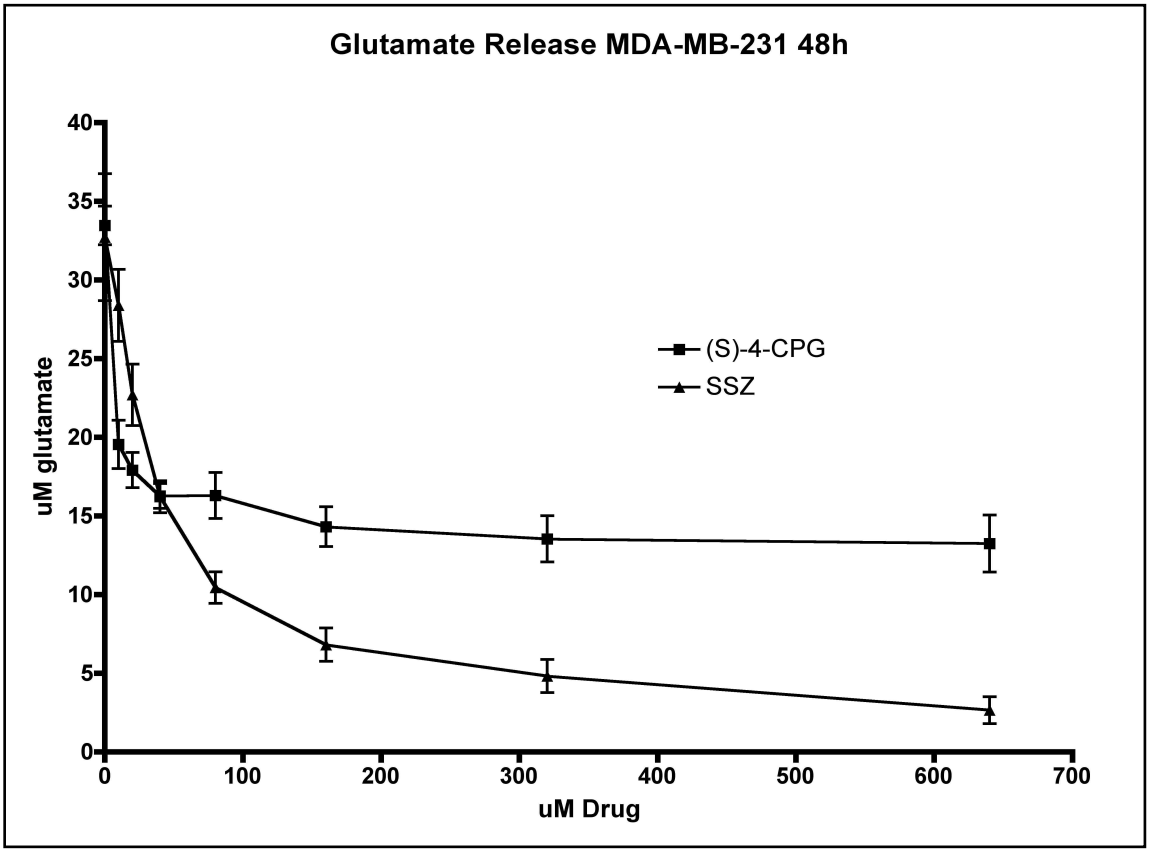

Figure 3.1 Absolute glutamate release in media from 10,000 seeded MDA-MB-231 over 48 hours at concentrations of SSZ and (S)-4-CPG between 0-640 μM. Both inhibitors exhibited a strong dose-response relationship. While (S)-4-CPG was the more effective inhibitor of glutamate secretion at concentrations below 40 μM, SSZ was more effective at doses above 40 μM. The absolute glutamate release of all cells as represented here is the most accurate *in vitro* demonstration of the glutamate release of tumour cells treated with SSZ and (S)-4-CPG *in vivo.*

Data are expressed as the mean of n=3 experiments ± the standard error of the mean (SEM).

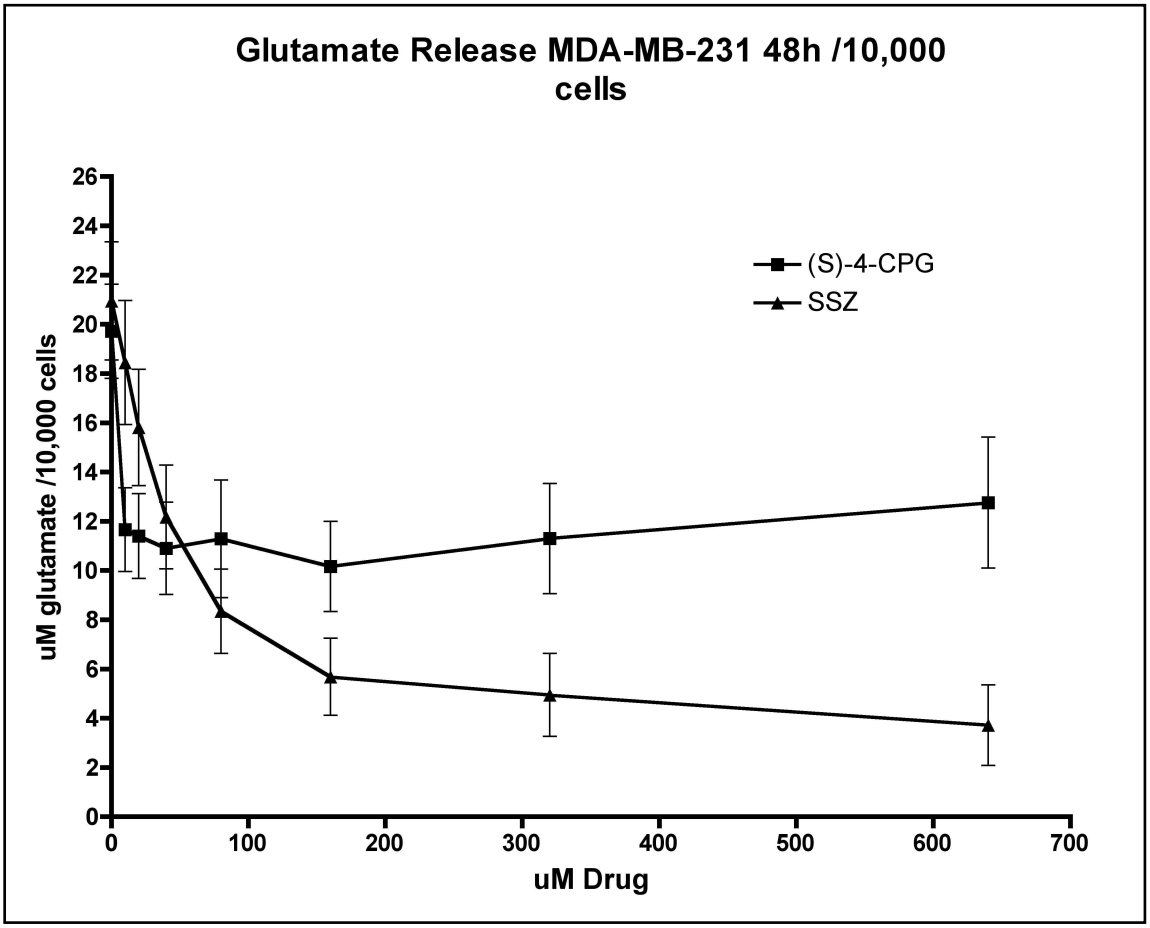

Figure 3.2 Glutamate release standardized to cell number and expressed per 10,000 cells in media from 10,000 seeded MDA-MB-231 over 48 hours at concentrations of SSZ and (S)-4-CPG between 0-640 μM. Both inhibitors maintained the strong dose-response relationship observed without standardization to cell number. While (S)-4-CPG was the more effective inhibitor of glutamate secretion at concentrations below 40 μM, SSZ was more effective at doses above

40 μM. Data are expressed as the mean of n=3 experiments ± the standard error of the mean (SEM).

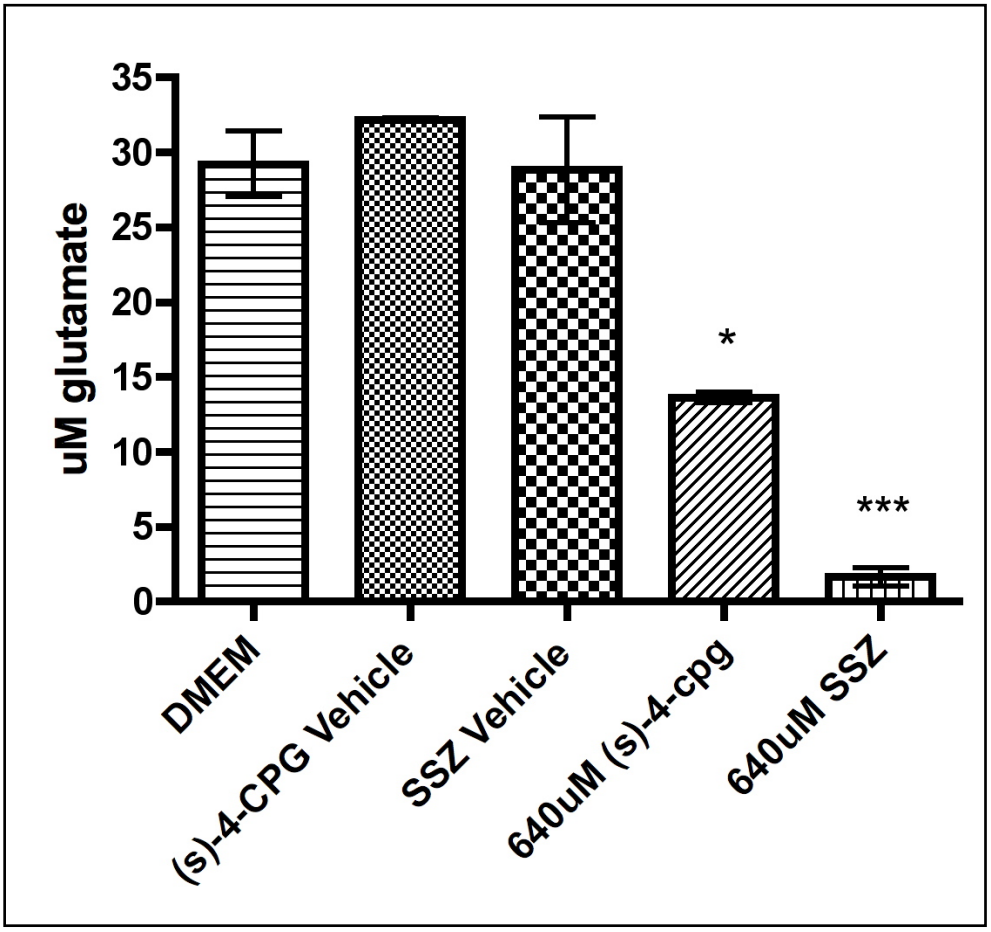

Figure 3.3 Absolute glutamate release in media from 10,000 seeded MDA-MB-231 over 48 hours in cells treated with: DMEM only (untreated), 640 μM SSZ, 640 μM (S)-4-CPG, and the respective dissolution vehicles for each drug at the equal volume and concentration to the 640 μM drug dose. This determined the absence of effect on glutamate secretion of either drug vehicle at the highest dose examined in all *in vitro* work. Data are expressed as the mean of n=3 experiments

± the standard error of the mean (SEM). Data was analyzed by one-way ANOVA followed by Bonferonni post hoc test. Significance is expressed in comparison to the DMEM only group 640 μM (S)-4-CPG $p<0.05$, 640 μM SSZ $p<0.001$.

The pattern of glutamate release in response to a single dose of SSZ and (S)-4-CPG over time was determined through a time-course release over 72 hours (Figure 3.4). This was necessary to determine the stability and pattern of each inhibitor's glutamate release inhibition over time. Transient inhibition where the glutamate secretion ability of the cells recovered quickly after an initial setback would have limited the desirability for use of that compound *in vivo*.

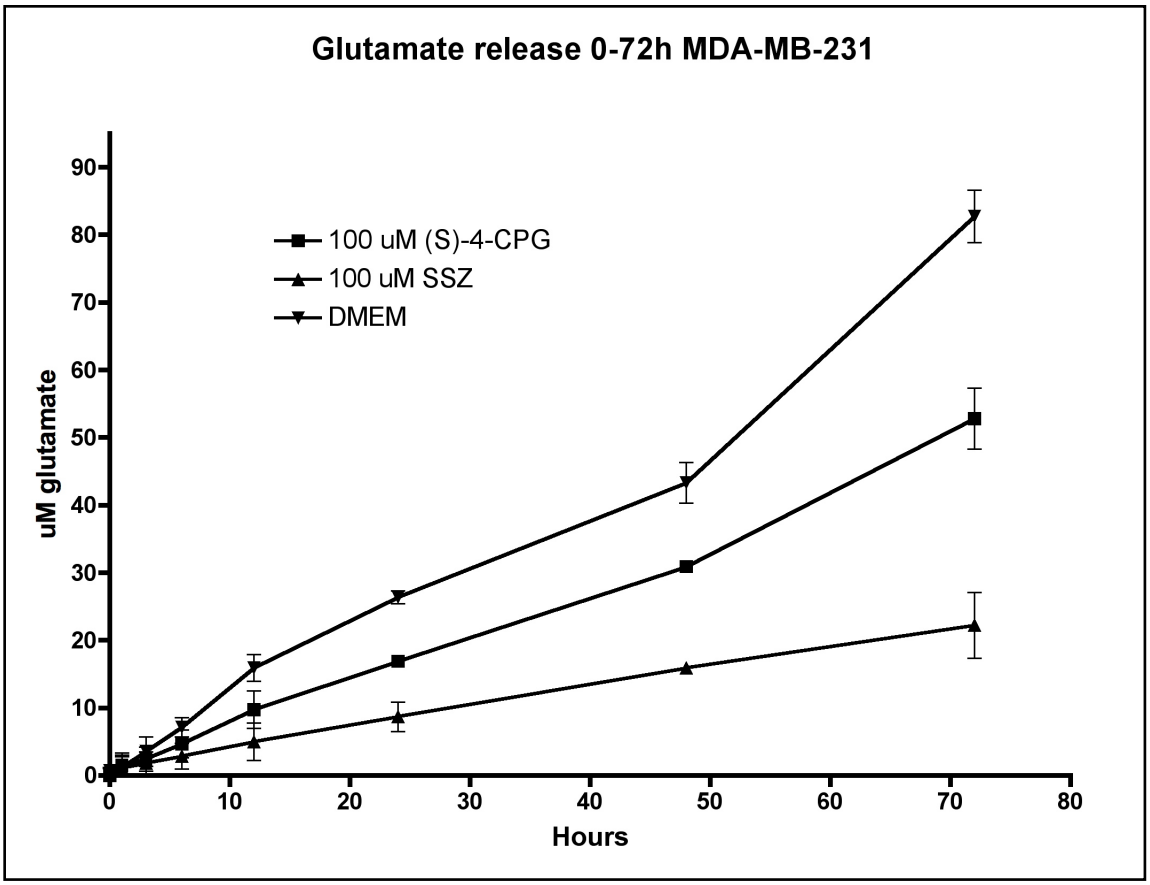

Figure 3.4 Absolute glutamate release in media from 10,000 seeded MDA-MB-231 in three groups: DMEM only (no treatment), 100 μM SSZ and 100 μM (S)-4-CPG. Measurements were taken at time points between 0-72 hours. This demonstrates the stability of the glutamate release inhibition of both drugs with an unreplenished single dose. Data are expressed as the mean of n=3 experiments ± the standard error of the mean (SEM).

Cell growth in response to both SSZ and (S)-4-CPG 0-640 μM dose ranges at 48 hours was nearly identical between groups as measured by crystal violet assay post media

collection (Figure 3.5). Normal MDA-MB-231 grown in DMEM + 10% FBS were observed to grow at a much faster rate than cells without added FBS. This similarity between treatment groups of cell number following 48 hours is in contrast to the differential abilities of SSZ and (S)-4-CPG to inhibit glutamate secretion from these cells. All wells were initially seeded with 10,000 cells, and all cells but the highest dose (640 μM) still allowed an increase in cell number over 48 hours. This is an essential feature of both inhibitors when used *in vivo*. A severe decrease in cell number *in vitro* would indicate a mortality effect on MDA-MB-231 that could limit the success rates of the animal bone tumour model, and would certainly contaminate any behavioural effects of drug treatment with decreased tumour size. The choice of SSZ and (S)-4-CPG doses for *in vivo* use that did not significantly affect cell survival isolates any observed behavioural drug-effects to the inhibition of glutamate secretion.

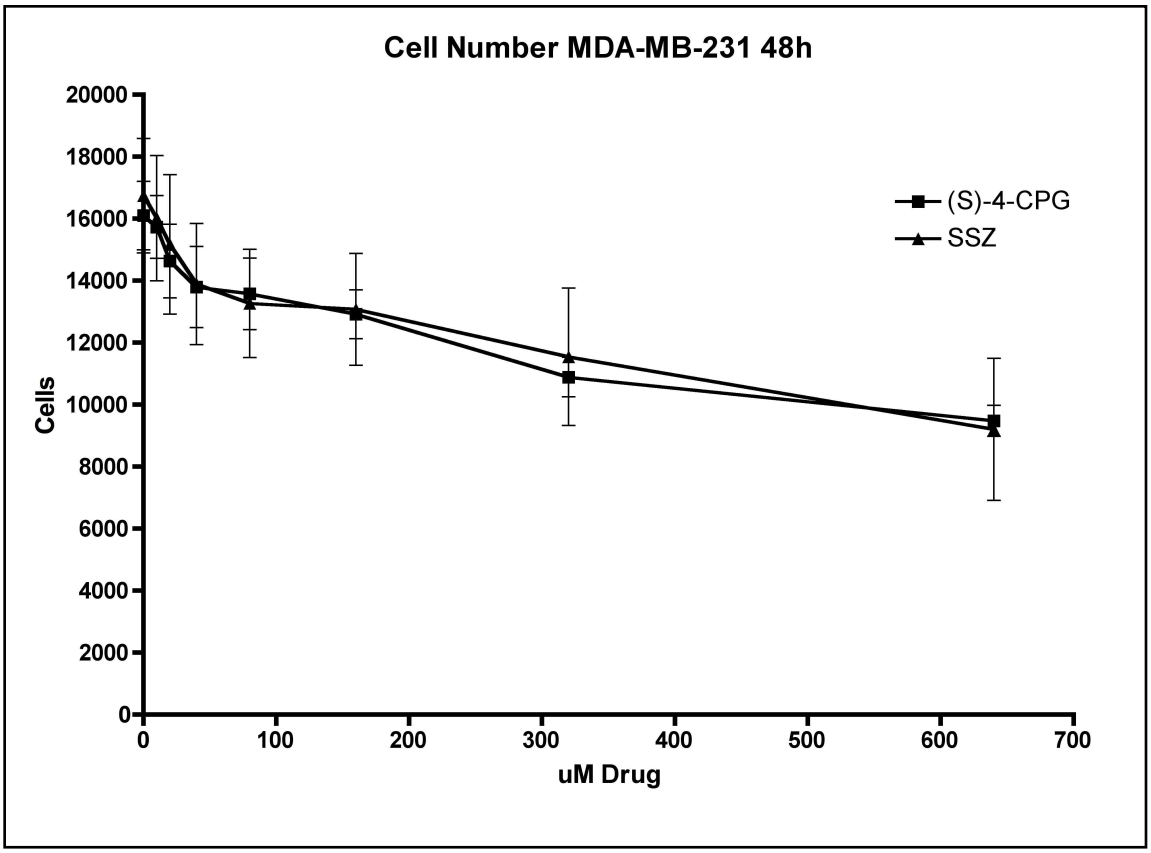

Figure 3.5 Cell number following 48 hour growth of 10,000 seeded MDA-MB-231 treated at concentrations of SSZ and (S)-4-CPG between 0-640 μM. Both inhibitors exhibited a dose-response relationship similar to the trend of glutamate release over the same treatments; however, cell number does not cease to decline at higher concentrations of (S)-4-CPG as occurs with glutamate release. It is important to note that the 640 μM treatment groups of both inhibitors were the only groups to elicit a decline in cell number. Data are expressed as the mean of n=3 experiments ± the standard error of the mean (SEM).

Behavioural Analysis

Mice injected with MDA-MB-231 at the distal epiphysis of a single femur reliably demonstrated behavioural evidence of pain corresponding to tumour presence in the ipsilateral limb and no behavioural evidence of pain in the contralateral hind limb as measured by both DWB and DPA machines. Animals that did not develop an osteolytic tumour in bone visible by radiograph also did not develop behavioural evidence of pain similar to confirmed tumour-bearing animals, and were removed from analysis. DWB and DPA measurements were very consistent with each other and were able to demonstrate daily changes in animal behaviour consistently across platforms. The animal model of Balb/c nu/nu female mice injected intrafemorally with 10^6 MDA-MB-231 human breast cancer cells was therefore validated as an animal model of human cancer-induced bone pain to investigate the effects of SSZ and (S)-4-CPG treatment on behavioural evidence of pain.

Drug treatments revealed modulating effects on pain in the SSZ treatment group (165.66 μM circulating dose, 6.6 mg/kg/day) and no behavioural evidence of effect in the (S)-4-CPG treatment group (20 μM circulating dose, 0.4 mg/kg/day). At the outset of this project it was expected that any effects of the inhibition of system x_C^- mediated glutamate secretion on pain would manifest as a reduction in early pain behaviours or a delay in the time until onset of pain evident as a shift to the right in the curve of normal cancer-induced bone pain behaviour. A large scale reduction in pain was not expected from a non-analgesic, mechanistic approach that might eliminate a potential source of pain, rather than broadly inhibit the transmission of nociceptive signalling.

SSZ treatment (165.66 μM) resulted in a trend toward a delay until onset of allodynia pain behaviour as measured by weight bearing with the DWB, although the overall treatment effect of SSZ compared to vehicle treatment past day 20 was statistically insignificant (P = 0.09) (Figure 3.6). Mice in the SSZ treatment group, however, maintained higher weight bearing on the tumour bearing limb for a longer duration, and did not exhibit a large mean decline in ipsilateral weight bearing until several days later than the vehicle group.

DPA analysis of SSZ treated animals was consistent with the evidence of a delay until the onset of pain behaviours observed with the DWB analysis. The two analyses mirrored each other very closely which supports their continued use as behavioural evaluations. As measured by DPA, SSZ treatment resulted in a delay until onset of allodynia and hyperalgesic pain behaviour. Unlike DWB analysis, DPA analysis of the treatment effect of SSZ compared to vehicle treatment past day 20 was statistically significant (P = 0. 04) (Figure 3.7).

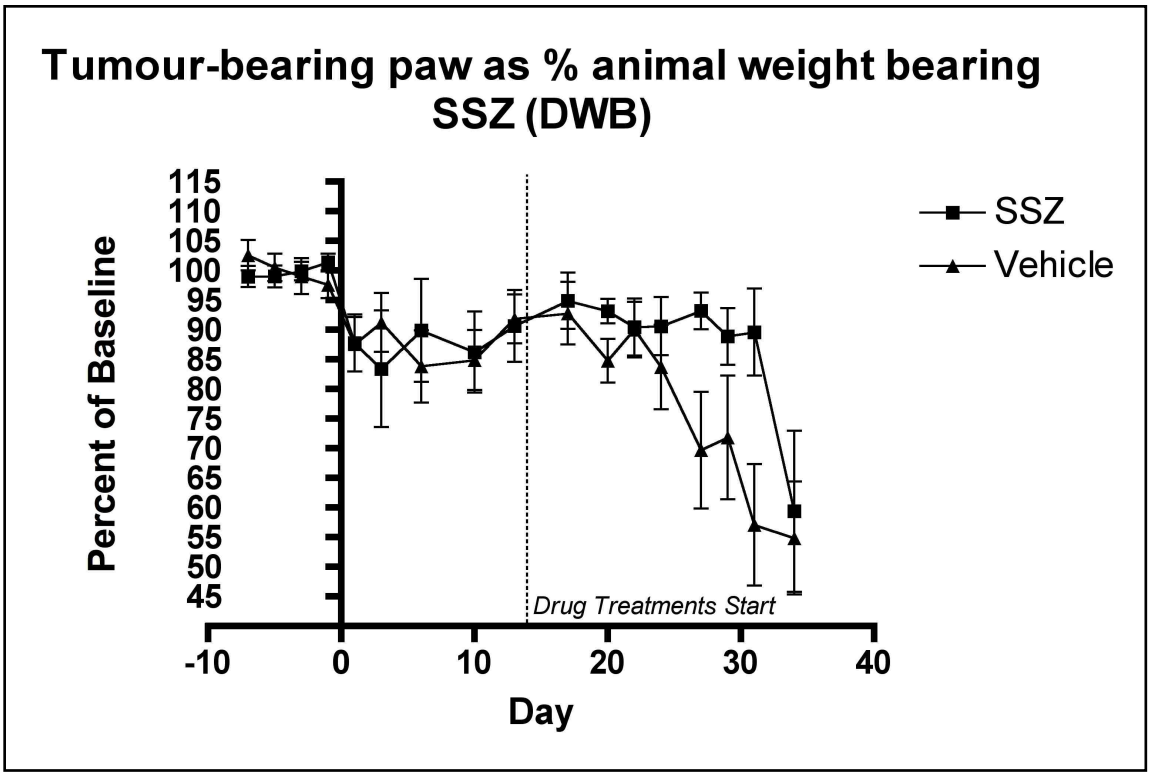

Figure 3.6 DWB analysis of the SSZ treated animals vs. vehicle treated animals. This chart displays a measurement of the weight borne by the tumour afflicted paw as a percentage of the whole animal weight, standardized to the animal's baseline scores for the same measurement. 100% on the y-axis is therefore equivalent to the animal's behaviour prior to tumour implantation surgery. Less than 100% on the y-axis indicates a decrease in weight borne by the tumour afflicted paw. SSZ treated animals display higher weight bearing in the tumour-afflicted limb for a longer duration than the vehicle treated animals displaying a resistance to allodynia manifested in the vehicle treated animals; however, statistical analysis revealed an insignificant difference due to treatment. One way repeated measures ANOVA on the measurements past Day 20 was not significant

for a treatment difference (P = 0.09). (SSZ): n=11; (Vehicle): n=14. Data are expressed as the mean ipsilateral weight bearing as a percentage of all weight bearing ± the standard error of the mean (SEM).

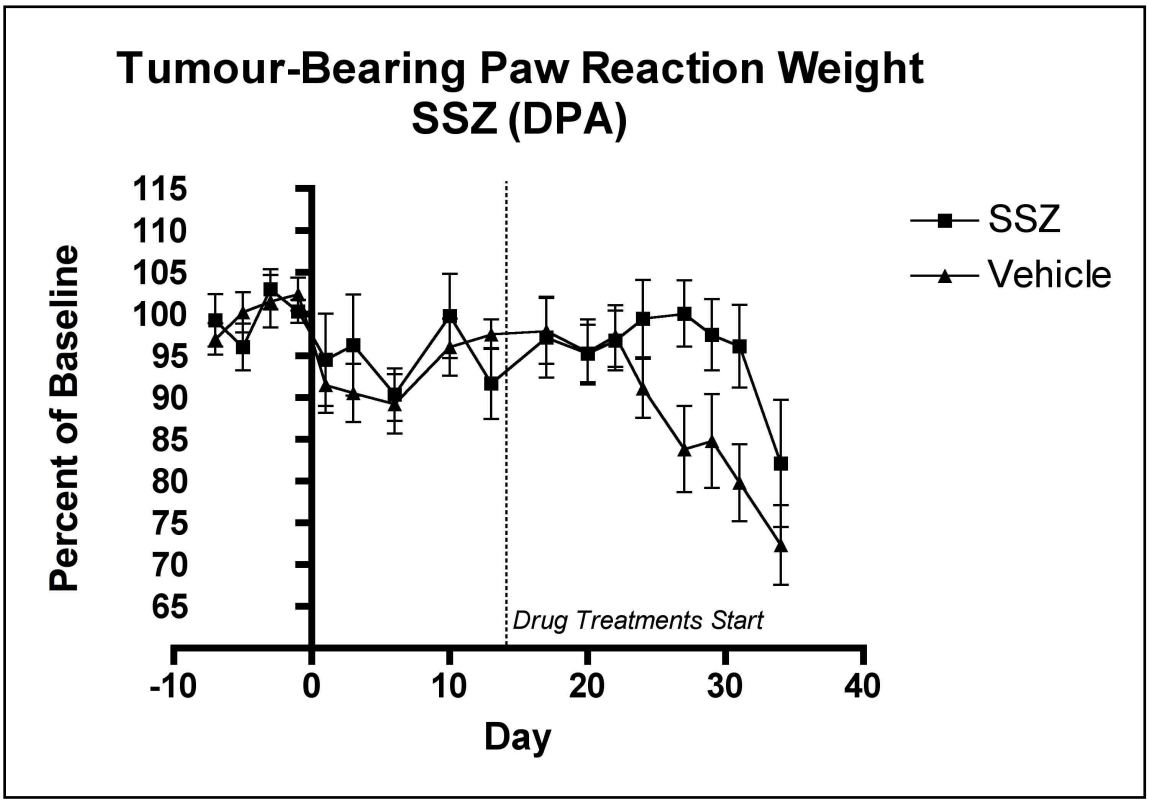

Figure 3.7 DPA analysis of the SSZ treated animals vs. vehicle treated animals. This chart displays a measurement of the threshold force withstood at reaction to a progressive stimulus on the plantar surface of the mouse ipsilateral hindpaw. The data provided is the force withstood by the ipsilateral tumour bearing paw only. Like the DWB chart above, 100% on the y-axis is equivalent to the animal's behaviour prior to tumour induction. Less than 100% on the y-axis indicates a decrease in the force withstood by the tumour afflicted paw. Consistent with the

DWB results for the same animals this data indicates a delay until the time of onset of pain behaviours. One way repeated measures ANOVA on the block past Day 20 was significant for a treatment difference ($P = 0.04$). (SSZ): n=11; (Vehicle): n=14. Data are expressed as the mean ipsilateral force withstood ± the standard error of the mean (SEM).

Treatment with (S)-4-CPG (20 μM) demonstrated no strong behavioural evidence of pain relief. No clear trends or significant differences were observed between (S)-4-CPG and vehicle treatment groups with measurement by DWB (Figure 3.8) or with DPA (Figure 3.9). This is inconsistent with expectations; however, if the SSZ data is a true representation of the effect of the inhibition of system x_C^- mediated glutamate secretion on pain, then it is possible that (S)-4-CPG did not manifest the same behavioural results from either a failure to reach the pharmacological target, or that it was delivered at too low a dose for impact. The unknown safety profile of intraperitoneal (S)-4-CPG did not appear to have limited behavioural results, as no distinct events indicating poor tolerance of the drug were observed.

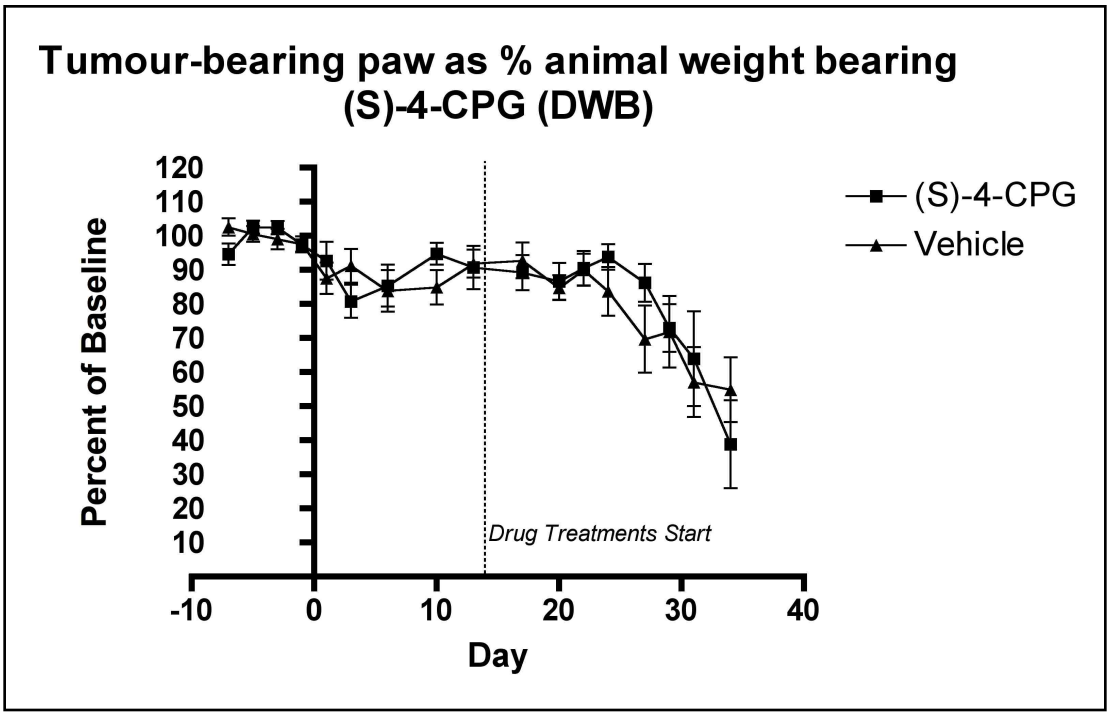

Figure 3.8 DWB analysis of (S)-4-CPG treated animals vs. vehicle treated animals. This chart indicates no significant difference in the time until onset of pain behaviours, or any differences otherwise in pain behaviours between groups. This result is consistent with DPA measurement. One way repeated measures ANOVA on the measurements past Day 20 was not significant for a treatment difference ($P = 0.7$). ((S)-4-CPG): n=12; (Vehicle): n=14. Data are expressed as the mean ipsilateral weight bearing as a percentage of all weight bearing ± the standard error of the mean (SEM).

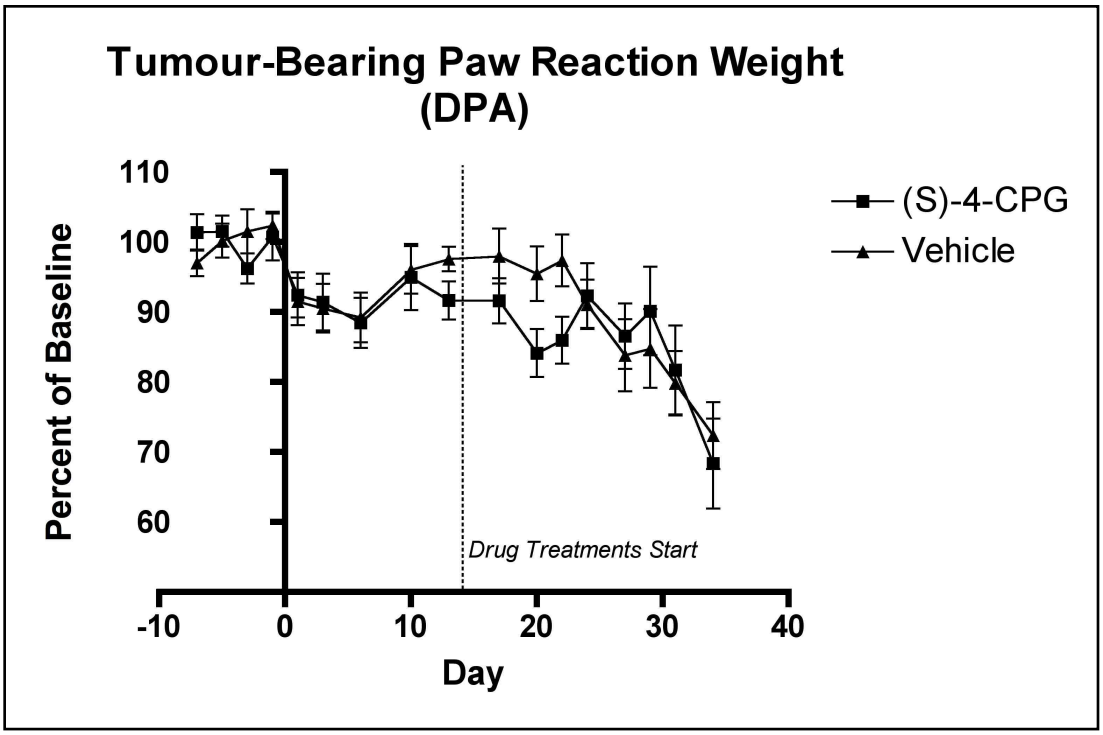

Figure 3.9 DPA analysis of (S)-4-CPG treated animals vs. vehicle treated animals. This chart indicates no significant difference in the time until onset of pain behaviours, or any differences otherwise in pain behaviours between groups. This result is consistent with DWB measurement. The groups do display an early divergence; however, it is not sustained. One way repeated measures ANOVA on the block past Day 20 was not significant for a treatment difference (P = 0.8). ((S)-4-CPG): n=12; (Vehicle): n=14. Data are expressed as the mean ipsilateral force withstood ± the standard error of the mean (SEM).

For comparison, the above data is repeated below in single charts for the DWB (Figure 3.10) and DPA (Figure 3.11) measurements. Included in these charts are all

treatment groups (SSZ, (S)-4-CPG, and vehicle) without error bars to facilitate comparison between groups. The similarity of the (S)-4-CPG and vehicle treatment animals that becomes apparent when directly contrasted with the SSZ group that displays a clearly divergent trend from both.

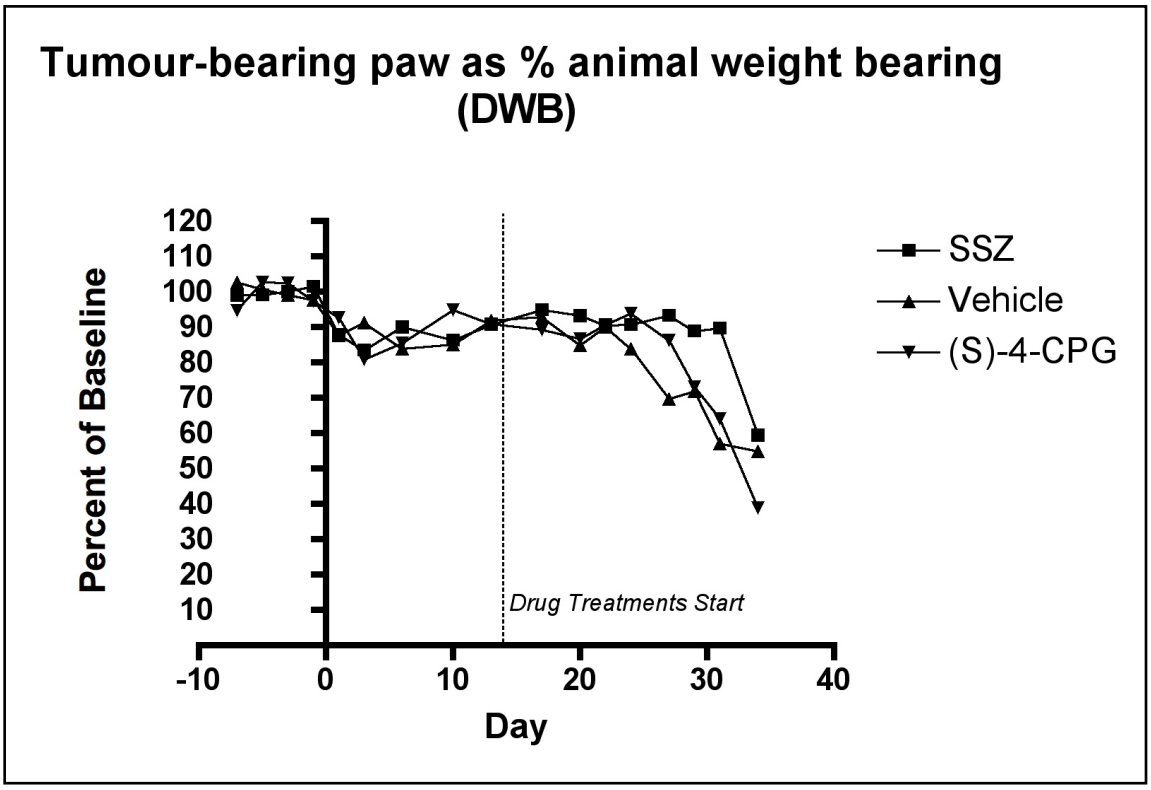

Figure 3.10 DWB analysis of all groups. Error bars have been removed to facilitate comparison. (SSZ): n=11; ((S)-4-CPG): n=12; (Vehicle): n=14.

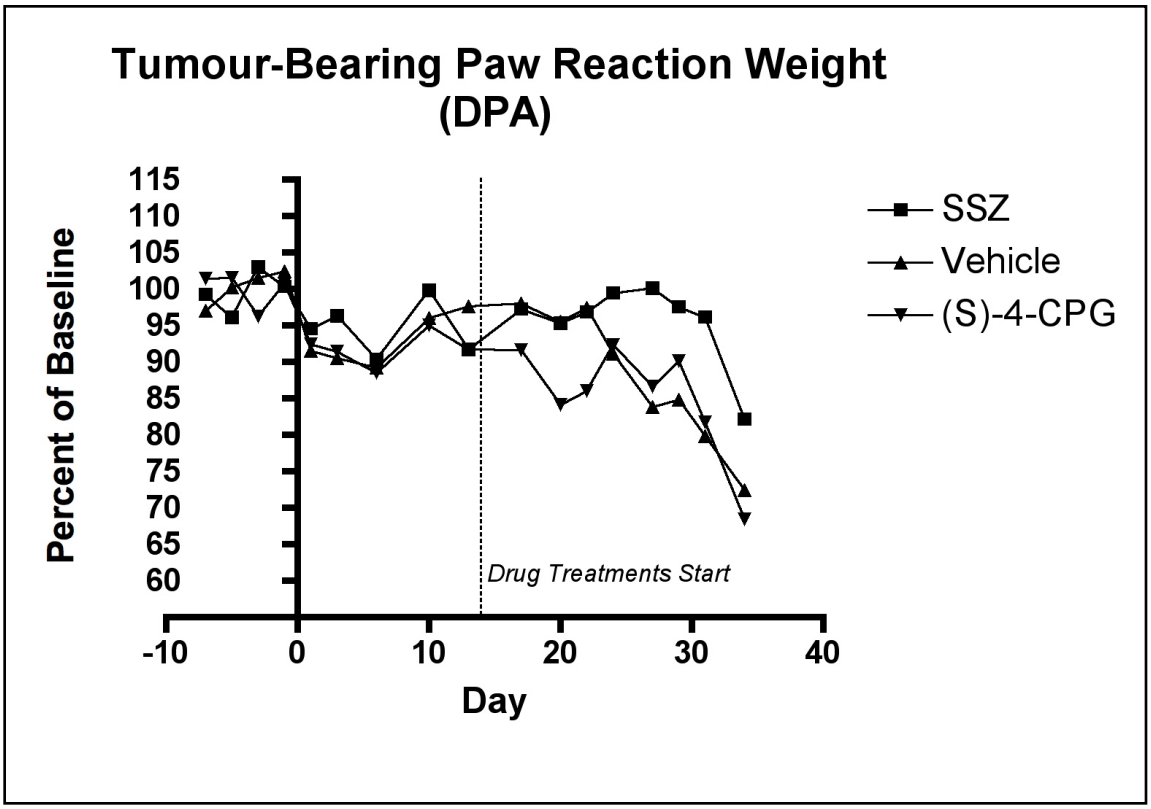

Figure 3.11 DPA analysis of all groups. Error bars have been removed to facilitate comparison. (SSZ): n=11; ((S)-4-CPG): n=12; (Vehicle): n=14.

As is clear from the above evidence, no treatment group demonstrated a strong reduction of pain behaviours at animal endpoint. This effective period of SSZ treatment as indicated above is at the onset of pain, and the treatment effect of SSZ appears to induce a temporal delay until the onset of pain when compared with vehicle treatment animals. No such delay was observed in the (S)-4-CPG treatment group. To isolate this effect, the day at which behavioural scores for tumour bearing animals fell irreversibly below 70% of that animal's baseline score for the same measurement was plotted as a

survival curve. This was calculated for 70% as individually measured by both DWB and DPA. Comparison between groups as measured by DWB (Figure 3.12) revealed a significant difference between vehicle and SSZ treatment group, with SSZ treated animals exhibiting a later achievement of irreversible 70% pain (P = 0.04). There was no significant difference between the (S)-4-CPG and vehicle treatment groups (P = 0.9). Comparison between groups as measured by DPA (Figure 3.13) revealed no significant differences for either SSZ (P = 0.1), or (S)-4-CPG (P = 0.8), when compared with vehicle.

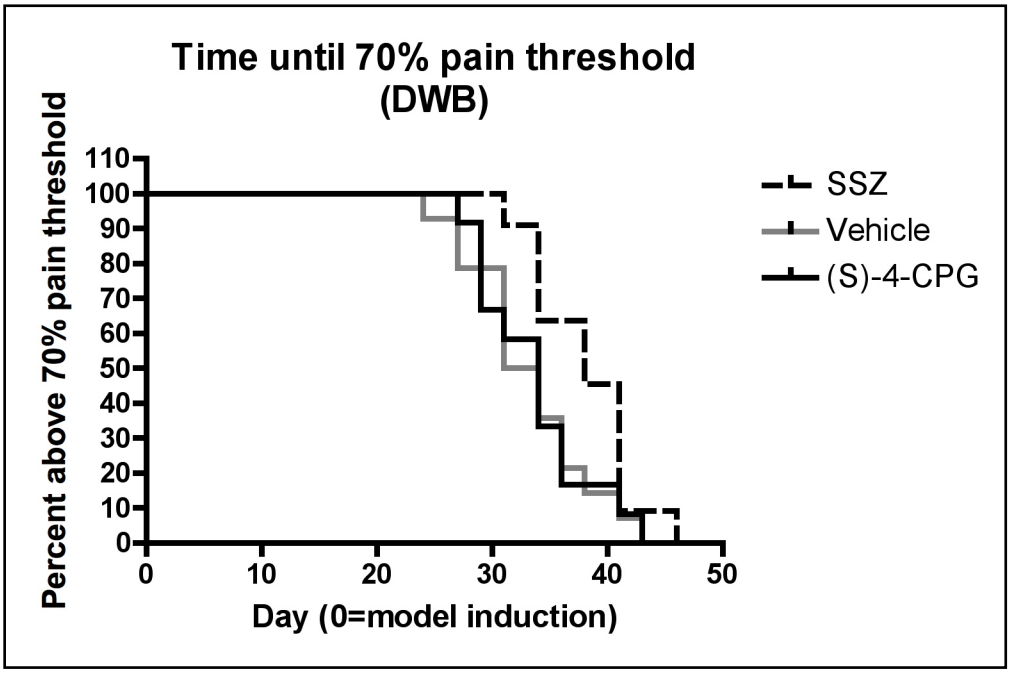

Figure 3.12 DWB analysis of the percent of animals of each group above the 70% of baseline score for ipsilateral limb weight bearing as a percentage of total animal weight bearing. SSZ treated animals display a delay in the onset of pain behaviours relative to vehicle treated animals (P = 0.04). (S)-4-CPG treated

animals display no significant difference relative to vehicle treated animals (P = 0.9). (SSZ): n=11; ((S)-4-CPG): n=12; (Vehicle): n=14.

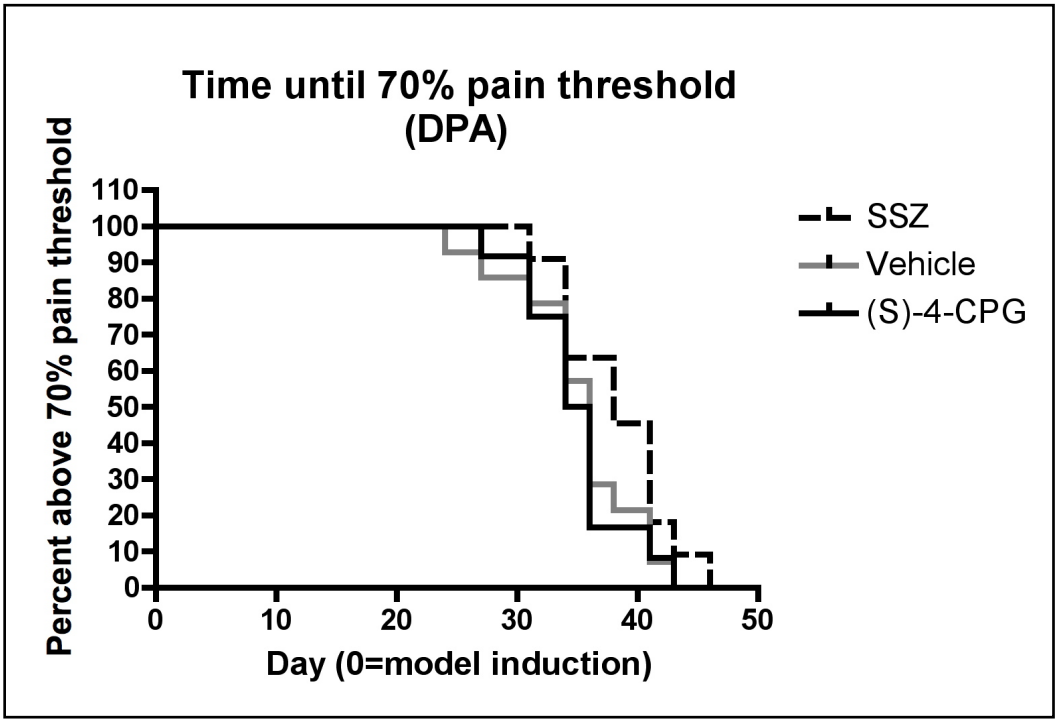

Figure 3.13 DPA analysis of the percent of animals of each group above the 70% of baseline score for ipsilateral limb threshold force at reaction. Neither SSZ nor (S)-4-CPG treated animals displayed a significant difference relative to vehicle treated animals (P = 0.1), and (P = 0.8), respectively. (SSZ): n=11; ((S)-4-CPG): n=12; (Vehicle): n=14.

Power Analysis

A retroactive power analysis indicated that the sample sizes chosen were sufficient to observe effect sizes comparable to the few larger differences seen in the period of group divergence between the SSZ and vehicle groups for both DWB and DPA methods of behavioural comparison. With a type II error (β=20%), and a type I error (α=5%) at an effect size of 0.4, DWB comparisons on days 24-31 and DPA comparisons on days 27-31 were attainable with current sample sizes. Sample sizes were not sufficient to detect smaller potential differences observed just prior to the major period of group divergence in the SSZ and vehicle comparisons, and any differences between the (S)-4-CPG and vehicle treatment groups excluding DWB day 27.

Radiographic Analysis

All radiographic images taken immediately following sacrifice were examined prior to the amalgamation of all behavioural data to investigate model success, and to ensure that only data from animals that successfully developed tumours were included. Osteolytic lesions were readily apparent in the ipsilateral femurs of model animals, while contralateral femurs demonstrated no signs of disruption. The sham injected animal retained normal bone patterns in both femurs (Figures 3.14, 3.15).

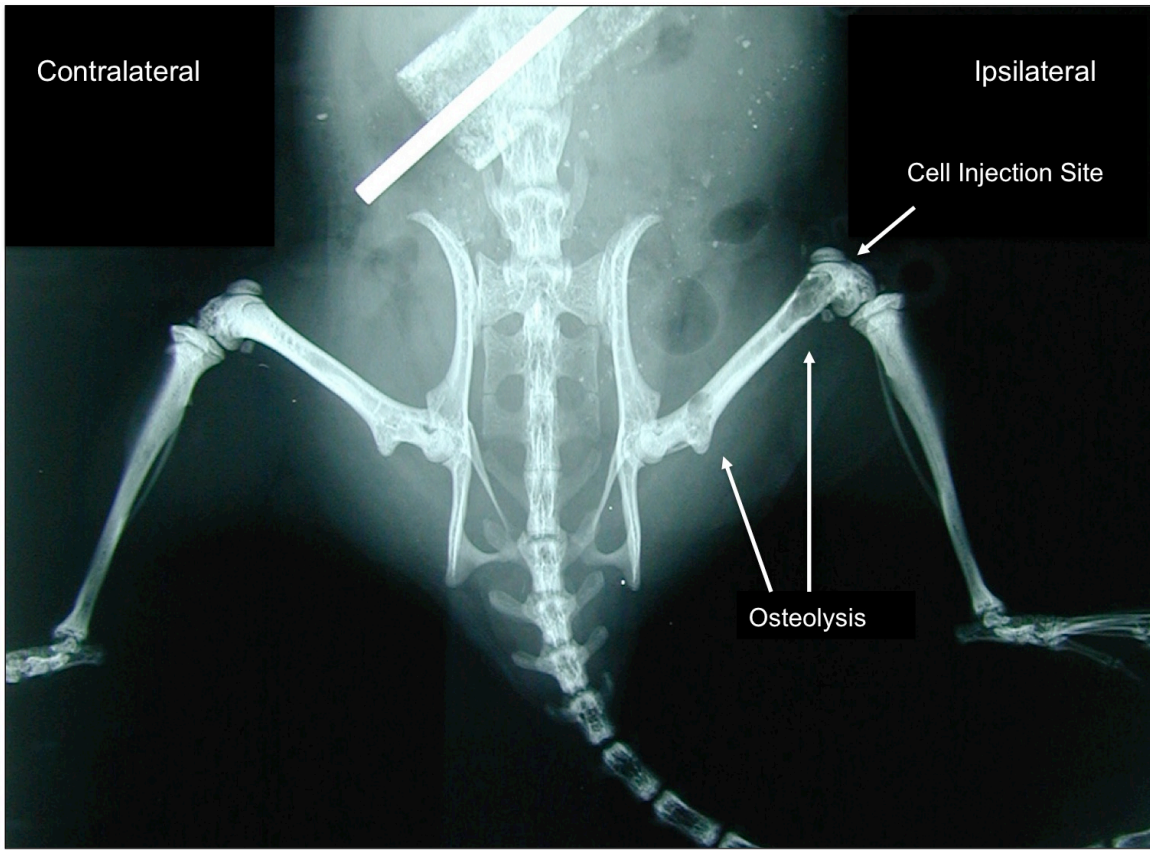

Figure 3.14 Post-mortem radiograph of tumour-bearing animal. This animal exhibits a large osteolytic lesion near the distal epiphysis of the ipsilateral femur near the site of injection that continues into the diaphysis, and a second large lesion nearer to the proximal epiphysis. The contralateral femur displays no signs of excessive osteolysis and normal anatomical features.

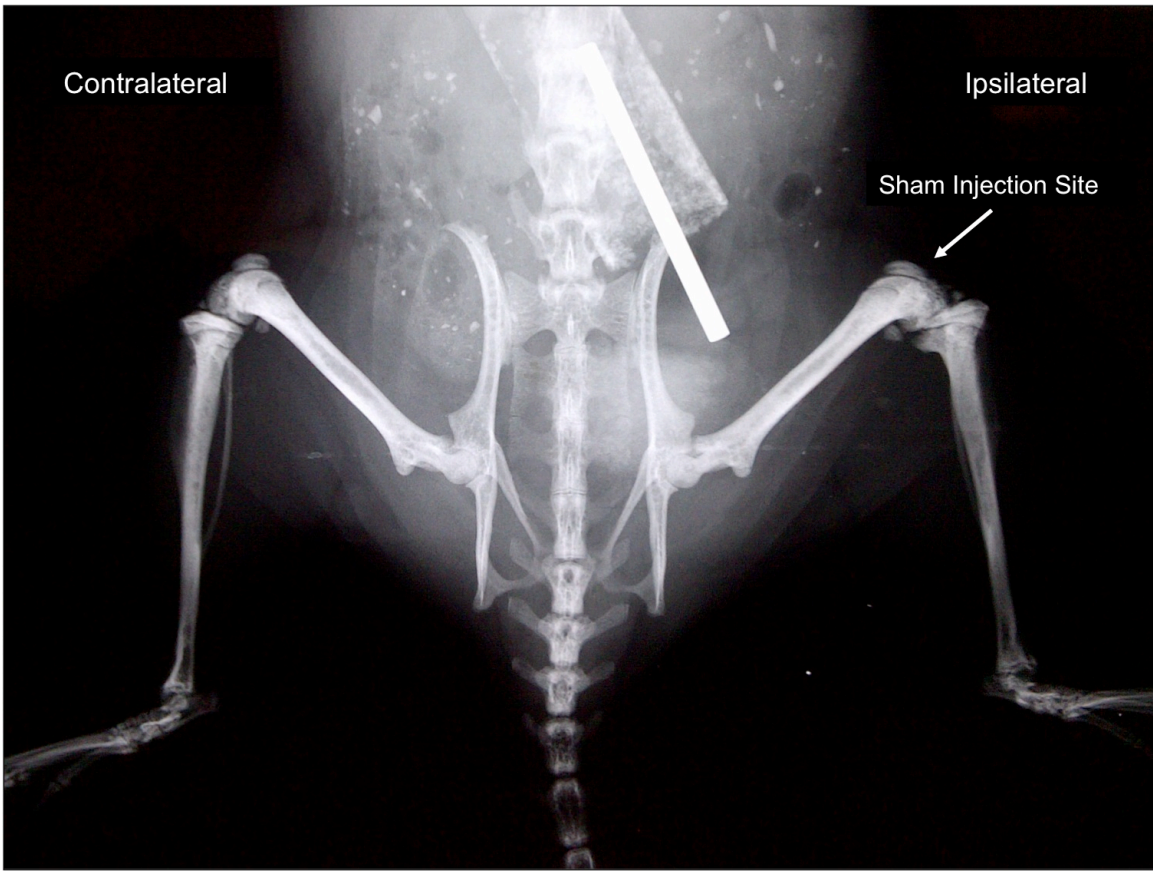

Figure 3.15 Post-mortem radiograph of the sham-injected animal. This animal exhibits no signs of tumour or excessive osteolysis in either femur. The site of injection appears normal and without visible signs of tissue damage.

The extent of osteolytic lesions in the ipsilateral femurs of all mice as imaged as a loss of bone density by post-mortem radiograph was scored using a custom four point (0-3) scale of bone destruction (See Methods, Figure 2.2 for tumour scale). This analysis revealed a trend of all visible lesions towards extensive lysis, which was expected and consistent with the practice of sacrifice at endpoint utilized in this study (Figure 3.16).

No treatment groups were overrepresented in any lesion category, demonstrating the absence of an overall effect of treatment on tumour size at endpoint. This is reassuring as it demonstrates the lack of a large effect of both SSZ and (S)-4-CPG on tumour growth as was intended at the administered doses; however, it is still possible that the tumour growth was delayed in either of the treatment groups, as that would not be indicated with this analysis of lesion size at endpoint. All behavioural data were analyzed when isolated for tumour group; however, no trends emerged that differed from the data analyzed for all tumour bearing animals.

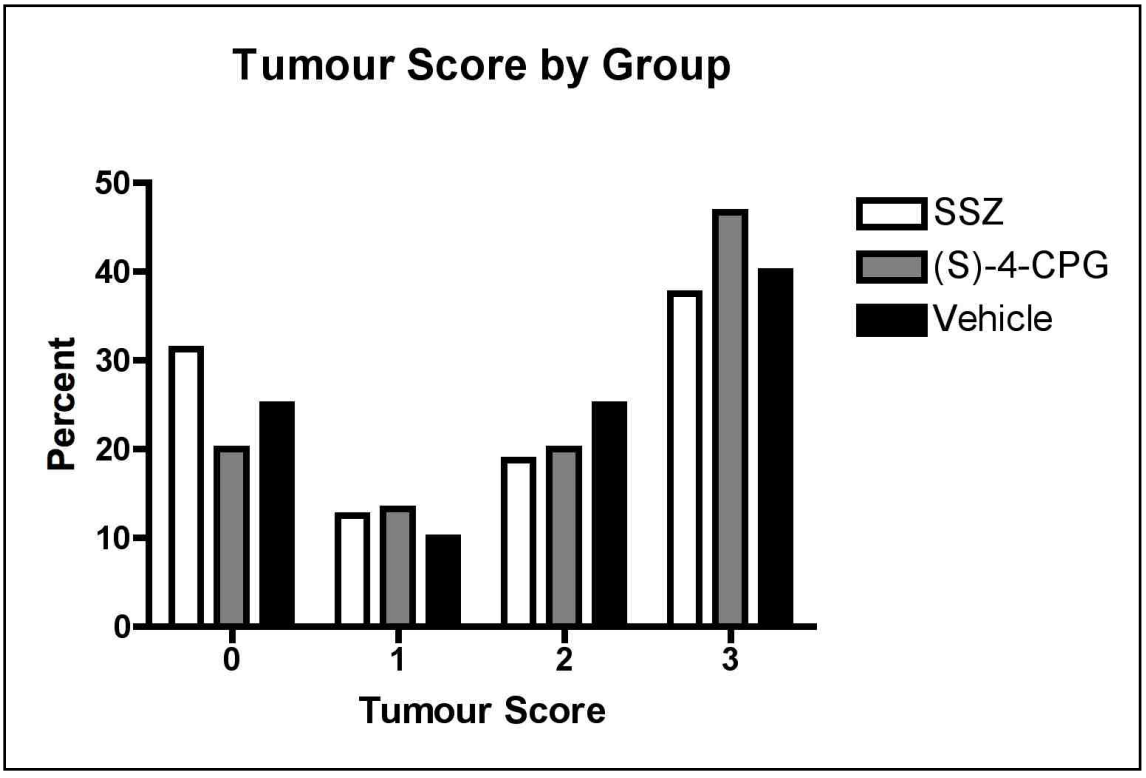

Figure 3.16 Percentage of animals of each treatment group by tumour lesion score. The scale designations are: (0): Normal bone, no visible lesion; (1): minor loss of bone density, minimal lesion; (2): Moderate to substantial loss of bone

density, lesion limited to bone trabecula and cortex; (3): substantial loss of bone density, lesion includes clear periosteal involvement or fracture. There is an overall trend towards larger lesions across all groups; however, no individual treatment group shows any strong trend apart from this. All attempted tumour model animals are included. (SSZ): n=16; ((S)-4-CPG): n=15; (Vehicle): n=20.

Histology

Haematoxylin and eosin staining revealed the proliferation of tumour cells throughout the ipsilateral femurs of animals that radiographically demonstrated lytic lesions. Tumour was commonly found within the distal epiphysis and diaphysis of ipsilateral femurs, and less frequently at the proximal epiphysis of the femur and throughout the periosteum and surrounding muscle and joint space of the knee. Bone marrow, bone trabeculae and cortical bone all demonstrated invasion. In contralateral femurs and the sham injected mouse, no evidence of extensive osteolysis or tumour was found (Figures 3.17, 3.18).

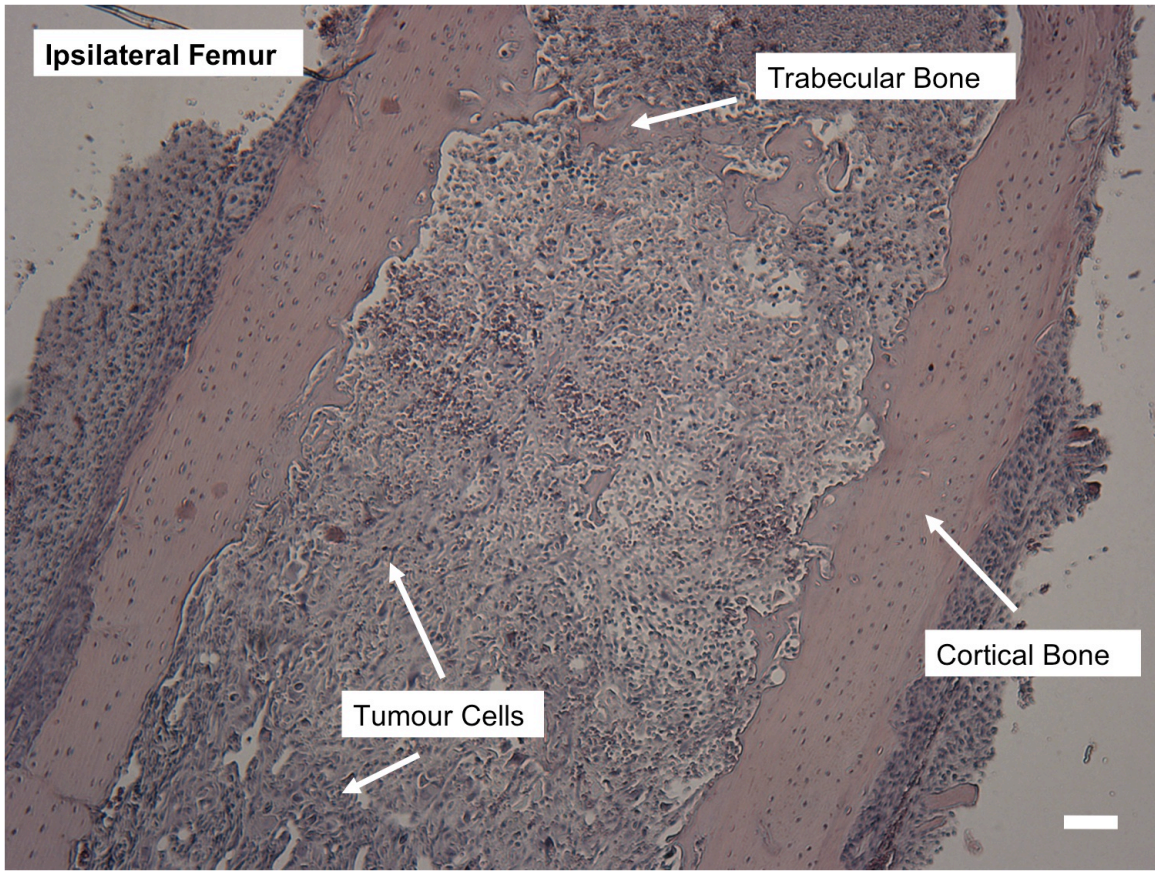

Figure 3.17 Haematoxylin and eosin staining of the ipsilateral femur of a tumour bearing mouse at the diaphysis. This femur exhibits large unpatterned tumour cells occupying the place of the trabecular bone and the bone marrow. The trabecular bone appears only in small islands, and the inner face of the cortical bone appears ragged and lytic. This photograph demonstrates the structural contrast with the corresponding location of the femur in the contralateral femur of the same animal (Figure 3.18). Scale bar = 100 μm.

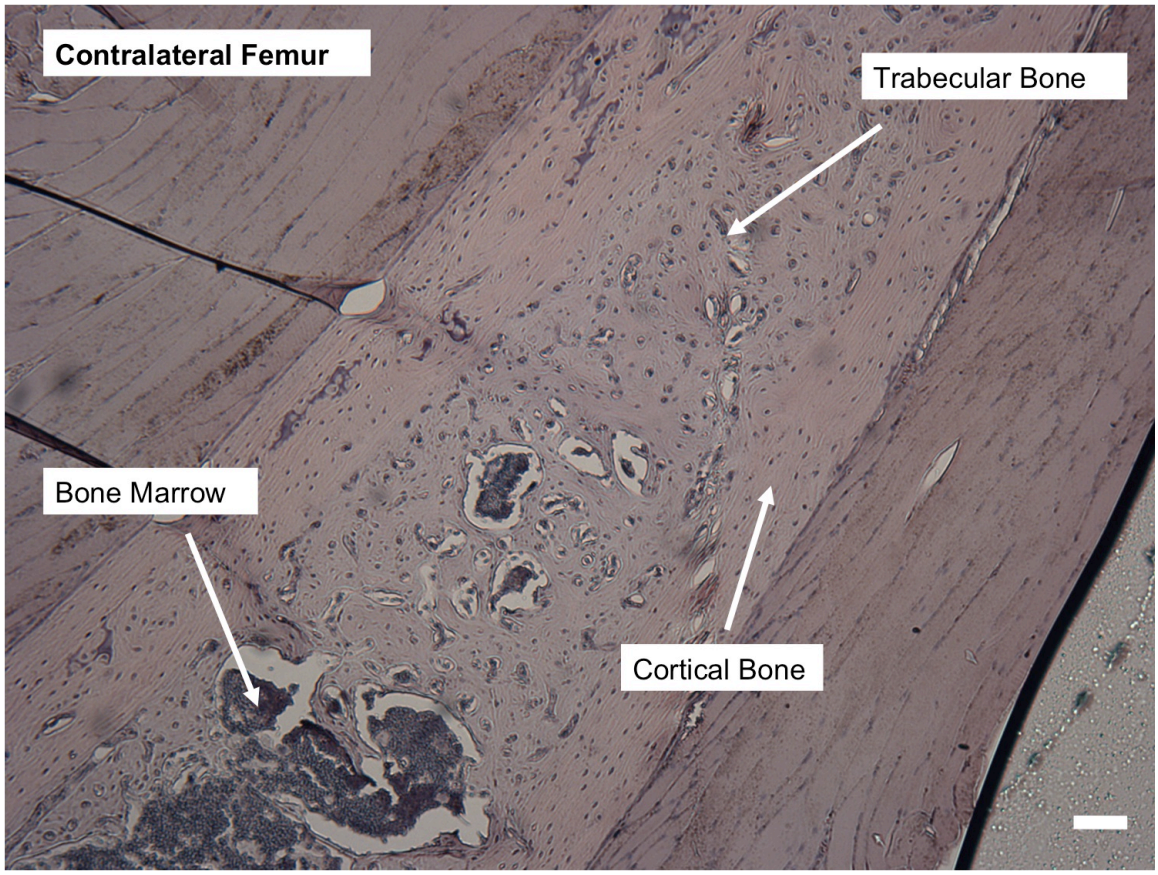

Figure 3.18 Haematoxylin and eosin staining of the contralateral femur of a tumour bearing mouse at the diaphysis. Cortical and trabecular bone and bone marrow appear patterned and without displacement or lysis. This photograph demonstrates the structural contrast with the corresponding location of the femur in the ipsilateral femur of the same animal (Figure 3.17). Scale bar = 100 μm.

Staining with the anti-glutamate antibody revealed implanted tumour cells to be the major source of glutamate in model animal bone across all treatment groups (Figures 3.19, 3.20, 3.21). Bone marrow and the cells of the bone growth plate also stained darkly

for glutamate, but they were most often far less prevalent than the tumour in ipsilateral femurs.

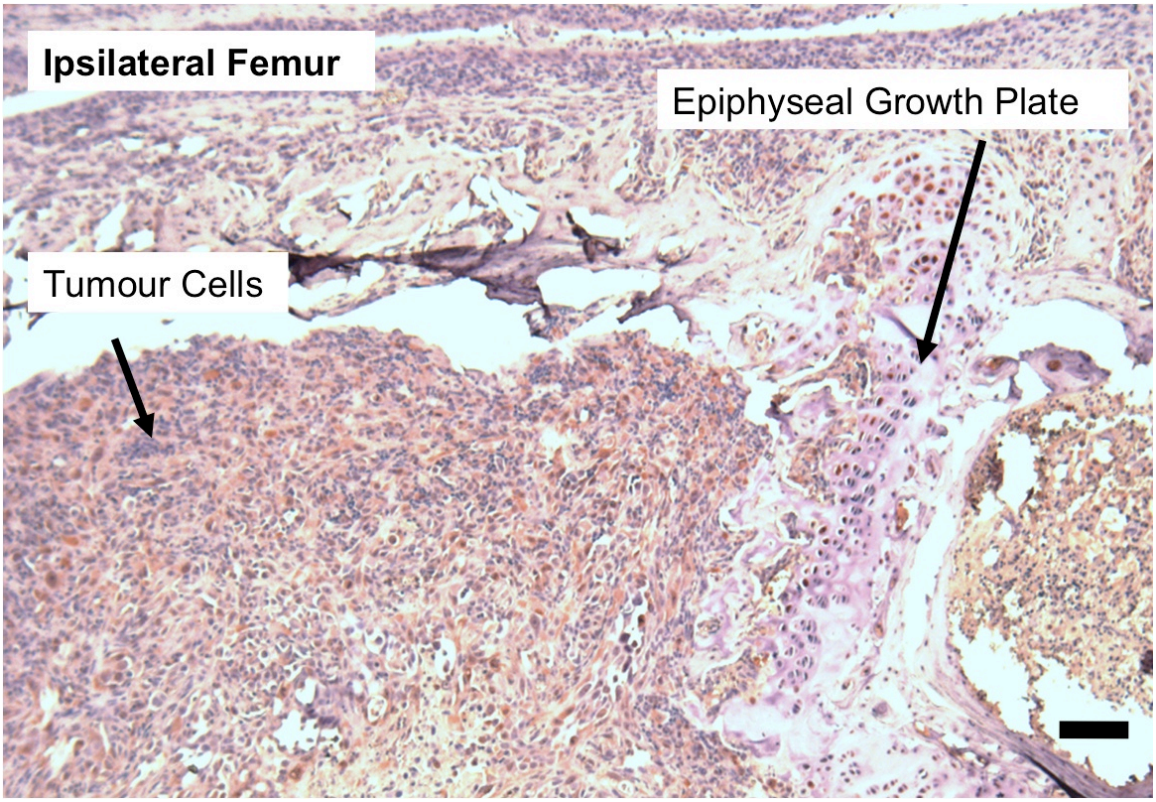

Figure 3.19 Glutamate immunostain and haematoxylin counterstain of the ipsilateral femur of a tumour bearing mouse at the metaphysis. This femur exhibits tumour cells distal and proximal to the epiphyseal growth plate. Bone is largely degraded excluding at the epiphyseal plate and some cortical bone. Glutamate (red) is most predominantly stained in the tumour. Scale bar = 100 μm.

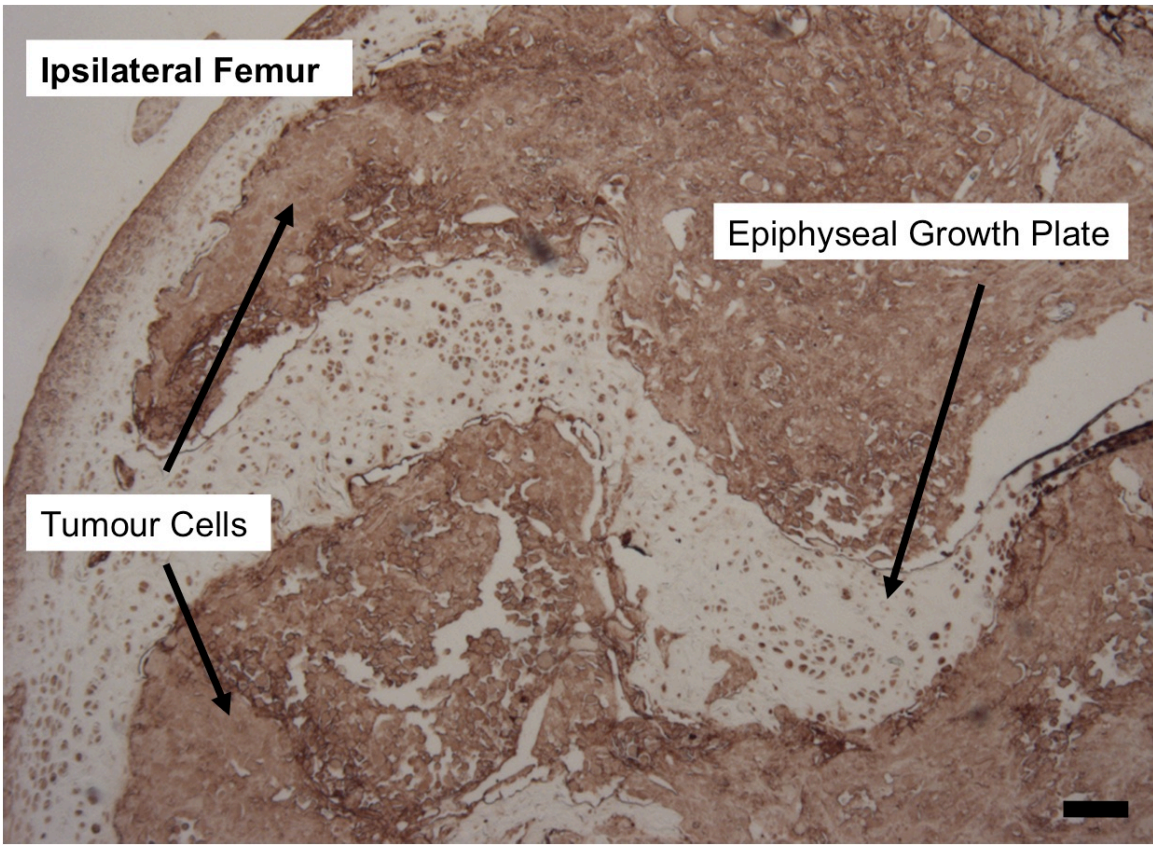

Figure 3.20 Glutamate immunostain without counterstain of the ipsilateral femur of a tumour bearing mouse at the epiphysis. This femur exhibits tumour cells distal and proximal to the epiphyseal growth plate. Bone is largely degraded excluding at the epiphyseal plate and some cortical bone. Glutamate staining can be easily observed without counterstain, and is most predominantly stained in the tumour. The cells within the epiphyseal growth plate also stain darkly for glutamate. Mineralized bone does not stain at all. Scale bar = 100 μm.

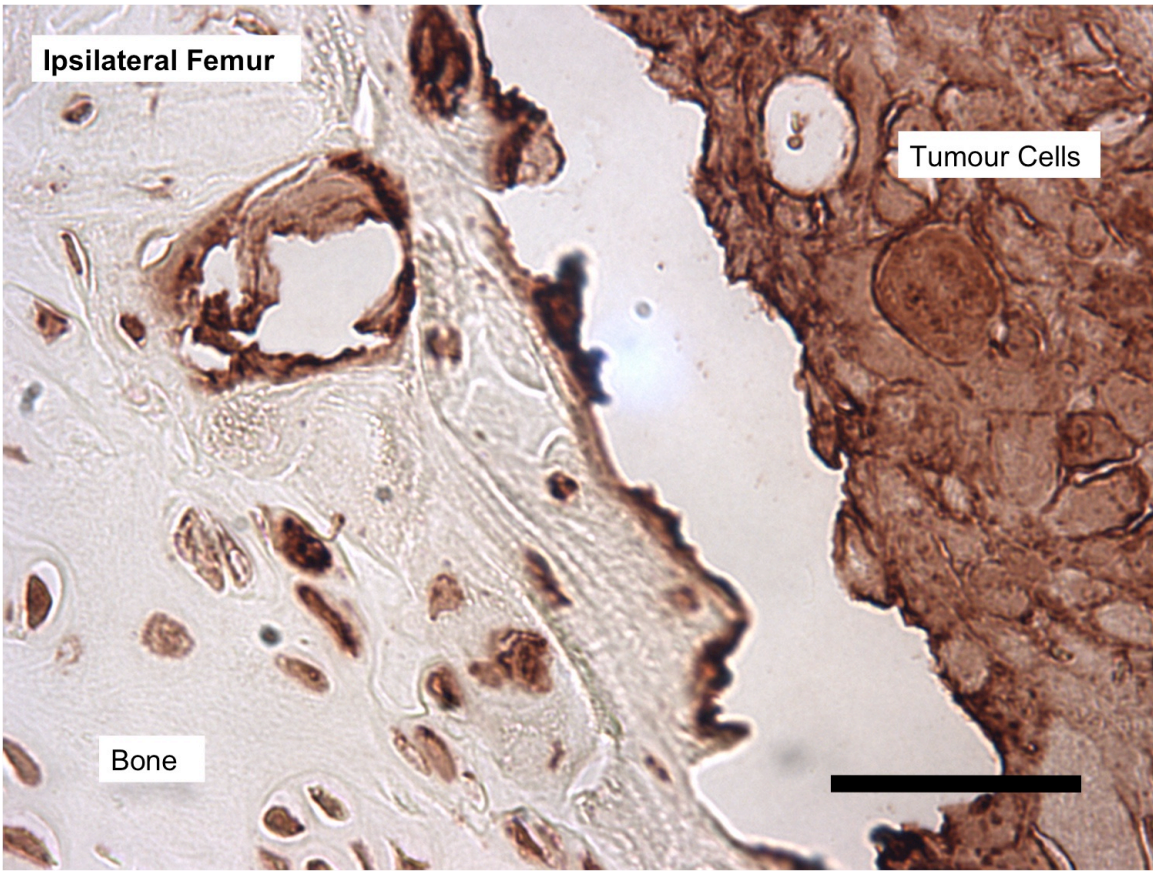

Figure 3.21 Glutamate immunostain without counterstain of the ipsilateral femur of a tumour bearing mouse at the metaphysis. This high magnification photograph clearly demonstrates the distinction between glutamate staining levels in mineralized bone and in tumours. Scale bar = 50 μm.

The extent of glutamate staining in tumours of all treatment groups was analyzed using a custom three point (1-3) scale of staining colour of the tumour near to an interface with bone (See Methods page , Figure 2.3 for scale). This analysis did not reveal a strong association of tumours staining with any treatment group, although there was a trend

towards darker staining within the SSZ treatment group relative to the vehicle treatment group (Figure 3.22). The (S)-4-CPG treatment group was more evenly distributed between staining levels. The inability to properly distinguish between cytoplasmic and extracellular glutamate has clear implications for the usefulness of this scale with this animal model. The darkest staining (Group 3) was mostly located in tumours treated with SSZ or (S)-4-CPG. This could be an indication of the accumulation of intracellular glutamate in the tumour cells that could not export through system x_c^-. It must be noted that this comparison between groups is a strictly qualitative measurement.

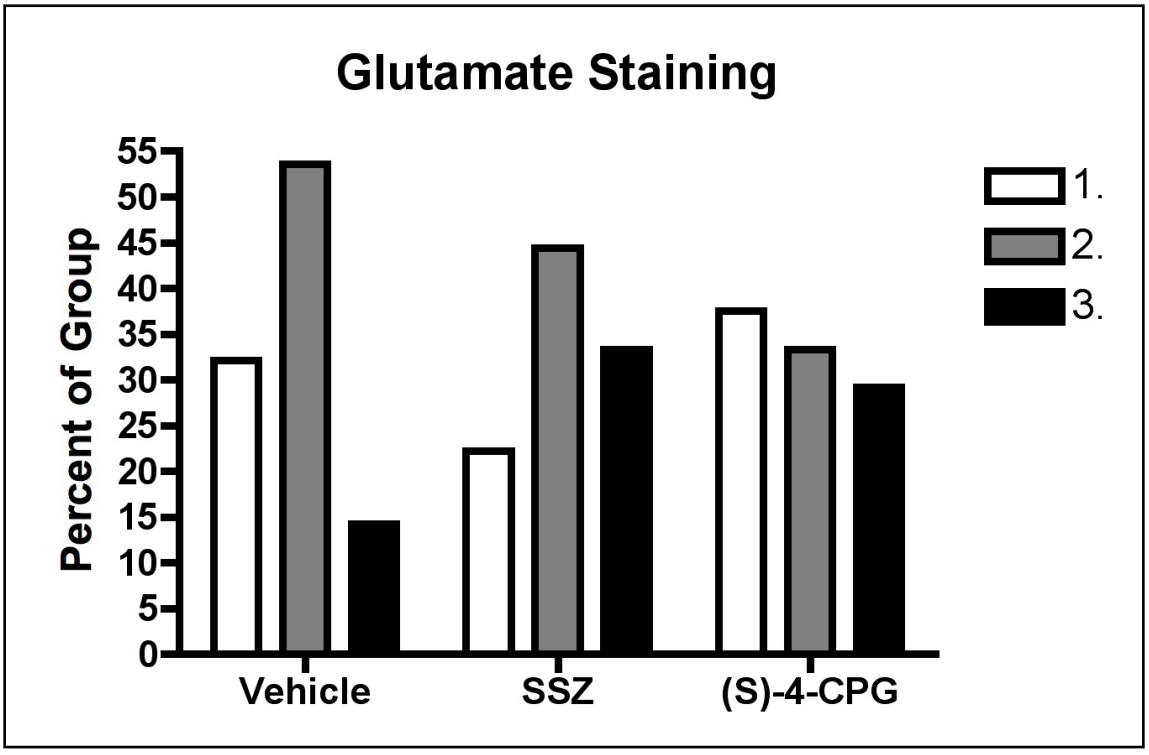

Figure 3.22 Percentage of animals of each treatment group by the extent of tumour glutamate staining. These staining designations are: (1): mild glutamate staining; (2): moderate glutamate staining; (3): heavy glutamate staining. This

analysis shows a possible trend towards the darkest staining in tumours treated with SSZ and (S)-4-CPG. This may indicate cytoplasmic sequestration of glutamate that would be released to the extracellular environment in vehicle treated animals. This analysis was performed for all animals with two separately stained and evaluated slides of each sample.

Chapter 4: Discussion

Breast cancers are the most common source of metastases to bone, where they are responsible for a host of pathologies, including cancer-induced bone pain, that result in reduced patient functional status, quality of life and survival (Mercadante, 1997). Cancer-induced bone pain is a complex condition that arises from a multiplicity of factors including from weak and fractured bone, inflammation, neuropathy, and from disruptive cell signalling and nociceptive factors released directly from or induced to be released from the growing tumour. This indicates that cancer-induced bone pain is induced not only through direct action of the tumour, but also indirectly through tumour–induced dysregulation of the host tissue. Cancer-induced bone pain has also been partially alleviated in multiple instances through targeting the influence of cancer on its host tissue, rather than through the obstruction of signals of pain to the CNS as is done with analgesic treatment.

This project sought to investigate the relief of cancer-induced bone pain through the removal of a stimulus of pain from the bone tissue microenvironment. Glutamate has the potential to act as a stimulus of pain in bone through action on bone cells which natively utilize glutamatergic signalling in the regulation of bone remodelling, and through the direct stimulus of glutamate receptors on peripheral nociceptors in bone. Breast cancer cells including the human breast adenocarcinoma cell line MDA-MB-231 have been demonstrated to release glutamate *in vitro* through the system x_C^-

cystine/glutamate antiporter (Sharma et al., 2010). It was therefore hypothesized that the inhibition of the system x_C^- transporter would limit the release of glutamate from cancer cells implanted in mouse bone, resulting in a reduced experience of cancer-induced bone pain.

Two system x_C^- inhibitors were evaluated for this purpose; the well established drug SSZ, and the glutamate analogue (S)-4-CPG, both of which have been recognized as among the most efficient inhibitors of system x_C^- (Shukla et al., 2011). Prior to this project SSZ had been administered to animal models of cancer by intraperitoneal injection (Chung et al., 2005), but (S)-4-CPG could only be confirmed to have been administered intrathecally in non-cancer animal models at much lower doses than were chosen for this project (Yashpal et al., 2001). Dose-response curves from 0-640 μM for glutamate release from MDA-MB-231 were established for both inhibitors (Figures 3.1, 3.2) to determine their effectiveness from which *in vivo* doses would be selected. It was determined that (S)-4-CPG was more effective at limiting glutamate release than SSZ at concentrations below 40 μM, and SSZ was most effective above 40 μM, while both had remarkably similar effects on cell growth (Figure 3.5). This effectiveness of (S)-4-CPG at low concentrations is largely consistent with reports of (S)-4-CPG to exhibit a lower IC_{50} than SSZ in the inhibition of cystine uptake through system x_C^- inhibition (Shukla et al., 2011). Neither drug was able to entirely negate glutamate secretion from the cells at the tested concentrations, and higher concentrations of either drug were not attainable in our animal model. Doses were selected for each inhibitor that reflected a relatively high inhibition of glutamate release without a major effect on cell growth. This was desirable

as it was necessary to isolate the mechanism of the inhibition of glutamate release in the attenuation of pain without compounding any effects with those of limiting tumour growth. The well-characterized safety profile of SSZ and the relatively unknown safety of intraperitoneal (S)-4-CPG were also taken into account for *in vivo* use. Selected doses for each drug were calculated to be, for SSZ: 165.66 μM circulating (6.6 mg/kg/day); and for (S)-4-CPG: 20 μM circulating (0.4 mg/kg/day).

Drugs were to be delivered *via* intraperitoneal Alzet mini-osmotic pumps that relieved the need for daily injections. Although these pumps were not directly tested in this project for their reliability to release SSZ and (S)-4-CPG in solution, all pumps were utilized within the manufacturer's specifications regarding compatible vehicle substances, proper filling technique and length of implantation in the animal. Alzet mini-osmotic pumps have been used *in vitro* and *in vivo* in our lab in the past, and were previously verified in our lab for reliability of use in metronomic, timed release over several weeks in animal models of cancer (Foebel & Singh, 2006). A limitation of the reliance on the correct performance of these pumps is the inability to properly verify the amount of either drug released into the animal circulation from the pumps. No assays for the detection of either SSZ or (S)-4-CPG, apart from spectrophotometry or liquid chromatography requiring excessive blood samples from model mice, could be found for use in our lab, and so verification of the synchronized function of the pumps with the test substances and of the access of test substances to their target sites could not be performed.

An animal model of cancer-induced bone pain was developed to reflect a realistic course of human metastasis and treatment. Human cancer cells were implanted on day 0,

with the implantation of drug pumps following at day 14 to allow the unencumbered establishment of the tumour and to reflect the delay between tumour metastasis and treatment of a cancer in humans. Measurement of behavioural outcomes was performed through weight bearing analysis with the DWB machine for spontaneous pain behaviours, and through paw withdrawal force analysis with the DPA machine for induced pain behaviours. Reductions in both weight bearing and withdrawal force were accepted as behavioural indications of pain. Both machines were developed in the interests of reducing inherent subjectivity in the classical behavioural measures of the incapacitance test and the von Frey hair assessment, for the DWB and DPA, respectively. With the DPA I believe this outcome was achieved. It has also been reported; however, that with repetitive DPA use, a training effect can develop in which latency to withdraw decreases over time in normal rats (K. D. Anderson et al., 2005). If this training effect did occur in the mice of this project, we expect that it would have occurred equally in contralateral limbs between groups; however, effects of sensitization in ipsilateral limbs, if differential between groups, have the potential to influence this effect.

The DWB machine also succeeds in reducing subjectivity through the operator influence on a the state of the animal as the data capture occurs, for with the DWB, the animal is unrestrained and the capture occurs as a mean over the duration of several minutes. The manual validation stage; however, where the operator must match paws to pressure points through the use of custom software introduces a layer of subjectivity not present in a classical incapacitance test. This occurs through the determination of how to evaluate the data in terms of measurement thresholds, and acceptable moments of capture.

For this project, all validation was performed by one operator and so all measurements and procedures regarding data validation were easily standardized and repeatable.

Behavioural results indicated reduced indicators of pain and a delay until the time of onset of pain behaviours in animals treated with SSZ. Weight bearing assessment revealed a trend towards these characteristics, with the onset of a clear mean decrease in weight bearing on the tumour-afflicted limbs beginning several days later than the corresponding mean decrease in vehicle treated animals (Figures 3.6, 3.12). Paw withdrawal data was consistent with this trend towards reduced and later onset of pain, and revealed a significant difference between the vehicle treatment group and the SSZ treatment group in the later stages of the model (Figures 3.7, 3.13). Behavioural results showed no such trend for the alternate system x_C^- inhibitor, (S)-4-CPG. In weight bearing results there is a very slight difference between the (S)-4-CPG and vehicle treatment groups around the time of onset of significant pain behaviours in favour of the (S)-4-CPG group (Figures 3.8, 3.12); however, this difference is not maintained in later days, nor is it substantiated in the paw withdrawal data which displays no instances of relevant difference between (S)-4-CPG and vehicle groups (Figures 3.9, 3.13).

The delay until the time of onset of pain behaviours is a rational outcome of the inhibition of glutamate secretion into bone from metastatic cancer cells. Glutamate is a signalling molecule involved in the regulation of bone remodelling (Seidlitz et al., 2010b), and is also directly recognizable by nociceptors in bone (Mach et al., 2002), and known to directly provoke pain when subcutaneously injected (Carlton et al., 1995). The influx of exogenous glutamate from a tumour growing in bone; therefore, has the

potential to disrupt normal intracellular bone signalling, contributing to dysregulated bone remodelling, and to directly stimulate afferent nociceptors in bone. Cancer-induced bone pain; however, is a complex and little-understood pain state that involves many stimuli assuredly apart from glutamate. The observed delay of cancer-induce bone pain in SSZ treated animals may indicate a delay in the onset of central sensitization or osteolytic lesion development as induced by exogenous glutamate in vehicle treated animals. In later stages of the disease it is expected that other stimuli of pain including tumour induced nerve destruction and bone fractures would progress regardless of glutamate and would overwhelm any effects on pain of extracellular glutamate.

It is possible that this delay of pain onset may also reflect a delay in tumour growth as induced by SSZ. The rate of lesion development between groups could not be evaluated in this animal model without repeated anaesthesia and radiographs that would have had a disruptive influence on both tumour growth and behavioural responses. Doses of both SSZ and (S)-4-CPG were selected so as to not have an influential effect on tumour growth, and following weeks of growth *in vivo*, it is unlikely that there would be a measurable difference in tumour development or size between groups. At endpoints, there were no notable associations between osteolytic lesion size and treatment group (Figure 3.16). If it is the case that the inhibition of glutamate release is inexorably tied to tumour growth, then this does not invalidate the proposal of excess glutamate as an algogenic substance in bone, but it does imply that isolating the mechanisms of cancer-induced bone pain as provoked by glutamate release is a more delicate task than this animal model has allowed.

The discrepancy between the effect on pain of the SSZ treatment group and the lack thereof in the (S)-4-CPG treatment group was unexpected as both treatments were chosen for their reported efficiency over other inhibitors of system x_C^-, and for their effectiveness in inhibiting glutamate secretion from MDA-MB-231 cells *in vitro*. The dose selected for (S)-4-CPG was chosen based on the observed plateau of glutamate secretion inhibition *in vitro* and the uncharacterized safety of intraperitoneal administration. This dose is less inhibitory to glutamate release *in vitro* than the dose selected for SSZ. Both drugs could have accommodated a more than 50% reduction in their dose without a notable effect on glutamate release (Figure 3.1); however, it is possible that the selected dose of (S)-4-CPG was too small to accommodate *in vivo* use. No overt signs of toxicity were observed in (S)-4-CPG treated animals, so this study does nothing to preclude the use of higher doses of (S)-4-CPG in the future .

It is also a possibility that, independently of dose, (S)-4-CPG did not access target system x_C^- on cancer cells in bone to the same extent as SSZ. To investigate the possibility of (S)-4-CPG sequestration or loss of function in the mouse circulation, a retrospective *in vitro* glutamate release assay was performed with (S)-4-CPG at 20 μM either applied directly to MDA-MB-231 cells or first incubated with Balb/c nu/nu mouse serum or bovine serum albumin at several dilutions prior to application. Results following 48 hours indicated no evidence of (S)-4-CPG inactivity following exposure to animal blood proteins. Again, the determination of access of treatment drugs to their molecular target is limited by a lack of assay for the quantification of either SSZ or (S)-4-CPG. The slight trend towards darker immunohistochemical staining for glutamate may

indicate the efficacy of both substances at retaining glutamate within tumour cells, however this is a qualitative comparison (Figure 3.22). There is also no reason to expect that either SSZ or (S)-4-CPG were only effective for short periods of time. 72 hours glutamate secretion progressed mostly linearly without a strong recovery following a single initial treatment of both substances (Figure 3.4). In another retrospective investigation into the longevity of SSZ and (S)-4-CPG, both inhibitors were applied to MDA-MB-231 cells *in vitro* at concentrations between 0-640 μM for 24h hours and then removed, rinsed with PBS, and replaced with untreated DMEM for the following 24 hours to examine the resilience of each drug. The amount of glutamate in the media following the second 24 hours was quantified to determine any differences between inhibitors. No large differences were seen that would indicate poor longevity of (S)-4-CPG, or of SSZ. These brief retrospective investigations have not indicated poor inhibitory performance of (S)-4-CPG in a way that sheds light on its apparent inefficacy in pain relief.

As SSZ was engineered as a combination of the antibiotic sulfapyridine and the anti-inflammatory 5-aminosalicylic acid intended for administration as a prodrug that would activate following oral administration, the possibility has been raised that SSZ may act to relieve pain not intact at cancer cell system x_C^- in these animal models, but rather as its constituent anti-inflammatory 5-aminosalicylic acid. Cleavage of the azo bond that joins the two subsidiaries of SSZ; however, is solely performed in animals by intestinal bacteria (Peppercorn & Goldman, 1972). In humans with normal colonic states, only ~60% of the drug is metabolized to its two constituents when administered orally (Wahl

et al., 1998). The intraperitoneal route of administration in these animal models eliminates exposure of SSZ to colonic bacteria, and the sterile housing requirement of the nude mice further reduces bacterial exposure of the treated animals, eliminating the expectation that SSZ could be metabolized beyond its intact state in test animals.

SSZ is also currently being clinically investigated in the treatment of malignant glioma through action at the system x_C^- transporter on glioma cells (de Groot & Sontheimer, 2011). In higher concentrations than those utilized in this project, the more complete elimination of the system x_C^- transport function deprives the cancer cell of cystine for oxidative stress protection and eliminates the autocrine/paracrine growth and metastasis effects and host tissue destruction of glutamate to the extent that cell mortality is greatly increased (Chung et al., 2005), and cellular resistance to chemotherapy is decreased (Y. Huang & Sadée, 2006). This approach could also be investigated in the treatment of metastatic cancers in bone in conjunction with effects on the limitation of pain.

Conclusion

In cancer cells, glutamate release is understood to be a side-effect of the cellular response to oxidative stress to upregulate the expression and activity of system x_C^- to allow the increased uptake of cystine. The clinical implications of the attenuation of both cystine uptake and glutamate release extend to multiple types of cancers and to other diverse disease states. This is the first project to examine the inhibition of system x_C^- in the interests of pain management. Cancer-induced bone pain is a multifaceted and unique

pain state whose treatment has been approached from many angles, but remains elusive to control. Current therapies are limited by dose-dependent side-effects that negatively impact the quality of life of patients. This project has demonstrated a reduction in pain and a delay to the time of onset of pain in animal models of human breast cancer-induced bone pain through treatment with the system x_C^- inhibitor sulfasalazine.

The outcome of this project implies a mechanistic treatment of pain at the source of pain initiation. The elimination or reduction of glutamate secretion from a metastatic tumour in bone removes a disruptive cell signalling molecule and algogenic substance from the extracellular environment at the site of metastasis. If fully realized, this approach to pain management has the potential to limit central treatment induced side effects and to relieve the pathological states that are initially responsible for the provocation of pain.

Future Directions

This research can be continued in a plethora of directions. Our lab has begun to examine the influence of the above treatments on neurotrophin expression at the tumour site in bone, specifically NGF and BDNF, and their receptors TrkA, TrkB, and p75. Staining for the neuronal marker CGRP has also begun. Other models of cancer-induced bone pain have demonstrated the influence of the neurotrophins and of neurogenesis in the generation and maintenance of pain, and we are investigating any correlation between those and tumour-secreted glutamate.

It would be immediately valuable to evaluate the expression of xCT in patient-derived tumour samples. Functional system x_C^- has been confirmed in cultured cells immediately derived from patient tumours (Collins et al., 1998); however, as discussed earlier, the ability of cell-culture conditions to induce xCT expression and system x_C^- function in cells ensures that claims of system x_C^- function in cancers must be confirmed in patient tumours.

To directly assuage the concern of drug action at sites other than cancer cell system x_C^-, a relevant progression of this animal model could be to induce bone tumours with cancer cells molecularly modified to be without functional system x_C^-, provided the cells could survive implantation. To compare these models to those of normal cancer cell induced mice would not solve for tumour size discrepancies, as cancer cells without system x_C^- would likely exhibit limited growth, but pharmacological treatments would be unnecessary. This model could be used to assess both cancer-induced bone pain and tumour progression and response to treatment.

The sequestration of glutamate in cells in response to system x_C^- inhibition is a response that must be validated *in vitro.* Preliminary testing is underway through the growth of cells in exposure to SSZ and (S)-4-CPG, followed by their wash, harvest, and lysis. The resulting intracellular solution is measured for glutamate concentration uning the AMPLEX Red method.

Another use for this model is in the investigation of breakthrough cancer pain. Our lab has begun to investigate the possibility of the provocation of incident pain in

cancer-induced bone pain models through forced ambulation or exercise. To investigate the role of system x_C^- inhibition in the initiation of breakthrough pain, SSZ could be administered to model animals either steadily *via* osmotic pump, or prior to ambulation. Behavioural measurements taken before and after ambulation may indicate the extent of the influence of tumour derived glutamate in incident pain.

Reference List

Alzet. (2008). ALZET Technical Information Manual.

Anderson, H. C. (2003). Matrix vesicles and calcification. *Curr Rheumatol Rep, 5*(3), 222-226.

Angelini, G., Gardella, S., Ardy, M., Ciriolo, M. R., Filomeni, G., Di Trapani, G., Clarke, F., Sitia, R., & Rubartelli, A. (2002). Antigen-presenting dendritic cells provide the reducing extracellular microenvironment required for T lymphocyte activation. *Proc Natl Acad Sci U S A, 99*(3), 1491-1496.

Arcella, A., Carpinelli, G., Battaglia, G., D'Onofrio, M., Santoro, F., Ngomba, R. T., Bruno, V., Casolini, P., Giangaspero, F., & Nicoletti, F. (2005). Pharmacological blockade of group II metabotropic glutamate receptors reduces the growth of glioma cells in vivo. *Neuro Oncol, 7*(3), 236-245.

Armstrong, N., & Gouaux, E. (2000). Mechanisms for activation and antagonism of an AMPA-sensitive glutamate receptor: crystal structures of the GluR2 ligand binding core. *Neuron, 28*(1), 165-181.

Aslan, D., Andersen, M. D., Gede, L. B., de Franca, T. K., Jorgensen, S. R., Schwarz, P., & Jorgensen, N. R. (2012). Mechanisms for the bone anabolic effect of parathyroid hormone treatment in humans. *Scand J Clin Lab Invest, 72*(1), 14-22.

Balendiran, G. K., Dabur, R., & Fraser, D. (2004). The role of glutathione in cancer. *Cell Biochem Funct, 22*(6), 343-352.

Banjac, A., Perisic, T., Sato, H., Seiler, A., Bannai, S., Weiss, N., Kolle, P., Tschoep, K., Issels, R. D., Daniel, P. T., Conrad, M., & Bornkamm, G. W. (2008). The cystine/cysteine cycle: a redox cycle regulating susceptibility versus resistance to cell death. *Oncogene, 27*(11), 1618-1628.

Bannai, S. (1986). Exchange of cystine and glutamate across plasma membrane of human fibroblasts. *J Biol Chem, 261*(5), 2256-2263.

Bannai, S., & Ishii, T. (1988). A novel function of glutamine in cell culture: utilization of glutamine for the uptake of cystine in human fibroblasts. *J Cell Physiol, 137*(2), 360-366.

Bannai, S., & Kitamura, E. (1980). Transport interaction of L-cystine and L-glutamate in human diploid fibroblasts in culture. *J Biol Chem, 255*(6), 2372-2376.

Bassi, M. T., Gasol, E., Manzoni, M., Pineda, M., Riboni, M., Martin, R., Zorzano, A., Borsani, G., & Palacin, M. (2001). Identification and characterisation of human xCT that co-expresses, with 4F2 heavy chain, the amino acid transport activity system xc. *Pflugers Arch, 442*(2), 286-296.

Bellido, T., Ali, A. A., Plotkin, L. I., Fu, Q., Gubrij, I., Roberson, P. K., Weinstein, R. S., O'Brien, C. A., Manolagas, S. C., & Jilka, R. L. (2003). Proteasomal degradation of Runx2 shortens parathyroid hormone-induced anti-apoptotic signaling in osteoblasts. A putative explanation for why intermittent administration is needed for bone anabolism. *J Biol Chem, 278*(50), 50259-50272.

Benyamin, R., Trescot, A. M., Datta, S., Buenaventura, R., Adlaka, R., Sehgal, N., Glaser, S. E., & Vallejo, R. (2008). Opioid complications and side effects. *Pain Physician, 11*(2 Suppl), S105-120.

Bergstrom, J., Furst, P., Noree, L. O., & Vinnars, E. (1974). Intracellular free amino acid concentration in human muscle tissue. *J Appl Physiol, 36*(6), 693-697.

Bleakman, D., Alt, A., & Nisenbaum, E. S. (2006). Glutamate receptors and pain. *Semin Cell Dev Biol, 17*(5), 592-604.

Bloom, A. P., Jimenez-Andrade, J. M., Taylor, R. N., Castaneda-Corral, G., Kaczmarska, M. J., Freeman, K. T., Coughlin, K. A., Ghilardi, J. R., Kuskowski, M. A., & Mantyh, P. W. (2011). Breast cancer-induced bone remodeling, skeletal pain, and sprouting of sensory nerve fibers. *J Pain, 12*(6), 698-711.

Bord, S., Horner, A., Beavan, S., & Compston, J. (2001). Estrogen receptors alpha and beta are differentially expressed in developing human bone. *J Clin Endocrinol Metab, 86*(5), 2309-2314.

Boyce, S., & Hill, R. G. (2004). Substance P (NK1) Receptor Antagonists—Analgesics or Not? In P. Holzer (Ed.), (Vol. 164, pp. 441-457): Springer Berlin Heidelberg.

Brater, D. C. (1999). Effects of nonsteroidal anti-inflammatory drugs on renal function: focus on cyclooxygenase-2-selective inhibition. *Am J Med, 107*(6A), 65S-70S; discussion 70S-71S.

Brown, J., Barrios, C., Diel, I., Facon, T., Fizazi, K., & Ibrahim, T. (2010). *Incidence and outcomes of Osteonecrosis of the Jaw from an Integrated Analysis of Three Pivotal Randomized Double-Blind, Double-Dummy Phase 3 Trials Comparing Denosumab and Zoledronic Acid for Treatment of Bone Metastases in Advanced Cancer Patients or Myeloma*. Paper presented at the 10th International Conference on Cancer-Induced Bone Disease, Sheffield, UK.

Buckingham, S. C., Campbell, S. L., Haas, B. R., Montana, V., Robel, S., Ogunrinu, T., & Sontheimer, H. (2011). Glutamate release by primary brain tumors induces epileptic activity. *Nat Med, 17*(10), 1269-1274.

Burdo, J., Dargusch, R., & Schubert, D. (2006). Distribution of the cystine/glutamate antiporter system xc- in the brain, kidney, and duodenum. *J Histochem Cytochem, 54*(5), 549-557.

Cairns, B. E., Svensson, P., Wang, K., Castrillon, E., Hupfeld, S., Sessle, B. J., & Arendt-Nielsen, L. (2006). Ketamine attenuates glutamate-induced mechanical sensitization of the masseter muscle in human males. *Exp Brain Res, 169*(4), 467-472.

Caraceni, A., & Portenoy, R. K. (1999). An international survey of cancer pain characteristics and syndromes. IASP Task Force on Cancer Pain. International Association for the Study of Pain. *Pain, 82*(3), 263-274.

Carlton, S. M., & Coggeshall, R. E. (1999). Inflammation-induced changes in peripheral glutamate receptor populations. *Brain Res, 820*(1-2), 63-70.

Carlton, S. M., Hargett, G. L., & Coggeshall, R. E. (1995). Localization and activation of glutamate receptors in unmyelinated axons of rat glabrous skin. *Neurosci Lett, 197*(1), 25-28.

Casuccio, A., Mercadante, S., & Fulfaro, F. (2009). Treatment strategies for cancer patients with breakthrough pain. *Expert Opin Pharmacother, 10*(6), 947-953.

Chenu, C. (2002). Glutamatergic innervation in bone. *Microsc Res Tech, 58*(2), 70-76.

Chenu, C., Serre, C. M., Raynal, C., Burt-Pichat, B., & Delmas, P. D. (1998). Glutamate receptors are expressed by bone cells and are involved in bone resorption. *Bone, 22*(4), 295-299.

Chillarón, J., Roca, R., Valencia, A., Zorzano, A., & Palacin, M. (2001). Heteromeric amino acid transporters: biochemistry, genetics, and physiology. *Am J Physiol Renal Physiol, 281*(6), F995-1018.

Cho, Y., & Bannai, S. (1990). Uptake of glutamate and cysteine in C-6 glioma cells and in cultured astrocytes. *J Neurochem, 55*(6), 2091-2097.

Choi, D. W. (1988). Glutamate neurotoxicity and diseases of the nervous system. *Neuron, 1*(8), 623-634.

Christensen, H. N. (1984). Naming plan for membrane transport systems for amino acids. *Neurochem Res, 9*(12), 1757-1758.

Chung, W. J., Lyons, S. A., Nelson, G. M., Hamza, H., Gladson, C. L., Gillespie, G. Y., & Sontheimer, H. (2005). Inhibition of cystine uptake disrupts the growth of primary brain tumors. *J Neurosci, 25*(31), 7101-7110.

Cleeland, C. S., Gonin, R., Baez, L., Loehrer, P., & Pandya, K. J. (1997). Pain and treatment of pain in minority patients with cancer. The Eastern Cooperative Oncology Group Minority Outpatient Pain Study. *Ann Intern Med, 127*(9), 813-816.

Clines, G. A., & Guise, T. A. (2008). Molecular mechanisms and treatment of bone metastasis. *Expert Rev Mol Med, 10*, e7.

Coggeshall, R. E., & Carlton, S. M. (1998). Ultrastructural analysis of NMDA, AMPA, and kainate receptors on unmyelinated and myelinated axons in the periphery. *J Comp Neurol, 391*(1), 78-86.

Coleman, R. E. (1997). Skeletal complications of malignancy. *Cancer, 80*(8 Suppl), 1588-1594.

Coleman, R. E. (2006). Clinical features of metastatic bone disease and risk of skeletal morbidity. *Clin Cancer Res, 12*(20 Pt 2), 6243s-6249s.

Coleman, R. E., & Rubens, R. D. (1987). The clinical course of bone metastases from breast cancer. *Br J Cancer, 55*(1), 61-66.

Collins, C. L., Wasa, M., Souba, W. W., & Abcouwer, S. F. (1998). Determinants of glutamine dependence and utilization by normal and tumor-derived breast cell lines. *J Cell Physiol, 176*(1), 166-178.

Danbolt, N. C. (2001). Glutamate uptake. *Prog Neurobiol, 65*(1), 1-105.

de Groot, J., & Sontheimer, H. (2011). Glutamate and the biology of gliomas. *Glia, 59*(8), 1181-1189.

de Paula, F. J., & Rosen, C. J. (2010). Back to the future: revisiting parathyroid hormone and calcitonin control of bone remodeling. *Horm Metab Res, 42*(5), 299-306.

Dingledine, R., Borges, K., Bowie, D., & Traynelis, S. F. (1999). The glutamate receptor ion channels. *Pharmacol Rev, 51*(1), 7-61.

Dore-Savard, L., Otis, V., Belleville, K., Lemire, M., Archambault, M., Tremblay, L., Beaudoin, J. F., Beaudet, N., Lecomte, R., Lepage, M., Gendron, L., & Sarret, P. (2010). Behavioral, medical imaging and histopathological features of a new rat model of bone cancer pain. *PLoS One, 5*(10), e13774.

Doxsee, D. W., Gout, P. W., Kurita, T., Lo, M., Buckley, A. R., Wang, Y., Xue, H., Karp, C. M., Cutz, J. C., Cunha, G. R., & Wang, Y. Z. (2007). Sulfasalazine-induced cystine starvation: potential use for prostate cancer therapy. *Prostate, 67*(2), 162-171.

Drake, M. T., Clarke, B. L., & Khosla, S. (2008). Bisphosphonates: mechanism of action and role in clinical practice. *Mayo Clin Proc, 83*(9), 1032-1045.

Drdla, R., & Sandkuhler, J. (2008). Long-term potentiation at C-fibre synapses by low-level presynaptic activity in vivo. *Mol Pain, 4*, 18.

Duivenvoorden, W. C., Popovic, S. V., Lhotak, S., Seidlitz, E., Hirte, H. W., Tozer, R. G., & Singh, G. (2002). Doxycycline decreases tumor burden in a bone metastasis model of human breast cancer. *Cancer Res, 62*(6), 1588-1591.

Eck, H. P., & Droge, W. (1989). Influence of the extracellular glutamate concentration on the intracellular cyst(e)ine concentration in macrophages and on the capacity to release cysteine. *Biol Chem Hoppe Seyler, 370*(2), 109-113.

Eilon, G., & Mundy, G. R. (1978). Direct resorption of bone by human breast cancer cells in vitro. *Nature, 276*(5689), 726-728.

el-Hajj Fuleihan, G., Chen, C. J., Rivkees, S. A., Marynick, S. P., Stock, J., Pallotta, J. A., & Brown, E. M. (1989). Calcium-dependent release of N-terminal fragments and intact immunoreactive parathyroid hormone by human pathological parathyroid tissue in vitro. *J Clin Endocrinol Metab, 69*(4), 860-867.

Ferrarese, C., Pecora, N., Frigo, M., Appollonio, I., & Frattola, L. (1993). Assessment of reliability and biological significance of glutamate levels in cerebrospinal fluid. *Ann Neurol, 33*(3), 316-319.

Fiermonte, G., Palmieri, L., Todisco, S., Agrimi, G., Palmieri, F., & Walker, J. E. (2002). Identification of the mitochondrial glutamate transporter. Bacterial expression, reconstitution, functional characterization, and tissue distribution of two human isoforms. *J Biol Chem, 277*(22), 19289-19294.

Foebel, A., & Singh, G. (2006). *A combination metronomic chemotherapy model for prostate cancer.* Hamilton, ON: McMaster University.

Forslund, A. H., Hambraeus, L., van Beurden, H., Holmback, U., El-Khoury, A. E., Hjorth, G., Olsson, R., Stridsberg, M., Wide, L., Akerfeldt, T., Regan, M., & Young, V. R. (2000). Inverse relationship between protein intake and plasma free amino acids in healthy men at physical exercise. *Am J Physiol Endocrinol Metab, 278*(5), E857-867.

Fuller, K., Kirstein, B., & Chambers, T. J. (2007). Regulation and enzymatic basis of bone resorption by human osteoclasts. *Clin Sci (Lond), 112*(11), 567-575.

Fundytus, M. E. (2001). Glutamate receptors and nociception: implications for the drug treatment of pain. *CNS Drugs, 15*(1), 29-58.

Gabriel, A. F., Marcus, M. A., Walenkamp, G. H., & Joosten, E. A. (2009). The CatWalk method: assessment of mechanical allodynia in experimental chronic pain. *Behav Brain Res, 198*(2), 477-480.

Gasol, E., Jimenez-Vidal, M., Chillaron, J., Zorzano, A., & Palacin, M. (2004). Membrane topology of system xc- light subunit reveals a re-entrant loop with substrate-restricted accessibility. *J Biol Chem, 279*(30), 31228-31236.

Gatenby, R. A., Gawlinski, E. T., Gmitro, A. F., Kaylor, B., & Gillies, R. J. (2006). Acid-mediated tumor invasion: a multidisciplinary study. *Cancer Res, 66*(10), 5216-5223.

Gazerani, P., Wang, K., Cairns, B. E., Svensson, P., & Arendt-Nielsen, L. (2006). Effects of subcutaneous administration of glutamate on pain, sensitization and vasomotor responses in healthy men and women. *Pain, 124*(3), 338-348.

Genever, P. G., & Skerry, T. M. (2001). Regulation of spontaneous glutamate release activity in osteoblastic cells and its role in differentiation and survival: evidence for intrinsic glutamatergic signaling in bone. *FASEB J, 15*(9), 1586-1588.

Giacometti, T. (1979). Free and bound glutamate in natural products. In L. Filer, S. Garattini, M. Kare, W. Reynolds & R. Wurtman (Eds.), *Glutamic acid: advances in biochemistry and physiology* (pp. 25–34). New York: Raven Press.

Gochenauer, G. E., & Robinson, M. B. (2001). Dibutyryl-cAMP (dbcAMP) up-regulates astrocytic chloride-dependent L-[3H]glutamate transport and expression of both system xc(-) subunits. *J Neurochem, 78*(2), 276-286.

Gout, P. W., Buckley, A. R., Simms, C. R., & Bruchovsky, N. (2001). Sulfasalazine, a potent suppressor of lymphoma growth by inhibition of the x(c)- cystine transporter: a new action for an old drug. *Leukemia, 15*(10), 1633-1640.

Gruetter, R., Seaquist, E. R., Kim, S., & Ugurbil, K. (1998). Localized in vivo 13C-NMR of glutamate metabolism in the human brain: initial results at 4 tesla. *Dev Neurosci, 20*(4-5), 380-388.

Gu, Y., Genever, P. G., Skerry, T. M., & Publicover, S. J. (2002). The NMDA type glutamate receptors expressed by primary rat osteoblasts have the same electrophysiological characteristics as neuronal receptors. *Calcif Tissue Int, 70*(3), 194-203.

Guan, J., Lo, M., Dockery, P., Mahon, S., Karp, C. M., Buckley, A. R., Lam, S., Gout, P. W., & Wang, Y. Z. (2009). The xc- cystine/glutamate antiporter as a potential therapeutic target for small-cell lung cancer: use of sulfasalazine. *Cancer Chemother Pharmacol, 64*(3), 463-472.

Guise, T. A., Yin, J. J., Taylor, S. D., Kumagai, Y., Dallas, M., Boyce, B. F., Yoneda, T., & Mundy, G. R. (1996). Evidence for a causal role of parathyroid hormone-related protein in the pathogenesis of human breast cancer-mediated osteolysis. *J Clin Invest, 98*(7), 1544-1549.

Hadjidakis, D. J., & Androulakis, II. (2006). Bone remodeling. *Ann N Y Acad Sci, 1092*, 385-396.

Halliwell, B. (2007). Oxidative stress and cancer: have we moved forward? *Biochem J, 401*(1), 1-11.

Halvorson, K. G., Sevcik, M. A., Ghilardi, J. R., Rosol, T. J., & Mantyh, P. W. (2006). Similarities and differences in tumor growth, skeletal remodeling and pain in an osteolytic and osteoblastic model of bone cancer. *Clin J Pain, 22*(7), 587-600.

Hanahan, D., & Weinberg, R. A. (2011). Hallmarks of cancer: the next generation. *Cell, 144*(5), 646-674.

Harrington, J. F., Messier, A. A., Bereiter, D., Barnes, B., & Epstein, M. H. (2000). Herniated lumbar disc material as a source of free glutamate available to affect pain signals through the dorsal root ganglion. *Spine (Phila Pa 1976), 25*(8), 929-936.

Hawkins, R. A., DeJoseph, M. R., & Hawkins, P. A. (1995). Regional brain glutamate transport in rats at normal and raised concentrations of circulating glutamate. *Cell Tissue Res, 281*(2), 207-214.

Hinoi, E., Fujimori, S., Nakamura, Y., & Yoneda, Y. (2001). Group III metabotropic glutamate receptors in rat cultured calvarial osteoblasts. *Biochem Biophys Res Commun, 281*(2), 341-346.

Hinoi, E., Fujimori, S., Takarada, T., Taniura, H., & Yoneda, Y. (2002). Facilitation of glutamate release by ionotropic glutamate receptors in osteoblasts. *Biochem Biophys Res Commun, 297*(3), 452-458.

Hinoi, E., Fujimori, S., Takemori, A., Kurabayashi, H., Nakamura, Y., & Yoneda, Y. (2002). Demonstration of expression of mRNA for particular AMPA and kainate receptor subunits in immature and mature cultured rat calvarial osteoblasts. *Brain Res, 943*(1), 112-116.

Hinoi, E., Fujimori, S., & Yoneda, Y. (2003). Modulation of cellular differentiation by N-methyl-D-aspartate receptors in osteoblasts. *FASEB J, 17*(11), 1532-1534.

Hinoi, E., Takarada, T., & Yoneda, Y. (2004). Glutamate signaling system in bone. *J Pharmacol Sci, 94*(3), 215-220.

Ho, M. L., Tsai, T. N., Chang, J. K., Shao, T. S., Jeng, Y. R., & Hsu, C. (2005). Down-regulation of N-methyl D-aspartate receptor in rat-modeled disuse osteopenia. *Osteoporos Int, 16*(12), 1780-1788.

Honore, P., Luger, N. M., Sabino, M. A., Schwei, M. J., Rogers, S. D., Mach, D. B., O'Keefe P, F., Ramnaraine, M. L., Clohisy, D. R., & Mantyh, P. W. (2000). Osteoprotegerin blocks bone cancer-induced skeletal destruction, skeletal pain and pain-related neurochemical reorganization of the spinal cord. *Nat Med, 6*(5), 521-528.

Honore, P., Rogers, S. D., Schwei, M. J., Salak-Johnson, J. L., Luger, N. M., Sabino, M. C., Clohisy, D. R., & Mantyh, P. W. (2000). Murine models of inflammatory, neuropathic and cancer pain each generates a unique set of neurochemical changes in the spinal cord and sensory neurons. *Neuroscience, 98*(3), 585-598.

Huang, J., Chang, J. Y., Woodward, D. J., Baccala, L. A., Han, J. S., Wang, J. Y., & Luo, F. (2006). Dynamic neuronal responses in cortical and thalamic areas during different phases of formalin test in rats. *Exp Neurol, 200*(1), 124-134.

Huang, J. C., Sakata, T., Pfleger, L. L., Bencsik, M., Halloran, B. P., Bikle, D. D., & Nissenson, R. A. (2004). PTH differentially regulates expression of RANKL and OPG. *J Bone Miner Res, 19*(2), 235-244.

Huang, Y., Dai, Z., Barbacioru, C., & Sadee, W. (2005). Cystine-glutamate transporter SLC7A11 in cancer chemosensitivity and chemoresistance. *Cancer Res, 65*(16), 7446-7454.

Huang, Y., & Sadée, W. (2006). Membrane transporters and channels in chemoresistance and -sensitivity of tumor cells. *Cancer Lett, 239*(2), 168-182.

Huang, Y., Zhou, Y., Fan, Y., & Zhou, D. (2008). Celastrol inhibits the growth of human glioma xenografts in nude mice through suppressing VEGFR expression. *Cancer Lett, 264*(1), 101-106.

Hwang, C., Sinskey, A. J., & Lodish, H. F. (1992). Oxidized redox state of glutathione in the endoplasmic reticulum. *Science, 257*(5076), 1496-1502.

IARC. (2010). Globocan 2008. from http://globocan.iarc.fr/factsheets/populations/factsheet.asp?uno=900

Ishii, I., Akahoshi, N., Yu, X. N., Kobayashi, Y., Namekata, K., Komaki, G., & Kimura, H. (2004). Murine cystathionine gamma-lyase: complete cDNA and genomic sequences, promoter activity, tissue distribution and developmental expression. *Biochem J, 381*(Pt 1), 113-123.

Ishii, T., Sugita, Y., & Bannai, S. (1987). Regulation of glutathione levels in mouse spleen lymphocytes by transport of cysteine. *J Cell Physiol, 133*(2), 330-336.

Ishiuchi, S., Tsuzuki, K., Yoshida, Y., Yamada, N., Hagimura, N., Okado, H., Miwa, A., Kurihara, H., Nakazato, Y., Tamura, M., Sasaki, T., & Ozawa, S. (2002). Blockage of Ca(2+)-permeable AMPA receptors suppresses migration and induces apoptosis in human glioblastoma cells. *Nat Med, 8*(9), 971-978.

Jang, J. H., Kim, D. W., Sang Nam, T., Se Paik, K., & Leem, J. W. (2004). Peripheral glutamate receptors contribute to mechanical hyperalgesia in a neuropathic pain model of the rat. *Neuroscience, 128*(1), 169-176.

Jimenez-Andrade, J. M., Ghilardi, J. R., Castaneda-Corral, G., Kuskowski, M. A., & Mantyh, P. W. (2011). Preventive or late administration of anti-NGF therapy attenuates tumor-induced nerve sprouting, neuroma formation, and cancer pain. *Pain, 152*(11), 2564-2574.

Jimenez-Andrade, J. M., Mantyh, W. G., Bloom, A. P., Ferng, A. S., Geffre, C. P., & Mantyh, P. W. (2010). Bone cancer pain. *Ann N Y Acad Sci, 1198*, 173-181.

Kaleeba, J. A., & Berger, E. A. (2006). Kaposi's sarcoma-associated herpesvirus fusion-entry receptor: cystine transporter xCT. *Science, 311*(5769), 1921-1924.

Kato, S., Ishita, S., Sugawara, K., & Mawatari, K. (1993). Cystine/glutamate antiporter expression in retinal Muller glial cells: implications for DL-alpha-aminoadipate toxicity. *Neuroscience, 57*(2), 473-482.

Kato, S., Negishi, K., Mawatari, K., & Kuo, C. H. (1992). A mechanism for glutamate toxicity in the C6 glioma cells involving inhibition of cystine uptake leading to glutathione depletion. *Neuroscience, 48*(4), 903-914.

Kau, K. S., Madayag, A., Mantsch, J. R., Grier, M. D., Abdulhameed, O., & Baker, D. A. (2008). Blunted cystine-glutamate antiporter function in the nucleus accumbens promotes cocaine-induced drug seeking. *Neuroscience, 155*(2), 530-537.

Kim, J. W., & Dang, C. V. (2006). Cancer's molecular sweet tooth and the Warburg effect. *Cancer Res, 66*(18), 8927-8930.

Kim, J. Y., Kanai, Y., Chairoungdua, A., Cha, S. H., Matsuo, H., Kim, D. K., Inatomi, J., Sawa, H., Ida, Y., & Endou, H. (2001). Human cystine/glutamate transporter: cDNA cloning and upregulation by oxidative stress in glioma cells. *Biochim Biophys Acta, 1512*(2), 335-344.

Komarova, S. V. (2005). Mathematical model of paracrine interactions between osteoclasts and osteoblasts predicts anabolic action of parathyroid hormone on bone. *Endocrinology, 146*(8), 3589-3595.

Kousteni, S., Almeida, M., Han, L., Bellido, T., Jilka, R. L., & Manolagas, S. C. (2007). Induction of osteoblast differentiation by selective activation of kinase-mediated actions of the estrogen receptor. *Mol Cell Biol, 27*(4), 1516-1530.

Koyama, Y., Ishibashi, T., & Baba, A. (1995). Increase in chloride-dependent L-glutamate transport activity in synaptic membrane after in vitro ischemic treatment. *J Neurochem, 65*(4), 1798-1804.

Kroemer, G., & Pouyssegur, J. (2008). Tumor cell metabolism: cancer's Achilles' heel. *Cancer Cell, 13*(6), 472-482.

Le, A., Cooper, C. R., Gouw, A. M., Dinavahi, R., Maitra, A., Deck, L. M., Royer, R. E., Vander Jagt, D. L., Semenza, G. L., & Dang, C. V. (2010). Inhibition of lactate dehydrogenase A induces oxidative stress and inhibits tumor progression. *Proc Natl Acad Sci U S A, 107*(5), 2037-2042.

Lee, J., Weber, M., Mejia, S., Bone, E., Watson, P., & Orr, W. (2001). A matrix metalloproteinase inhibitor, batimastat, retards the development of osteolytic bone metastases by MDA-MB-231 human breast cancer cells in Balb C nu/nu mice. *Eur J Cancer, 37*(1), 106-113.

Lee, W. J., Hawkins, R. A., Vina, J. R., & Peterson, D. R. (1998). Glutamine transport by the blood-brain barrier: a possible mechanism for nitrogen removal. *Am J Physiol, 274*(4 Pt 1), C1101-1107.

Lewerenz, J., Sato, H., Albrecht, P., Henke, N., Noack, R., Methner, A., & Maher, P. (2011). Mutation of ATF4 mediates resistance of neuronal cell lines against oxidative stress by inducing xCT expression. *Cell Death Differ*.

Liao, J., Li, X., Koh, A. J., Berry, J. E., Thudi, N., Rosol, T. J., Pienta, K. J., & McCauley, L. K. (2008). Tumor expressed PTHrP facilitates prostate cancer-induced osteoblastic lesions. *Int J Cancer, 123*(10), 2267-2278.

Lim, J. C., & Donaldson, P. J. (2011). Focus on molecules: the cystine/glutamate exchanger (System x(c)(-)). *Exp Eye Res, 92*(3), 162-163.

Lin, T. H., Yang, R. S., Tang, C. H., Wu, M. Y., & Fu, W. M. (2008). Regulation of the maturation of osteoblasts and osteoclastogenesis by glutamate. *Eur J Pharmacol, 589*(1-3), 37-44.

Liotta, L. A. (2001). An attractive force in metastasis. *Nature, 410*(6824), 24-25.

Liu, D., Jiang, L. S., & Dai, L. Y. (2007). Substance P and its receptors in bone metabolism. *Neuropeptides, 41*(5), 271-283.

Ljusberg, J., Wang, Y., Lang, P., Norgard, M., Dodds, R., Hultenby, K., Ek-Rylander, B., & Andersson, G. (2005). Proteolytic excision of a repressive loop domain in tartrate-resistant acid phosphatase by cathepsin K in osteoclasts. *J Biol Chem, 280*(31), 28370-28381.

Llinas, R., Steinberg, I. Z., & Walton, K. (1981). Relationship between presynaptic calcium current and postsynaptic potential in squid giant synapse. *Biophys J, 33*(3), 323-351.

Lo, M., Ling, V., Wang, Y. Z., & Gout, P. W. (2008). The xc- cystine/glutamate antiporter: a mediator of pancreatic cancer growth with a role in drug resistance. *Br J Cancer, 99*(3), 464-472.

Lo, M., Wang, Y. Z., & Gout, P. W. (2008). The x(c)- cystine/glutamate antiporter: a potential target for therapy of cancer and other diseases. *J Cell Physiol, 215*(3), 593-602.

Loeser, J. D., & Treede, R. D. (2008). The Kyoto protocol of IASP Basic Pain Terminology. *Pain, 137*(3), 473-477.

Lyons, S. A., Chung, W. J., Weaver, A. K., Ogunrinu, T., & Sontheimer, H. (2007). Autocrine glutamate signaling promotes glioma cell invasion. *Cancer Res, 67*(19), 9463-9471.

Mach, D. B., Rogers, S. D., Sabino, M. C., Luger, N. M., Schwei, M. J., Pomonis, J. D., Keyser, C. P., Clohisy, D. R., Adams, D. J., O'Leary, P., & Mantyh, P. W. (2002). Origins of skeletal pain: sensory and sympathetic innervation of the mouse femur. *Neuroscience, 113*(1), 155-166.

Mackie, E. J. (2003). Osteoblasts: novel roles in orchestration of skeletal architecture. *Int J Biochem Cell Biol, 35*(9), 1301-1305.

MacLean, D. M. (2009). The delta2 glutamate-like receptor undergoes similar conformational changes as other ionotropic glutamate receptors. *J Neurosci, 29*(21), 6767-6768.

Mak, I. W., Seidlitz, E. P., Cowan, R. W., Turcotte, R. E., Popovic, S., Wu, W. C., Singh, G., & Ghert, M. (2010). Evidence for the role of matrix metalloproteinase-13 in bone resorption by giant cell tumor of bone. *Hum Pathol, 41*(9), 1320-1329.

Mann, K. A., Lee, J., Arrington, S. A., Damron, T. A., & Allen, M. J. (2008). Predicting distal femur bone strength in a murine model of tumor osteolysis. *Clin Orthop Relat Res, 466*(6), 1271-1278.

Mantyh, P. W., Koltzenburg, M., Mendell, L. M., Tive, L., & Shelton, D. L. (2011). Antagonism of nerve growth factor-TrkA signaling and the relief of pain. *Anesthesiology, 115*(1), 189-204.

Mantyh, W. G., Jimenez-Andrade, J. M., Stake, J. I., Bloom, A. P., Kaczmarska, M. J., Taylor, R. N., Freeman, K. T., Ghilardi, J. R., Kuskowski, M. A., & Mantyh, P. W. (2010). Blockade of nerve sprouting and neuroma formation markedly attenuates the development of late stage cancer pain. *Neuroscience, 171*(2), 588-598.

Marie, P. J. (2008). Transcription factors controlling osteoblastogenesis. *Arch Biochem Biophys, 473*(2), 98-105.

Mason, D. J., Suva, L. J., Genever, P. G., Patton, A. J., Steuckle, S., Hillam, R. A., & Skerry, T. M. (1997). Mechanically regulated expression of a neural glutamate transporter in bone: a role for excitatory amino acids as osteotropic agents? *Bone, 20*(3), 199-205.

Massie, A., Schallier, A., Mertens, B., Vermoesen, K., Bannai, S., Sato, H., Smolders, I., & Michotte, Y. (2008). Time-dependent changes in striatal xCT protein expression in hemi-Parkinson rats. *Neuroreport, 19*(16), 1589-1592.

Mayer, M. L. (2005). Glutamate receptor ion channels. *Curr Opin Neurobiol, 15*(3), 282-288.

McKenzie, J. A., Bixby, E. C., & Silva, M. J. (2011). Differential gene expression from microarray analysis distinguishes woven and lamellar bone formation in the rat ulna following mechanical loading. *PLoS One, 6*(12), e29328.

McNearney, T., Speegle, D., Lawand, N., Lisse, J., & Westlund, K. N. (2000). Excitatory amino acid profiles of synovial fluid from patients with arthritis. *J Rheumatol, 27*(3), 739-745.

Meldrum, B. S. (2000). Glutamate as a neurotransmitter in the brain: review of physiology and pathology. *J Nutr, 130*(4S Suppl), 1007S-1015S.

Meloni, F., Brocchieri, A., Ballabio, P. C., Tua, A., Grignani, G., & Grassi, G. G. (1998). Bombesin, calcium homeostasis and tumour growth. *Monaldi Arch Chest Dis, 53*(4), 405-409.

Mercadante, S. (1997). Malignant bone pain: pathophysiology and treatment. *Pain, 69*(1-2), 1-18.

Mercadante, S. (1999). Pain treatment and outcomes for patients with advanced cancer who receive follow-up care at home. *Cancer, 85*(8), 1849-1858.

Merighi, A., Salio, C., Ghirri, A., Lossi, L., Ferrini, F., Betelli, C., & Bardoni, R. (2008). BDNF as a pain modulator. *Prog Neurobiol, 85*(3), 297-317.

Meuser, T., Pietruck, C., Radbruch, L., Stute, P., Lehmann, K. A., & Grond, S. (2001). Symptoms during cancer pain treatment following WHO-guidelines: a longitudinal follow-up study of symptom prevalence, severity and etiology. *Pain, 93*(3), 247-257.

Miyaji, T., Echigo, N., Hiasa, M., Senoh, S., Omote, H., & Moriyama, Y. (2008). Identification of a vesicular aspartate transporter. *Proc Natl Acad Sci U S A, 105*(33), 11720-11724.

Morimoto, R., Uehara, S., Yatsushiro, S., Juge, N., Hua, Z., Senoh, S., Echigo, N., Hayashi, M., Mizoguchi, T., Ninomiya, T., Udagawa, N., Omote, H., Yamamoto, A., Edwards, R. H., & Moriyama, Y. (2006). Secretion of L-glutamate from osteoclasts through transcytosis. *EMBO J, 25*(18), 4175-4186.

Müller, A., Homey, B., Soto, H., Ge, N., Catron, D., Buchanan, M. E., McClanahan, T., Murphy, E., Yuan, W., Wagner, S. N., Barrera, J. L., Mohar, A., Verastegui, E., & Zlotnik, A. (2001). Involvement of chemokine receptors in breast cancer metastasis. *Nature, 410*(6824), 50-56.

Mundy, G. R. (2002). Metastasis to bone: causes, consequences and therapeutic opportunities. *Nat Rev Cancer, 2*(8), 584-593.

Murphy, T. H., Miyamoto, M., Sastre, A., Schnaar, R. L., & Coyle, J. T. (1989). Glutamate toxicity in a neuronal cell line involves inhibition of cystine transport leading to oxidative stress. *Neuron, 2*(6), 1547-1558.

Murphy, T. H., Schnaar, R. L., & Coyle, J. T. (1990). Immature cortical neurons are uniquely sensitive to glutamate toxicity by inhibition of cystine uptake. *FASEB J, 4*(6), 1624-1633.

Nagae, M., Hiraga, T., Wakabayashi, H., Wang, L., Iwata, K., & Yoneda, T. (2006). Osteoclasts play a part in pain due to the inflammation adjacent to bone. *Bone, 39*(5), 1107-1115.

Narang, V. S., Pauletti, G. M., Gout, P. W., Buckley, D. J., & Buckley, A. R. (2003). Suppression of cystine uptake by sulfasalazine inhibits proliferation of human mammary carcinoma cells. *Anticancer Res, 23*(6C), 4571-4579.

Naveh-Many, T. (2010). Minireview: the play of proteins on the parathyroid hormone messenger ribonucleic Acid regulates its expression. *Endocrinology, 151*(4), 1398-1402.

Nedergaard, M., Takano, T., & Hansen, A. J. (2002). Beyond the role of glutamate as a neurotransmitter. *Nat Rev Neurosci, 3*(9), 748-755.

Niswender, C. M., & Conn, P. J. (2010). Metabotropic glutamate receptors: physiology, pharmacology, and disease. *Annu Rev Pharmacol Toxicol, 50*, 295-322.

Noble, B. S. (2008). The osteocyte lineage. *Arch Biochem Biophys, 473*(2), 106-111.

O'Kane, R. L., Martinez-Lopez, I., DeJoseph, M. R., Vina, J. R., & Hawkins, R. A. (1999). Na(+)-dependent glutamate transporters (EAAT1, EAAT2, and EAAT3) of the blood-brain barrier. A mechanism for glutamate removal. *J Biol Chem, 274*(45), 31891-31895.

Okuno, S., Sato, H., Kuriyama-Matsumura, K., Tamba, M., Wang, H., Sohda, S., Hamada, H., Yoshikawa, H., Kondo, T., & Bannai, S. (2003). Role of cystine transport in intracellular glutathione level and cisplatin resistance in human ovarian cancer cell lines. *Br J Cancer, 88*(6), 951-956.

Omote, K., Kawamata, T., Kawamata, M., & Namiki, A. (1998). Formalin-induced release of excitatory amino acids in the skin of the rat hindpaw. *Brain Res, 787*(1), 161-164.

Orr, F. W., Lee, J., Duivenvoorden, W. C., & Singh, G. (2000). Pathophysiologic interactions in skeletal metastasis. *Cancer, 88*(12 Suppl), 2912-2918.

Ottaviano, F. G., Handy, D. E., & Loscalzo, J. (2008). Redox regulation in the extracellular environment. *Circ J, 72*(1), 1-16.

Paget, S. (1889). The distribution of secondary growths in cancer of the breast. . *Lancet, 1*, 571-573.

Pampliega, O., Domercq, M., Soria, F. N., Villoslada, P., Rodriguez-Antiguedad, A., & Matute, C. (2011). Increased expression of cystine/glutamate antiporter in multiple sclerosis. *J Neuroinflammation, 8*, 63.

Pargeon, K. L., & Hailey, B. J. (1999). Barriers to effective cancer pain management: a review of the literature. *J Pain Symptom Manage, 18*(5), 358-368.

Patel, S. A., Rajale, T., O'Brien, E., Burkhart, D. J., Nelson, J. K., Twamley, B., Blumenfeld, A., Szabon-Watola, M. I., Gerdes, J. M., Bridges, R. J., & Natale, N. R. (2010). Isoxazole analogues bind the system xc- transporter: structure-activity relationship and pharmacophore model. *Bioorg Med Chem, 18*(1), 202-213.

Patel, S. A., Warren, B. A., Rhoderick, J. F., & Bridges, R. J. (2004). Differentiation of substrate and non-substrate inhibitors of transport system xc(-): an obligate exchanger of L-glutamate and L-cystine. *Neuropharmacology, 46*(2), 273-284.

Peet, N. M., Grabowski, P. S., Laketic-Ljubojevic, I., & Skerry, T. M. (1999). The glutamate receptor antagonist MK801 modulates bone resorption in vitro by a mechanism predominantly involving osteoclast differentiation. *FASEB J, 13*(15), 2179-2185.

Peppercorn, M. A., & Goldman, P. (1972). The role of intestinal bacteria in the metabolism of salicylazosulfapyridine. *J Pharmacol Exp Ther, 181*(3), 555-562.

Perry, T. L. (1982). Cerebral amino acid pools. . In L. J. Filer (Ed.), *Handbook of neurochemistry* . (2nd ed., Vol. 1, pp. 151-180). New York: Plenum.

Peters, C. M., Ghilardi, J. R., Keyser, C. P., Kubota, K., Lindsay, T. H., Luger, N. M., Mach, D. B., Schwei, M. J., Sevcik, M. A., & Mantyh, P. W. (2005). Tumor-induced injury of primary afferent sensory nerve fibers in bone cancer pain. *Exp Neurol, 193*(1), 85-100.

Pfizer. (2009). A study of tanezumab as add-on therapy to opioid medication in patients with pain due to cancer that has spread to bone. NCT00545129., from http://clinicaltrials.gov

Pham, A. N., Blower, P. E., Alvarado, O., Ravula, R., Gout, P. W., & Huang, Y. (2010). Pharmacogenomic approach reveals a role for the x(c)- cystine/glutamate antiporter in growth and celastrol resistance of glioma cell lines. *J Pharmacol Exp Ther, 332*(3), 949-958.

Piani, D., & Fontana, A. (1994). Involvement of the cystine transport system xc- in the macrophage-induced glutamate-dependent cytotoxicity to neurons. *J Immunol, 152*(7), 3578-3585.

Powles, T., Paterson, A., McCloskey, E., Schein, P., Scheffler, B., Tidy, A., Ashley, S., Smith, I., Ottestad, L., & Kanis, J. (2006). Reduction in bone relapse and improved survival with oral clodronate for adjuvant treatment of operable breast cancer [ISRCTN83688026]. *Breast Cancer Res, 8*(2), R13.

Reichel, A., Begley, D. J., & Abbott, N. J. (2000). Carrier-mediated delivery of metabotrophic glutamate receptor ligands to the central nervous system: structural tolerance and potential of the L-system amino acid transporter at the blood-brain barrier. *J Cereb Blood Flow Metab, 20*(1), 168-174.

Rimaniol, A. C., Mialocq, P., Clayette, P., Dormont, D., & Gras, G. (2001). Role of glutamate transporters in the regulation of glutathione levels in human macrophages. *Am J Physiol Cell Physiol, 281*(6), C1964-1970.

Robe, P. A., Bentires-Alj, M., Bonif, M., Rogister, B., Deprez, M., Haddada, H., Khac, M. T., Jolois, O., Erkmen, K., Merville, M. P., Black, P. M., & Bours, V. (2004). In vitro and in vivo activity of the nuclear factor-kappaB inhibitor sulfasalazine in human glioblastomas. *Clin Cancer Res, 10*(16), 5595-5603.

Robe, P. A., Martin, D., Albert, A., Deprez, M., Chariot, A., & Bours, V. (2006). A phase 1-2, prospective, double blind, randomized study of the safety and efficacy of Sulfasalazine for the treatment of progressing malignant gliomas: study protocol of [ISRCTN45828668]. *BMC Cancer, 6*, 29.

Robe, P. A., Martin, D. H., Nguyen-Khac, M. T., Artesi, M., Deprez, M., Albert, A., Vanbelle, S., Califice, S., Bredel, M., & Bours, V. (2009). Early termination of ISRCTN45828668, a phase 1/2 prospective, randomized study of sulfasalazine for the treatment of progressing malignant gliomas in adults. *BMC Cancer, 9*, 372.

Rochon, J. (1991). Sample size calculations for two-group repeated-measures experiments. *Biometrics, 47*(December), 1383-1398.

Rodan, G. A., & Martin, T. J. (2000). Therapeutic approaches to bone diseases. *Science, 289*(5484), 1508-1514.

Rosendal, L., Larsson, B., Kristiansen, J., Peolsson, M., Sogaard, K., Kjaer, M., Sorensen, J., & Gerdle, B. (2004). Increase in muscle nociceptive substances and anaerobic metabolism in patients with trapezius myalgia: microdialysis in rest and during exercise. *Pain, 112*(3), 324-334.

Rothstein, J. D., Patel, S., Regan, M. R., Haenggeli, C., Huang, Y. H., Bergles, D. E., Jin, L., Dykes Hoberg, M., Vidensky, S., Chung, D. S., Toan, S. V., Bruijn, L. I., Su, Z. Z., Gupta, P., & Fisher, P. B. (2005). Beta-lactam antibiotics offer neuroprotection by increasing glutamate transporter expression. *Nature, 433*(7021), 73-77.

Roubertoux, P. L., Le Roy, I., Tordjman, S., Cherfou, A., & Migliore-Samour, D. (2003). Analysis of quantitative trait loci for behavioral laterality in mice. *Genetics, 163*(3), 1023-1030.

Roudier, M. P., Vesselle, H., True, L. D., Higano, C. S., Ott, S. M., King, S. H., & Vessella, R. L. (2003). Bone histology at autopsy and matched bone scintigraphy findings in patients with hormone refractory prostate cancer: the effect of bisphosphonate therapy on bone scintigraphy results. *Clin Exp Metastasis, 20*(2), 171-180.

Rzeski, W., Turski, L., & Ikonomidou, C. (2001). Glutamate antagonists limit tumor growth. *Proc Natl Acad Sci U S A, 98*(11), 6372-6377.

Sabino, M. A., & Mantyh, P. W. (2005). Pathophysiology of bone cancer pain. *J Support Oncol, 3*(1), 15-24.

Sanchez-Sweatman, O. H., Lee, J., Orr, F. W., & Singh, G. (1997). Direct osteolysis induced by metastatic murine melanoma cells: role of matrix metalloproteinases. *Eur J Cancer, 33*(6), 918-925.

Sanchez-Sweatman, O. H., Orr, F. W., & Singh, G. (1998). Human metastatic prostate PC3 cell lines degrade bone using matrix metalloproteinases. *Invasion Metastasis, 18*(5-6), 297-305.

Sasaki, H., Sato, H., Kuriyama-Matsumura, K., Sato, K., Maebara, K., Wang, H., Tamba, M., Itoh, K., Yamamoto, M., & Bannai, S. (2002). Electrophile response element-mediated induction of the cystine/glutamate exchange transporter gene expression. *J Biol Chem, 277*(47), 44765-44771.

Sato, H., Kuriyama-Matsumura, K., Hashimoto, T., Sasaki, H., Wang, H., Ishii, T., Mann, G. E., & Bannai, S. (2001). Effect of oxygen on induction of the cystine transporter by bacterial lipopolysaccharide in mouse peritoneal macrophages. *J Biol Chem, 276*(13), 10407-10412.

Sato, H., Nomura, S., Maebara, K., Sato, K., Tamba, M., & Bannai, S. (2004). Transcriptional control of cystine/glutamate transporter gene by amino acid deprivation. *Biochem Biophys Res Commun, 325*(1), 109-116.

Sato, H., Tamba, M., Kuriyama-Matsumura, K., Okuno, S., & Bannai, S. (2000). Molecular cloning and expression of human xCT, the light chain of amino acid transport system xc. *Antioxid Redox Signal, 2*(4), 665-671.

Schwei, M. J., Honore, P., Rogers, S. D., Salak-Johnson, J. L., Finke, M. P., Ramnaraine, M. L., Clohisy, D. R., & Mantyh, P. W. (1999). Neurochemical and cellular reorganization of the spinal cord in a murine model of bone cancer pain. *J Neurosci, 19*(24), 10886-10897.

Seidlitz, E. P., Sharma, M. K., Saikali, Z., Ghert, M., & Singh, G. (2009). Cancer cell lines release glutamate into the extracellular environment. *Clin Exp Metastasis, 26*(7), 781-787.

Seidlitz, E. P., Sharma, M. K., & Singh, G. (2010a). A by-product of glutathione production in cancer cells may cause disruption in bone metabolic processes. *Can J Physiol Pharmacol, 88*(3), 197-203.

Seidlitz, E. P., Sharma, M. K., & Singh, G. (2010b). Extracellular glutamate alters mature osteoclast and osteoblast functions. *Can J Physiol Pharmacol, 88*(9), 929-936.

Sethi, N., Dai, X., Winter, C. G., & Kang, Y. (2011). Tumor-derived JAGGED1 promotes osteolytic bone metastasis of breast cancer by engaging notch signaling in bone cells. *Cancer Cell, 19*(2), 192-205.

Sharma, M. K., Seidlitz, E. P., & Singh, G. (2010). Cancer cells release glutamate via the cystine/glutamate antiporter. *Biochem Biophys Res Commun, 391*(1), 91-95.

Shigeri, Y., Seal, R. P., & Shimamoto, K. (2004). Molecular pharmacology of glutamate transporters, EAATs and VGLUTs. *Brain Res Brain Res Rev, 45*(3), 250-265.

Shih, A. Y., & Murphy, T. H. (2001). xCt cystine transporter expression in HEK293 cells: pharmacology and localization. *Biochem Biophys Res Commun, 282*(5), 1132-1137.

Shukla, K., Thomas, A. G., Ferraris, D. V., Hin, N., Sattler, R., Alt, J., Rojas, C., Slusher, B. S., & Tsukamoto, T. (2011). Inhibition of xc transporter-mediated cystine uptake by sulfasalazine analogs. *Bioorg Med Chem Lett, 21*(20), 6184-6187.

Skerry, T. M. (2008). The role of glutamate in the regulation of bone mass and architecture. *J Musculoskelet Neuronal Interact, 8*(2), 166-173.

Solomayer, E. F., Diel, I. J., Meyberg, G. C., Gollan, C., & Bastert, G. (2000). Metastatic breast cancer: clinical course, prognosis and therapy related to the first site of metastasis. *Breast Cancer Res Treat, 59*(3), 271-278.

Suematsu, A., Tajiri, Y., Nakashima, T., Taka, J., Ochi, S., Oda, H., Nakamura, K., Tanaka, S., & Takayanagi, H. (2007). Scientific basis for the efficacy of combined use of antirheumatic drugs against bone destruction in rheumatoid arthritis. *Mod Rheumatol, 17*(1), 17-23.

Sun, Y. X., Schneider, A., Jung, Y., Wang, J., Dai, J., Cook, K., Osman, N. I., Koh-Paige, A. J., Shim, H., Pienta, K. J., Keller, E. T., McCauley, L. K., & Taichman, R. S. (2005). Skeletal localization and neutralization of the SDF-1(CXCL12)/CXCR4

axis blocks prostate cancer metastasis and growth in osseous sites in vivo. *J Bone Miner Res, 20*(2), 318-329.

Takada, A., & Bannai, S. (1984). Transport of cystine in isolated rat hepatocytes in primary culture. *J Biol Chem, 259*(4), 2441-2445.

Takano, T., Lin, J. H., Arcuino, G., Gao, Q., Yang, J., & Nedergaard, M. (2001). Glutamate release promotes growth of malignant gliomas. *Nat Med, 7*(9), 1010-1015.

Takarada, T., Hinoi, E., Fujimori, S., Tsuchihashi, Y., Ueshima, T., Taniura, H., & Yoneda, Y. (2004). Accumulation of [3H] glutamate in cultured rat calvarial osteoblasts. *Biochem Pharmacol, 68*(1), 177-184.

Takarada, T., & Yoneda, Y. (2008). Pharmacological topics of bone metabolism: glutamate as a signal mediator in bone. *J Pharmacol Sci, 106*(4), 536-541.

Tetreault, P., Dansereau, M. A., Dore-Savard, L., Beaudet, N., & Sarret, P. (2011). Weight bearing evaluation in inflammatory, neuropathic and cancer chronic pain in freely moving rats. *Physiol Behav, 104*(3), 495-502.

Thomas, R. J., Guise, T. A., Yin, J. J., Elliott, J., Horwood, N. J., Martin, T. J., & Gillespie, M. T. (1999). Breast cancer cells interact with osteoblasts to support osteoclast formation. *Endocrinology, 140*(10), 4451-4458.

Uno, K., Takarada, T., Hinoi, E., & Yoneda, Y. (2007). Glutamate is a determinant of cellular proliferation through modulation of nuclear factor E2 p45-related factor-2 expression in osteoblastic MC3T3-E1 cells. *J Cell Physiol, 213*(1), 105-114.

Väänänen, H. K., Karhukorpi, E. K., Sundquist, K., Wallmark, B., Roininen, I., Hentunen, T., Tuukkanen, J., & Lakkakorpi, P. (1990). Evidence for the presence of a proton pump of the vacuolar H(+)-ATPase type in the ruffled borders of osteoclasts. *J Cell Biol, 111*(3), 1305-1311.

Väänänen, H. K., & Laitala-Leinonen, T. (2008). Osteoclast lineage and function. *Arch Biochem Biophys, 473*(2), 132-138.

Vene, R., Castellani, P., Delfino, L., Lucibello, M., Ciriolo, M. R., & Rubartelli, A. (2011). The cystine/cysteine cycle and GSH are independent and crucial antioxidant systems in malignant melanoma cells and represent druggable targets. *Antioxid Redox Signal, 15*(9), 2439-2453.

Verrey, F., Closs, E. I., Wagner, C. A., Palacin, M., Endou, H., & Kanai, Y. (2004). CATs and HATs: the SLC7 family of amino acid transporters. *Pflugers Arch, 447*(5), 532-542.

Vukmirovic-Popovic, S., Colterjohn, N., Lhotak, S., Duivenvoorden, W. C., Orr, F. W., & Singh, G. (2002). Morphological, histomorphometric, and microstructural alterations in human bone metastasis from breast carcinoma. *Bone, 31*(4), 529-535.

Wahl, C., Liptay, S., Adler, G., & Schmid, R. M. (1998). Sulfasalazine: a potent and specific inhibitor of nuclear factor kappa B. *J Clin Invest, 101*(5), 1163-1174.

Wang, H., Tamba, M., Kimata, M., Sakamoto, K., Bannai, S., & Sato, H. (2003). Expression of the activity of cystine/glutamate exchange transporter, system x(c)(-), by xCT and rBAT. *Biochem Biophys Res Commun, 305*(3), 611-618.

Wang, L., Hinoi, E., Takemori, A., Nakamichi, N., & Yoneda, Y. (2006). Glutamate inhibits chondral mineralization through apoptotic cell death mediated by retrograde operation of the cystine/glutamate antiporter. *J Biol Chem, 281*(34), 24553-24565.

Wang, L. N., Yang, J. P., Zhan, Y., Ji, F. H., Wang, X. Y., Zuo, J. L., & Xu, Q. N. (2012). Minocycline-induced reduction of brain-derived neurotrophic factor expression in relation to cancer-induced bone pain in rats. *J Neurosci Res, 90*(3), 672-681.

Warburg, O., Wind, F., & Negelein, E. (1927). The Metabolism of Tumors in the Body. *J Gen Physiol, 8*(6), 519-530.

Warr, O., Takahashi, M., & Attwell, D. (1999). Modulation of extracellular glutamate concentration in rat brain slices by cystine-glutamate exchange. *J Physiol, 514 (Pt 3)*, 783-793.

Watanabe, H., & Bannai, S. (1987). Induction of cystine transport activity in mouse peritoneal macrophages. *J Exp Med, 165*(3), 628-640.

WHO. (1996). *Cancer Pain Relief* (2nd ed.). Geneva: World Health Organization.

Wolfe, M. M., Lichtenstein, D. R., & Singh, G. (1999). Gastrointestinal toxicity of nonsteroidal antiinflammatory drugs. *N Engl J Med, 340*(24), 1888-1899.

Wolosker, H. (2006). D-serine regulation of NMDA receptor activity. *Sci STKE, 2006*(356), pe41.

Wu, G., Fang, Y. Z., Yang, S., Lupton, J. R., & Turner, N. D. (2004). Glutathione metabolism and its implications for health. *J Nutr, 134*(3), 489-492.

Yamasaki, M., Miyazaki, T., Azechi, H., Abe, M., Natsume, R., Hagiwara, T., Aiba, A., Mishina, M., Sakimura, K., & Watanabe, M. (2011). Glutamate receptor delta2 is essential for input pathway-dependent regulation of synaptic AMPAR contents in cerebellar Purkinje cells. *J Neurosci, 31*(9), 3362-3374.

Yashpal, K., Fisher, K., Chabot, J. G., & Coderre, T. J. (2001). Differential effects of NMDA and group I mGluR antagonists on both nociception and spinal cord protein kinase C translocation in the formalin test and a model of neuropathic pain in rats. *Pain, 94*(1), 17-29.

Yates, A. J., Gutierrez, G. E., Smolens, P., Travis, P. S., Katz, M. S., Aufdemorte, T. B., Boyce, B. F., Hymer, T. K., Poser, J. W., & Mundy, G. R. (1988). Effects of a synthetic peptide of a parathyroid hormone-related protein on calcium homeostasis, renal tubular calcium reabsorption, and bone metabolism in vivo and in vitro in rodents. *J Clin Invest, 81*(3), 932-938.

Yavas, O., Hayran, M., & Ozisik, Y. (2007). Factors affecting survival in breast cancer patients following bone metastasis. *Tumori, 93*(6), 580-586.

Ye, Z. C., Rothstein, J. D., & Sontheimer, H. (1999). Compromised glutamate transport in human glioma cells: reduction-mislocalization of sodium-dependent glutamate transporters and enhanced activity of cystine-glutamate exchange. *J Neurosci, 19*(24), 10767-10777.

Ye, Z. C., & Sontheimer, H. (1999). Glioma cells release excitotoxic concentrations of glutamate. *Cancer Res, 59*(17), 4383-4391.

Yin, J. J., Mohammad, K. S., Kakonen, S. M., Harris, S., Wu-Wong, J. R., Wessale, J. L., Padley, R. J., Garrett, I. R., Chirgwin, J. M., & Guise, T. A. (2003). A causal role

for endothelin-1 in the pathogenesis of osteoblastic bone metastases. *Proc Natl Acad Sci U S A, 100*(19), 10954-10959.

Yoneda, T., Hata, K., Nakanishi, M., Nagae, M., Nagayama, T., Wakabayashi, H., Nishisho, T., Sakurai, T., & Hiraga, T. (2011). Involvement of acidic microenvironment in the pathophysiology of cancer-associated bone pain. *Bone, 48*(1), 100-105.

Zech, D. F., Grond, S., Lynch, J., Hertel, D., & Lehmann, K. A. (1995). Validation of World Health Organization Guidelines for cancer pain relief: a 10-year prospective study. *Pain, 63*(1), 65-76.

Zhao, Y., Bachelier, R., Treilleux, I., Pujuguet, P., Peyruchaud, O., Baron, R., Clement-Lacroix, P., & Clezardin, P. (2007). Tumor alphavbeta3 integrin is a therapeutic target for breast cancer bone metastases. *Cancer Res, 67*(12), 5821-5830.

Zhu, M., & Bowden, G. T. (2004). Molecular mechanism(s) for UV-B irradiation-induced glutathione depletion in cultured human keratinocytes. *Photochem Photobiol, 80*(2), 191-196.

Zhu, W., Yang, M. L., Yang, G. Y., Boden, G., & Li, L. (2011). Changes in Serum Runt-related Transcription Factor 2 Levels After a 6-months Treatment with Recombinant Human Parathyroid Hormone in Patients with Osteoporosis. *J Endocrinol Invest*.